

Norwegian University of Life Sciences
Faculty of Veterinary Medicine
Department of Paraclinical Sciences (ParaFag)

Philosophiae Doctor (PhD)
Thesis 2023:62

In vitro investigations on infections with bovine coronavirus and Cryptosporidium parvum

In vitro-undersøkelser av infeksjoner med
bovintkoronavirus og *Cryptosporidium*
parvum

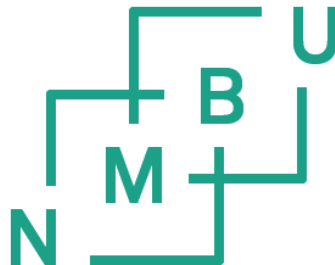
Ruchika Shakya

***In vitro* investigations on infections with bovine
coronavirus and *Cryptosporidium parvum***

In vitro-undersøkelser av infeksjoner med bovint
koronavirus og *Cryptosporidium parvum*

Philosophiae Doctor (PhD) Thesis
Ruchika Shakya

Faculty of Veterinary Medicine
Department of Paraclinical Sciences
Norwegian University of Life Sciences
Ås, 2023



Thesis number 2023:62
ISSN 1894-6402
ISBN 978-82-575-2091-5

Supervisors and Evaluation Committee

Main supervisor: Professor Mette Myrmed, NMBU, Norway
Co-supervisor: Professor Lucy Jane Robertson, NMBU, Norway
Co-supervisor: Shokouh Makvandi-Nejad, Norwegian
Veterinary Institute, Norway

Jonas Petter Johansson Wensman	National Veterinary Institute (SVA), Uppsala, Sweden
Marta García Sánchez	University of Dundee, Eastern Scotland, UK
Professor Charles McLean Press	NMBU, Norway

Acknowledgements

I would like to express my sincere appreciation to:

My main supervisor Mette Myrmel for the constant supervision, guidance, and encouragement. Her critical review and comments helped me think analytically and critically. I would like to thank her for providing me with all the materials, resources, and links that I could not possibly have discovered on my own. For her unwavering support, patience, I am truly grateful.

My co-supervisor Lucy J. Robertson for your unreserved support throughout my thesis. You have pushed me to excel not just in my thesis but encouraged me to take part in conferences, gatherings, meetings, and other collaborative works. I cannot miss out on thanking you for proof-reading my manuscripts and thesis with your skilful English knowledge. I always admire your knowledge, hard-working attitude, and the sense of humour.

Shokouh Makvandi-Nejad, my other co-supervisor for all the help with bioinformatics. Thanks for excellent teaching, guidance, and positive attitude.

Alejandro Jimenez Meléndez, for your selfless supervision, guidance, and support. You have stepped in as a supervisor, helped me constantly throughout my lab works. It was always easy to approach you be it for help with lab works, writings, presentations or even for small talks.

Mamata Khatri for your constant support throughout dissertation and lab works but also other pursuits of life. Thank you for patiently listening to my frustrations, smiling through, and joyfully giving me suggestions.

Turhan Markussen for enthusiastically stepping in to help us with bioinformatic skills and for providing guidance and feedbacks.

Professor Elisabeth A. Innes, Postdoc Alison Burrells, and others at the Moredun Research Institute (MRI), Scotland for being kind to host me at the Moredun Research Institute, Scotland, UK for helping me with my accommodation and adjustment to the new laboratory setting.

Thank you, my officemate Mathilde Svensen Varegg, for lighting up the room with your smile, social nature, and positive attitude. It was always fun discussing our projects and working together.

Preben Boysen for helping us with the gating for the flow cytometry and result analysis.

Hilde Raanaas Kolstad and Lene Cecilie Hermansen at the NMBU Imaging Centre for joyfully agreeing to help me with long sessions of confocal microscopy and TEM.

Britt Gjerset and Lars Austbø at the Norwegian Veterinary Institute for providing primers, probes, and qPCR protocol for the EHV-1.

Stanislav Iakhno for helping with scripts on RNASeq.

Ian Woolsey for sharing the protocols and scientific inputs to work with *C. parvum*.

Tamirat Tefera Temesgen for happily agreeing to share the *C. parvum* oocysts, helping with sequencing of isolated oocysts from calf faeces and Bioanalyzer for RNASeq.

Antje Hofgaard from University of Oslo for being so easy to collaborate with on TEM.

All the colleagues at the virology (Espen, Øystein, Elisabeth, Stine, Ingvild, Ingrid, Nina) and parasitology department (Ingrid, Elliott, Tsega) for offering me a nice working environment, technical support, and encouragement. For my former colleagues at NMBU, I would like to thank Henning, Gabriela, Özgün, Mari, Hege, Grethe, John and Kiru for their support.

Saksham Krishna Suvedi for his love, patience, and encouragement.

My sister Hausala Shakya and brother-in-law Bishwa Ale for working throughout the night with me on R and Python to prepare wonderful figures for my articles and keeping a positive attitude.

My parents, Kabir and Kusum Shakya, for unconditional love and support. Without their faith in me, I could not have accomplished and made it this far without them.

Lastly, I would like to dedicate my thesis to my grandparents (Ma and Ba) who impacted and inspired me and were always very proud of me.

Ruchika Shakya

Table of Contents

Supervisors and Evaluation Committee.....	ii
Acknowledgements	iii
1 List of abbreviations	1
2 List of papers.....	4
3 Summary	5
4 Norsk sammendrag.....	7
5 Introduction.....	9
5.1 Calf diarrhoea	9
5.2 Bovine coronavirus.....	11
5.2.1 The virus.....	11
5.2.2 Replication of BCoV	12
5.2.3 Epidemiology and transmission.....	13
5.2.4 Pathogenesis.....	14
5.2.5 Immune response	14
5.2.6 Diagnosis.....	15
5.2.7 Prevention and Treatment.....	16
5.3 <i>Cryptosporidium parvum</i>	17
5.3.1 The parasite	17
5.3.2 Life Cycle	17
5.3.3 Epidemiology and transmission of <i>C. parvum</i>	19
5.3.4 Pathogenesis.....	20
5.3.5 Immune response	21
5.3.6 Diagnosis.....	21
5.3.7 Prevention and Treatment.....	22
5.4 <i>In vitro</i> studies (2D and 3D cell-culture models) on BCoV and <i>C. parvum</i>	23
5.4.1 2D cell-culture models	23
5.4.2 3D cell-culture: Organoids	24
5.5 <i>In vivo</i> studies	26

6	Knowledge gaps.....	27
7	Aims of the study.....	28
8	Materials and methods	29
9	Methodological considerations	33
9.1	2D cell culture.....	33
9.2	3D cell culture – Bovine enteroids	33
	35	
9.3	Nucleic acid extraction	35
9.4	(RT)-qPCR.....	35
9.5	Flow cytometry	36
9.6	Immunostaining.....	37
9.7	Transmission electron microscopy.....	37
9.8	RNA sequencing (RNASeq)	38
9.9	Bioinformatic analysis	38
9.10	Statistical analysis.....	39
10	Results.....	40
10.1	Bovine coronavirus attaches to <i>C. parvum</i> during co-inoculation (Paper I and additional results).....	40
10.2	Marked pro-inflammatory response in BCoV- and co-infected HCT-8 cells (Paper II - Manuscript under review)	42
10.3	Bovine enteroids are permissive for BCoV (Paper III and additional results)	48
11	Discussion	50
12	Conclusions.....	57
13	Future perspectives	58
14	References.....	60
15	Papers	79

1 List of abbreviations

APC- Antigen presenting cell
BCoV- Bovine coronavirus
BNoV- Bovine norovirus
bp- Base pair
BRoV- Bovine rotavirus
BSA- Bovine serum albumin
CB- Cacodylate buffer
CEBPB- CCAAT (cytosine-cytosine-adenosine-adenosine-thymidine) enhancer binding protein beta
CEBPD- CCAAT Enhancer Binding Protein Delta
cGAS- Cyclic GMP-AMP synthase
CLmin- C-type lectin-like receptors
CO₂- Carbon dioxide
Ct- Cycle threshold
dH₂O- Distilled water
DAI- DNA-dependent activator of IRFs
DAPI- 4',6-diamidino-2-phenylindole
DC- Dendritic cells
DNA- Deoxyribonucleic acid
DPBS- Dulbecco's phosphate buffer saline
ECM- Extra cellular matrix
EDTA- Ethylenediaminetetraacetic acid
EHV-1- Equine herpes virus type-1
ELISA- Enzyme-linked immune-sorbent assay
ERGIC- Endoplasmic reticulum-Golgi intermediate compartment
FA- Fluorescence antibody
FBS- Foetal bovine serum
FPKM- Fragments per kilobase of exon per million mapped reads
FITC- Fluorescein isothiocyanate
gDNA- genomic DNA
GO- Gene ontology

Gp- Glycoprotein
GRO-a- Growth Regulated Oncogene-a
HCl- Hydrochloric acid
HCT-8- Human ileocecal adenocarcinoma
HEPES-4-(2-hydroxyethyl)-1-piperazineethanesulfonic acid
hpi- hour post inoculation
HRT-18G- Human rectal tumour cells
hsp- Heat shock protein
ICTV- International Committee on Taxonomy of Viruses
IFAT- Immunofluorescent antibody testing
IFN- Interferon
IFNG- Interferon gamma
IFI16- Gamma interferon (IFN- γ)-inducible protein 16
IgG- Immunoglobulin G
IL- Interleukin
IRF- Interferon regulatory factor
ISC- Intestinal stem cells
ISG- Interferon-stimulated gene
KEGG- Kyoto encyclopaedia of genes and genomes
LPS- Lipopolysaccharide
MAPK- Mitogen associated protein kinases
MAVS- Mitochondrial antiviral signalling
MDBK- Madin-Darby Bovine Kidney cells
MDCK1- Madin Darby Canine Kidney 1 cells
MERS- Middle East respiratory syndrome-related coronavirus
MOI- Multiplicity of infection
NA- Nucleic acid
NANS- N-Acetylneuraminase Synthase
Neu5Ac- N-acetyl neuraminic acid
NF- κ B- Nuclear factor kappa-light-chain-enhancer of activated B cells
NK- Natural killer
NLR- NOD-like receptor
PAMPs- Pathogen-associated molecular patterns
PBS- Phosphate buffered saline
PFA- Paraformaldehyde
PI- Propidium iodide
PRR- Pathogen recognizing receptor

PV- Parasitophorous vacuole
RdRp- RNA-dependent RNA polymerase
RHOA- Ras Homolog Family Member A
RLR- RIG-like receptors
RNA- Ribonucleic acid
RoV- Rotavirus
RPE- R-phycoerythrin
RER- Rough endoplasmic reticulum
RT-qPCR- Reverse transcriptase real-time quantitative polymerase chain reaction
SA- Sialic acid
Spp.-species
SRC- Proto-Oncogene, Non-Receptor Tyrosine Kinase Src
SSUrRNA- small subunit ribosomal RNA
STING- stimulator of interferon genes
TCID₅₀- The median tissue culture infectious dose (TCID₅₀)
TEM- Transmission electron microscopy
TLR- Toll-like receptor
T_m- Melting temperature
TNF- Tumour necrosis factor
TP53- Tumour protein P53
TRAF2- TNF Receptor Associated Factor 2
VNT- Virus neutralization test
VRCs- viral replication complexes

2 List of papers

Paper I.

Interactions between *Cryptosporidium parvum* and bovine corona virus during sequential and simultaneous infection of HCT-8 cells.

Authors: **Ruchika Shakya**, Alejandro Jiménez-Meléndez, Lucy J. Robertson, Mette Myrmel

Published: Microbes and Infection, 2022, 24 (3) 104909.

Manuscript II.

Gene expression profile of HCT-8 cells following single or co-infection with *Cryptosporidium parvum* and bovine coronavirus

Authors: Alejandro Jiménez-Meléndez, **Ruchika Shakya**, Turhan Markussen, Lucy J. Robertson, Mette Myrmel, Shokouh Makvandi-Nejad

Submitted to: Nature, Scientific Reports, 2023.

Paper III.

Bovine enteroids as an *in vitro* model for infection with bovine coronavirus

Authors: **Ruchika Shakya**, Alejandro Jiménez-Meléndez, Lucy J. Robertson, Mette Myrmel

Published: MDPI, Viruses, 2023, 15 (3) 635.

3 Summary

Intestinal infection causing diarrhoea is a major health problem among calves accounting for about 40% of calf diseases in Norway. Calves are especially susceptible to gastroenteritis during the first month of life of which bovine coronavirus (BCoV) and the intracellular parasite *Cryptosporidium parvum* (*C. parvum*) are the two major enteropathogens involved. Several studies have indicated that mixed infections are more common among diarrhoeal calves and that co-infections are associated with greater symptom severity. However, the pathogen-pathogen interplay and host-pathogen interaction during co-infection are unknown. Therefore, the overall objective of this thesis was to study the interplay between BCoV and *C. parvum* during infection and their possible effects on the host using *in vitro* models.

To study the BCoV and *C. parvum* interactions during infection, human HCT-8 cells were sequentially and simultaneously inoculated with the two pathogens. Quantitative results from (RT)-qPCR revealed prior inoculation of cells with one pathogen did not have any effect on replication of the other. Co-inoculation, however, showed an interesting result indicating binding of BCoV to *C. parvum* sporozoites. There was an increase in viral RNA in presence of sporozoites at 1 hpi (hours post inoculation) which was no longer evident at 24 hpi indicating entrapment of virus in the parasitophorous vacuole. To test whether the attachment between BCoV and *C. parvum* sporozoites could be specific, bovine norovirus (naked) and equine herpes virus-1 (enveloped), were included in the study. The results indicated no binding between sporozoites and these viruses, which strengthens our assumption that binding of BCoV to the sporozoites is specific. Furthermore, flow cytometry to study the proportion of single and co-infected cells at 72 hpi showed that *C. parvum* and BCoV infected 1-11% and 10-20% of the HCT-8 cells, respectively, with only 0.04% of double infected cells.

The host response was investigated with RNASeq of HCT-8 cells inoculated with BCoV alone, *C. parvum* alone, and BCoV/*C. parvum* simultaneously. There were more than 6000 differentially expressed genes (DEGs) in BCoV- and co-infected cells while only 52 DEGs were found for *C. parvum* infection at 72 hpi. Pathway (KEGG) and gene ontology (GO) analysis of BCoV- and co-infected cells revealed involvement of mostly immune related pathways (NF- κ B, TNF or, IL-17), apoptosis, and regulation of transcription while limited effect was exerted by *C.*

parvum under our experimental settings. The most enriched GO terms from *C. parvum*-infected cells at 24 hpi belonged to metabolic categories but at 72 hpi additional GO terms, such as cell death and responses to oxygen-containing compounds, occurred. Despite the modulation observed in the co-infection being dominated by the virus, which was probably due to differences in the infection rate of the pathogens, over 800 DEGs were exclusively expressed in co-infected cells at 72 hpi. Our findings provide insights on possible biomarkers associated with co-infection, which could be further explored *in vivo*.

Furthermore, a 3D bovine enteroid model (complex model due to heterogeneous cell population) was established as a replication system for BCoV. Immunostaining showed that the enteroids had a differentiated cell population. RT-qPCR results of the infected enteroids showed seven-fold increase in BCoV RNA at 72 hpi. The BCoV S-protein was detected by immunostaining, which indicates that virus particles might be produced. The expression of selected genes during BCoV infection of the enteroids was compared with the expression we previously found in HCT-8 cells. The pro-inflammatory responses of the enteroids such as IL-8 and IL-1A were comparable in the two models, while the expression of CXCL-3, MMP13, and TNF- α was significantly downregulated in the enteroids.

In conclusion, there was a limited impact of co-infections on replication of the two agents, but upon co-inoculation we found binding of BCoV to the sporozoites which inhibited viral replication. The host transcriptome study revealed that some of the genes exclusively expressed during co-infection could be suggestive of possible biomarkers of co-infections, and their role in the pathogenesis of these intestinal infections should be addressed using *in vitro* models (such as bovine enteroids) and *in vivo*. Bovine enteroids were able to support the replication of BCoV but need to be further explored for *C. parvum* infection. Comparative gene expression studies of enteroids and live animals are necessary to clarify whether the *in vitro* model represents a good alternative to replace *in vivo* experiments.

4 Norsk sammendrag

Tarminfeksjon som forårsaker diaré er et stort problem hos kalv og står bak om lag 40 % av sykdom hos kalv i Norge. Kalver er spesielt utsatte for gastroenteritt i løpet av den første levemåned. Bovint koronavirus (BCoV) og den intracellulære parasitten *Cryptosporidium parvum* (*C. parvum*) er blant de viktigste patogenene som er involvert. Flere studier har indikert at blandingsinfeksjoner er mer vanlig blant kalver med diaré og at ko-infeksjoner er assosiert med mer alvorlige symptomer. Likevel vet man lite om samspillet mellom patogener og mellom vert og patogen under ko-infeksjoner. Det overordnede målet for denne avhandlingen var derfor å studere samspillet mellom BCoV og *C. parvum* og deres mulige effekter på verten ved bruk av *in vitro*-modeller.

I den første studien (artikkel 1) ble HCT-8-celler inokulert med de to patogenene sekvensielt og samtidig. Kvantitative resultater fra (RT)-qPCR viste at tidligere inokulering av celler med det ene agenset ikke hadde noen effekt på replikasjon av det andre. Resultatene fra ko-inokulering indikerte imidlertid binding av BCoV til *C. parvum* sporozoitter. Det var en økning i cellene av viralt RNA i nærvær av sporozoitter ved 1 hpi (timer etter inokulering) som ikke lenger var tydelig ved 24 hpi. Dette tyder på hindring av virusreplikasjon, trolig på grunn av inneslutning av virus i parasittofore vakuoler. For å teste om bindingen mellom BCoV og sporozoittene kunne være spesifikk, ble bovint norovirus (nakent virus) og equint herpesvirus-1 (kappevirus), inkludert i studien. Resultatene indikerte ingen binding, noe som styrker vår antagelse om at binding av BCoV til sporozoittene er spesifikk. Videre viste flowcytometri at *C. parvum* og BCoV infiserte henholdsvis 1-11 % og 10-20 % av HCT-8-cellene, og kun 0,04 % ko-infiserte celler.

Vertscellenes respons (artikkel 2) ble undersøkt med RNASeq av HCT-8 celler som var inokulert med BCoV alene, *C. parvum* alene, og begge samtidig. Sammenliknet med ikke-infiserte celler var det mer enn 6000 differensielt uttrykte gener i BCoV- og ko-infiserte celler, mens kun 52 ble funnet for *C. parvum* ved 72 hpi. Pathway (KEGG) og genontologi (GO) analyse av BCoV- og ko-infiserte celler viste, hovedsakelig, regulering av immunrelaterte pathways (NF-κB, TNF eller, IL-17), apoptose og transkripsjon. De mest anrikede GO-termene i *C. parvum*-infiserte celler tilhørte metabolske kategorier ved 24 hpi, men ved 72 hpi forekom i tillegg GO-termer, som celledød og respons på oksygenholdige forbindelser. Til tross for

at moduleringen observert ved ko-infeksjon ble dominert av viruset, noe som trolig skyldtes høyere infeksjonsrate for viruset, ble over 800 gener utelukkende uttrykt i ko-infiserte celler ved 72 hpi. Funnene gir innsikt i mulige biomarkører for ko-infeksjon, noe som kan utforskes videre *in vivo*.

Videre ble en 3D bovin enteroide-modell (kompleks modell på grunn av en heterogen cellepopulasjon) etablert som et replikasjonssystem for BCoV (artikkel 3). Immunfarging av enteroidene viste en differensiert cellepopulasjon. RT-qPCR-resultater fra BCoV-infiserte enteroider viste syv ganger økning i BCoV RNA ved 72 hpi. BCoV S-protein ble påvist ved immunfarging og indikerer at viruspartikler kan produseres. Ekspresjonen av utvalgte gener under BCoV-infeksjon ble sammenlignet med ekspresjonen vi fant i HCT-8-celle. En pro-inflammatorisk respons (IL-8 og IL-1A) var felles for de to systemene, mens ekspresjon av CXCL-3, MMP13 og TNF- α var betydelig nedregulert i enteroidene.

Kort oppsummert var det en begrenset innvirkning av ko-infeksjon på replikasjon av de to agensene, men ved ko-inokulering fant vi en binding av BCoV til sporozoittene som hemmet virusreplikasjonen. Studien av vertens respons viste at en del gener kun var uttrykt under ko-infeksjon. Disse kan være mulige biomarkører for BCoV / *C. parvum* ko-infeksjoner og deres anvendbarhet bør studeres *in vivo*. Bovine enteroider kan støtte replikasjon av BCoV, men modellen må optimaliseres for *C. parvum*-infeksjon. Sammenlikning av genekspresjon i enteroider og levende dyr er nødvendig for å avklare om forsøk med *in vitro*-modellen representerer et godt alternativ til *in vivo* studier av tarminfeksjon i kalv.

5 Introduction

5.1 Calf diarrhoea

Calf diarrhoea is a major global health problem among cattle inflicting great impact on animal welfare, with increased morbidity, and elevated mortality rate, and reduced weight gain (Shaw et al., 2020). At the same time, it also causes a negative impact on the productivity and economy of dairy and cattle industries (Foster et al., 2009). Some of these production systems, especially those with high animal densities, poor sanitation, animal stress and discomfort, are favourable for the transmission of infectious diarrhoea among calves (Gulliksen et al., 2009). Calf diarrhoea can be non-infectious or infectious in origin and several enteric pathogens are associated with the development of disease (Bartels, 2010; Izzo, 2011). The most common agents worldwide include enterotoxigenic *Escherichia coli*, *Cryptosporidium* spp. ($\geq 85\%$ *C. parvum*), bovine rotavirus (BRoV), and bovine coronavirus (BCoV) (Meganck et al., 2014; Brunauer et al., 2021). Mixed infection is more common among diarrhoeal calves as compared to non-diarrhoeal calves, and several studies have indicated the presence of BCoV, BRoV, and *C. parvum* in co-infected diarrhoeal calves (Shaw et al., 2020; Renaud et al., 2021). BRoV and *C. parvum* individually account for the highest percentage of pathogens prevalent among diarrhoeal calves and have been studied extensively (Gulliksen et al., 2009; Bartels et al., 2010; Brandão et al., 2007). The pathogenesis of BCoV and BRoV are similar, with the infected cells being rapidly replaced by undifferentiated crypt cells, resulting in villous atrophy with decreased absorption leading to profuse diarrhoea (McGavin and Carlton, 1995; Singh et al., 2020). BCoV may result in increased mortality ($>50\%$) when combined with other viral, bacterial or *C. parvum* infections (Göhring et al., 2014; Metre et al., 2008; Asadi et al., 2015).

Calves are at the highest risk of developing diarrhoea from BCoV and *C. parvum* in the first month of age (Cruvinel et al., 2020). It is the phase when there is a major decline in specific antibodies as the colostrum is replaced with milk that is considered to have much lower antibody concentration (maternal antibody). The effect of prepartum vaccination of heifers/cows against BCoV diarrhoea to increase passive transfer of immunoglobulins in colostrum to calves has been controversial (Pinheiro et al., 2022). Besides immunity, several other factors, such as herd size, calf housing, environmental factors (e.g., birth season), feeding etc. play an

influential role in occurrence and prevalence of these pathogens (Windeyer et al., 2014).

BCoV infections are common among 1-3 weeks old calves, while the age of calves most likely to be infected with *C. parvum* varies from 0-24 weeks (Brunauer et al., 2021). Both BCoV and *C. parvum* are transmitted via the faecal-oral route and infect the enterocytes in the small intestine, leading to severe diarrhoea in new-born calves (Cho et al., 2014; Foster et al., 2009). BCoV also causes respiratory infections in calves and feedlot cattle and is hypothesized to be swallowed, eventually reaching the small intestine leading to diarrhoea (Oma et al., 2016; Hodnik et al., 2020). In addition, *C. parvum*-infected calves have been shown to be associated with more long-term health effects, such as reduced weight gain and respiratory tract infections, later in life (Renaud et al., 2021; Shaw et al., 2020).

Several serological studies on BCoV have indicated its endemic occurrence in Scandinavia (Hägglund et al., 2006; Bidokthi et al., 2009; Gulliksen et al., 2009b; Ohlson et al. 2010). According to the Norwegian Dairy Herd Recording System, diarrhoea accounted for almost 40% of calf diseases in Norway (Gulliksen et al., 2009). Østerås and others in 2007 estimated that the economic losses due to calf death was around 100 million Norwegian kroner in 2006, where the calf production rate was 280,000 head per year. According to Gulliksen et al., (2009), the seroprevalence of BCoV among Norwegian calves was 39.3%, while random sampling of 135 dairy herds showed a herd-level seropositivity reaching up to 80.7%. The overall prevalence of *Cryptosporidium* among calves in Norway was reported to be 12% while the herd prevalence was 53 % (Hamnes et al., 2006).

Co-infections with BCoV and *C. parvum* have been associated with a higher severity of symptoms as compared to single infections (Gomez et al., 2017; Trotz-Williams et al., 2007). However, the longer-term effects of infection from each pathogen in calves are not well understood (Thomson et al., 2017). Little research has been done to look at the significance of interaction between pathogens during co-infection with regards to clinical disease (severity and duration) (Gomez et al., 2017).

Therefore, the aim of the study was to investigate the use of *in vitro* systems to study the effect of BCoV and *C. parvum* co-infections, compared to single infections, as both are involved in calf diarrhoea infecting the same intestinal cells (enterocytes).

5.2 Bovine coronavirus

5.2.1 The virus

Bovine coronavirus (BCoV) belongs to the order *Nidovirales*, family *Coronaviridae*, subfamily *Orthocoronavirinae*. BCoV is an enveloped, positive-sense (+), single-stranded RNA (ssRNA) virus (Saif et al., 2010; Saif et al., 2018). BCoV belongs to genus *Betacoronavirus* (subgenus *Embecovirus*) measuring about 120-160 nm and with a genome of 31 Kb with 13 open reading frames (ICTV, 2019). The *Betacoronavirus* genus also includes human coronavirus-OC43, canine respiratory coronavirus, SARS-CoV, SARS-CoV-2 and Middle East respiratory syndrome-related coronavirus (MERS)-CoV (Saif et al., 2020).

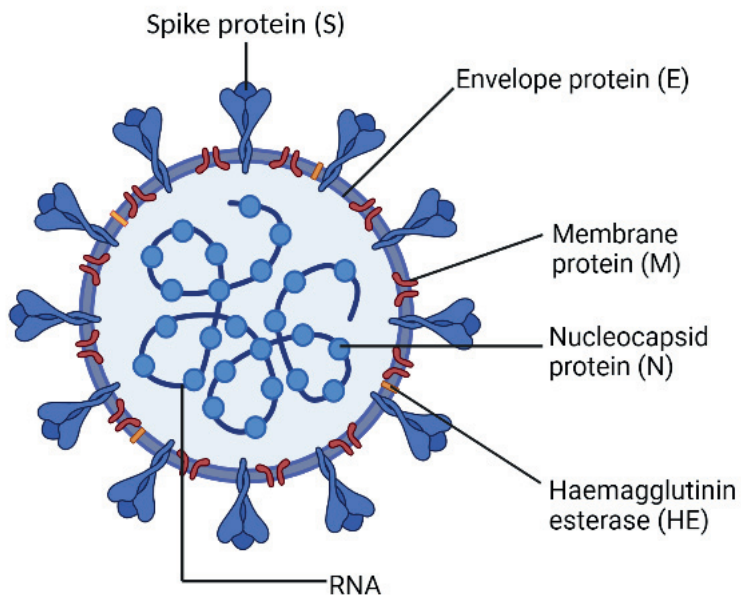


Figure 1: Schematic structure of coronavirus (Created in BioRender)

Credit: Ruchika Shakya

5.2.2 Replication of BCoV

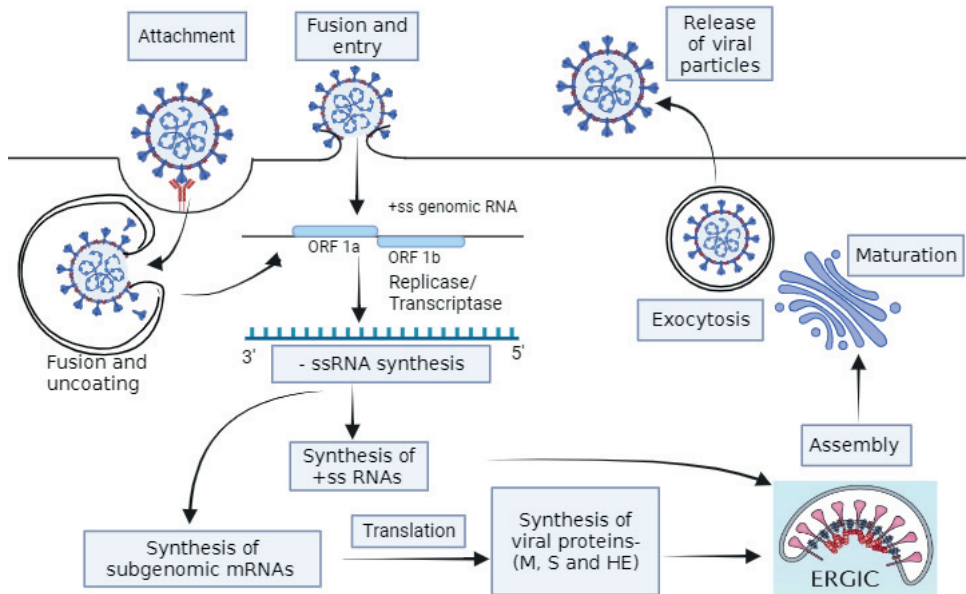


Figure 2: Replication cycle of Coronavirus (Created in BioRender)

Credit: Ruchika Shakya

The replication of BCoV is very similar to other Coronaviruses and the overall process of replication takes place in the cytoplasm of the host cell (Fig 2). BCoV contains five major structural proteins: the nucleocapsid (N), transmembrane (M), spike (S), envelope (E), and haemagglutinin/esterase (HE).

When BCoV infects a cell, the S glycoprotein (gp) attaches to the receptor (9-N acetyl neuraminic acid, Neu5Ac) on the target cell membrane (Schultze et al., 1992; Schwegmann-Wessels et al., 2006). The S-protein consists of two subunits (S1 and S2); the S1 subunit binds to the host cell receptors while the S2 helps in the fusion of the viral envelope to the host membrane (endosome). In the cytoplasm, the viral RNA attaches to the ribosomes to synthesize RNA-dependent RNA polymerase (RdRp), an enzyme transcribing the (+) strand RNA to a complementary (-) strand of RNA. A full-length genomic RNA and seven sub genomic (sgRNAs), which form a 3' nested set with common 3' ends, are then synthesized from the (-) strand serving as a template to produce (+) RNA progeny (Hofman et al., 1990).

The mRNAs coding for the non-structural and N proteins are translated on free ribosomes in the cell cytoplasm. The proteins- M, S and HE are synthesized on ribosomes at the rough endoplasmic reticulum (RER). The glycosylation process of M takes place once it reaches the Golgi apparatus. The S and HE are glycosylated at the RER during protein synthesis and the carbohydrate side chains subsequently modified during transport through the Golgi apparatus (Kienzle et al., 1990; Payne et al., 1990; Clark, 1993).

The interaction between N protein and the newly synthesized genomic RNA leads to the formation of nucleocapsids, which align on the cytoplasmic surface of the membranes of the RER and Golgi due to an interaction with the M proteins. The viral glycoproteins eventually embed in these membranes and the whole virions are pinched off and released into the lumen (budding). These viral replication complexes (VRCs) are assembled in the endoplasmic reticulum-Golgi intermediate compartment (ERGIC) and released from the cell, although a few particles are released by lysis of dying cells. Some of the S and HE gps that are not incorporated into virions are also transported to the plasma membrane. These S proteins cause the infected cells to fuse with the neighbouring cells forming a large, multinucleated cell known as syncytium enabling the virus to spread without being released into the extracellular space (Masters, 2006).

5.2.3 Epidemiology and transmission

BCoV is globally responsible for respiratory and enteric infections among cattle and other ruminants but can also be found in the respiratory and intestinal tracts of healthy cattle (Clark, 1993; Vlasova et al., 2021). Although, cattle either clinically or sub clinically infected are the main reservoir of BCoV, several studies have indicated BCoV-like CoVs in domesticated (water buffalo, sheep, goat, dromedary camel, alpaca, and llama) and wild ruminants (deer, wild cattle, antelopes, giraffes, and wild goats) (Ismail et al., 2001; Amer et al., 2018). However, transmission from other species to cattle has not been documented. Transmission of BCoV among cattle can be within the herd, either from mother to offspring or among the calves and older animals (Bidokthi et al., 2009). Transmission between farms may occur when the animals are purchased from another farm. The animals may be exposed to BCoV on clothing or

fomites. Transporting them to another herd may also act as a stressing factor that facilitates the onset of BCoV infection (Toftaker et al., 2016).

5.2.4 Pathogenesis

BCoV is mostly shed through nasal discharge and faeces of the infected animal and therefore reaches the respiratory epithelium via aerosol inhalation or the intestinal epithelium by ingestion. BCoV replicates in the nasal and tracheal epithelium and eventually the lungs, causing loss of cilia. The clinical picture in cattle may be present in three different ways: (a) calf diarrhoea at 1-2 weeks of age, (b) winter dysentery with haemorrhagic diarrhoea in adult cattle, and (c) respiratory diseases in both young and adult cattle (Fulton et al., 2013). Initially, the infected calves show respiratory signs such as fever, nasal discharge, sneezing, coughing, and interstitial pneumonia (Park et al., 2007). In the intestine, the infection starts at the proximal end of the small intestine and progresses towards the large intestine. The viral replication in these intestinal epithelial cells (enterocytes) of the villi damages them and immature cells replace these cells (Cho et al., 2014). This causes shortening and fusion of adjacent villi, loss of microvilli, and atrophy of colonic ridges. The immature cells do not secrete the required digestive enzymes thereby reducing digestion of feed ingredients (especially lactose in milk) and reducing the absorptive capacity of the small intestine. This causes osmotic imbalance as water is dragged into the lumen, leading to watery diarrhoea. The calves eventually get dehydrated and depressed due to severe diarrhoea with weakened sucking reflex (Boileau and Kapil, 2010).

5.2.5 Immune response

As first line of innate immune response the respiratory and intestinal epithelial cells have pathogen recognition receptors (PRRs) to recognize pathogen-associated molecular patterns (PAMPs). There are several known PRRs such as toll-like receptors (TLRs), NOD-like receptor (NLR), C-type lectin-like receptors (CLmin), and free-molecule receptors in the cytoplasm, such as Cyclic GMP-AMP synthase (cGAS), Gamma interferon (IFN- γ)-inducible protein 16 (IFI16), stimulator of interferon genes (STING), DNA-dependent activator of IRFs (DAI), and so on (Li et al., 2021).

Generally, coronaviruses are recognized by the ssRNA sensing TLRs in the cytosol, TLR3 and TLR7 in the endosomes, and cytosolic RIG-like receptors (RLRs) of the epithelial cells employing the mitochondrial antiviral signalling (MAVS) protein (Seth et al., 2005). This activates the interferon regulatory factor (IRF) 3, IRF7, and nuclear factor kappa-light-chain-enhancer of activated B cells (NF- κ B), inducing rapid production of type I interferon (IFN-I), IFN-III, and proinflammatory cytokines (Takeuchi et al., 2010). Many animal RNA viruses, including coronaviruses, have evolved mechanisms to counteract the host antiviral response (Hoffmann et al., 2015). The importance of addressing the IFN-I response during coronavirus infection can be exemplified by the well-studied human β -coronavirus SARS-CoV-2 that encodes at least ten proteins that target the induction and signalling pathways of IFN-I (Sa Ribero et al., 2020). The NF- κ B is the key regulator of pro-inflammatory response and innate immunity (Hayden and Ghosh, 2014). This, in turn, is essential for the induction of pro-inflammatory cytokines e.g., interleukin (IL) -6 and IL-8 and the early expression of IFN- β during RNA virus infection (Libermann and Baltimore, 1990; Kunsch and Rosen, 1993; Balachandran and Beg, 2011). A study on diarrhoeal calves infected with either BCoV showed an increase in mean IL-8 serum concentration from 0 to 24 h with a decline at 48 h also suggestive of IL-8 as a biomarker of intestinal injury (Ok et al., 2020).

Some of the significantly expressed genes predicted in BCoV infection in cattle, using *in silico* tools, include *TLR7*, *IRF1*, *TLR9*, *CEBPD*, *TRAF2*, *TP53*, *SRC*, *IL-6*, *RHOA*, *CEBPD*, *NANS* (Morenikeji et al., 2020).

5.2.6 Diagnosis

Brief history, clinical presentation, and age of diarrhoeal calves are informative to promptly identify BCoV infection. Rapid antigen tests (rainbow calf scours, BoviD-5 Ag Test Kit) (BCoV, *C. parvum*, and other pathogens including RoV, *E. coli* K99, *Clostridium perfringens*, *Giardia duodenalis*) include dipstick tests that can be used for on farm diagnostics (Wei et al., 2021). Faecal or nasal secretions collected from infected cattle are used to detect virus by using polymerase chain reaction (PCR), or enzyme-linked immune-sorbent assay (ELISA). Samples from acute phase of infection should be collected and processed immediately or transported on ice (Saif et al.,

2010). Serological screening methods include detection of BCoV specific antibodies in milk or sera using virus neutralization test (VNT) (Fulton et al. 2013), and ELISA (Alenius et al., 1991). BCoV-specific immunoglobulin G (IgG) can be detected for a long time after infection for up to 22 months; therefore, detection of IgM in serum for approximately one month could be essential for diagnosis of recent infection (Tråvén et al., 2001). For necropsy specimens, fluorescence antibody (FA) staining of tissue sample obtained from lungs, trachea, both small and large intestine, may be carried out (Boileau and Kapil, 2010). Viral RNA has also been detected in mesenteric lymph nodes, ileum, and colon from euthanized animals six weeks after infection (Oma et al., 2016). To isolate the virus from nasal or faecal secretions, a cloned line of human rectal tumour (HRT)-18 cells is most commonly used (Hasoksuz et al., 1999; Ellis, 2019).

5.2.7 Prevention and Treatment

Norway was the first country to launch a national control program against BCoV and BRoV in 2016 (Toftaker et al., 2016). The programme aims at implementing biosecurity measures to reduce the occurrence of BCoV among Norwegian cattle herds. The measures include separating the animals based on their BCoV antibody status (seropositive or seronegative), use of different transport vehicles, separate loading areas, and provision of sluices to provide clean clothes and footwear for farm visitors. The programme is voluntary, and the cost is shared among the producers and the industry (Stokstad et al., 2020).

There are intranasal vaccines such as BOVILIS Coronavirus (Merck & Co., Inc., Rahway, NJ, USA). However, these are not commonly administered in Norway.

Currently, there is no effective treatment for BCoV diarrhoea, only supportive therapy is available. Diarrhoeal calves or adults are given fluid, glucose, and electrolytes for oral or intravenous rehydration and to counteract hypoglycaemia, electrolyte imbalance, and acidosis (Boileau and Kapil, 2010). In severe cases of winter dysentery, blood transfusion, non-steroidal anti-inflammatory drugs and anti-haemorrhagic drugs are also prescribed (Abuelo and Perez-Santos, 2016; Chigerwe and Heller, 2018).

5.3 *Cryptosporidium parvum*

5.3.1 The parasite

Cryptosporidium spp. are Apicomplexan parasites responsible for causing cryptosporidiosis, which is characterized by watery diarrhoea, nausea, vomiting, fatigue, and several other symptoms. There are at least 44 species, and more than 120 genotypes of *Cryptosporidium*, of which many are host-specific, and many are considered to be non-zoonotic, while some can infect both humans and animals (Ryan et al., 2021). For species differentiation, the small subunit ribosomal RNA (SSUrRNA) gene or portions thereof are the most commonly used markers (Xiao, 2010). Of the several *Cryptosporidium* spp., *C. bovis*, *C. andersoni* and *C. ryanae* are the most common causes of cryptosporidiosis among cattle worldwide while *C. parvum* infections is especially common among neonatal calves (Szonyi et al., 2012). *C. parvum*, *C. ubiquitum*, and *C. hominis* and other species have been genetically characterized into various subtypes based on the 60 kDa glycoprotein gene (gp60) (Robinson et al., 2022). Several *C. parvum* gp60 subfamilies have been described and designated as IIa-IIo; among these, IIa, and IId are zoonotic and IIb, IIc, and IIe-IIt are not zoonotic (Lebbad et al., 2021; Ryan et al., 2014). Some other sub-typing markers, such as cgd1_470_1429, cgd4_2350_796, cgd5_10_310, cgd5_4490_2941; cgd6_4290, cgd8_4440_NC_506 and CGD8_4840_6355, with higher discriminatory capability than gp60 have been reported, but are not yet as widely implemented as the gp60 gene for subtyping (Robinson et al., 2022).

C. parvum oocysts are approximately 4 to 6 μm in diameter (Xiao et al., 2004). They are environmentally hardy and remarkably resistant to chemical disinfection (e.g., chlorination), but are susceptible to temperature extremes of freezing and heat (pasteurization) (Arrowood, 2002).

5.3.2 Life Cycle

Humans and animals acquire *C. parvum* infection via ingestion of oocysts, sometimes via contaminated food and water, which can result in extensive outbreaks with hundreds, or thousands infected. Calves and humans, especially vet students, are prone to being infected with cryptosporidiosis when exposed to fresh calf faeces, as

the oocysts are excreted fully sporulated (Fayer et al., 2008). *C. parvum* undergoes both asexual and sexual replication within a single host and transmission between hosts occurs through meiotic spores called oocysts (Leitch et al., 2011). Each oocyst contains four infective sporozoites. The *C. parvum* oocyst is exposed to gastric acid and body temperature in the stomach, while excystation is triggered only upon reaching the small intestine where the pH is elevated (intestinal bile secretion) (Leitch et al., 2011; Robertson et al., 1993). The actively motile sporozoites are then released that specifically attach themselves to the cells at the ileocecal junction and invade the enterocytes (Thomson et al., 2017). Following invasion, a parasitophorous vacuole is formed at the apical surface of the host cell and the parasites replicate inside it, remaining intracellular but extra cytoplasmic (McDonald et al., 1995).

Within 24 h of invasion, sporozoites mature into trophozoites and progress further through asexual replication to produce type I meronts containing 6-8 merozoites. These merozoites either go through repeated asexual reproduction and infect new epithelial cells, or progress to type II meronts (with 4 merozoites) which, later, progress to the sexual stages (macro- and microgamonts). After fertilization, oocysts are formed and sporulate inside the host as either thin- or thick-walled oocysts. The thin-walled oocysts are released into the lumen and re-infect the current host, while the thick-walled oocysts are shed in high numbers in the faeces (Cacciò et al., 2014).

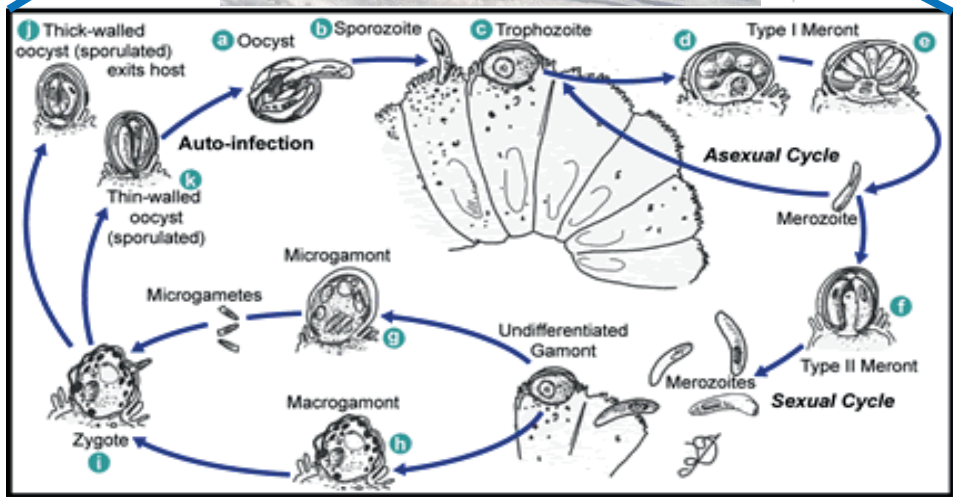


Figure 3: Outline of the *Cryptosporidium parvum* life cycle

Source: CDC, 2015; Picture credit: Norwegian red calf- Turi Nordengen/ Geno

5.3.3 Epidemiology and transmission of *C. parvum*

C. parvum, along with other *Cryptosporidium* species, such as *C. bovis*, *C. andersoni*, and *C. ryanae*, have been reported to be of clinical significance in bovine cryptosporidiosis (Robertson et al., 2014). *C. parvum* has been documented worldwide and has been shown to be prevalent as a major cause of neonatal enteritis among both beef and dairy cattle (Featherstone et al., 2010; Fayer et al., 2006; Brook et al., 2008; Joachim et al., 2003). *Cryptosporidium* has been reported from all age groups, while *C. parvum* infection is mostly common among pre-weaned monogastric calves up to 2 months of age (Brook et al., 2009; Fayer et al., 2007). *C. parvum* is the

most dominant species infecting European cattle (Quílez et al., 2008b; Imre et al., 2011; Plutzer and Karanis, 2007; Soba and Logar, 2008; Silverlås et al. 2013), Transmission mostly occurs by the faeco-oral route, by consumption of food or water contaminated with oocysts or when animals are housed in close proximity. Calves are often infected from their dams soon after birth (Faubert and Litvinsky et al., 2000; Thomson et al., 2019). On the other hand, the parasite may also be transmitted via susceptible calves, animals, or other farm workers through fomites on human clothing, hands, and shoes (Blanchard, 2012).

5.3.4 Pathogenesis

An experimental study among neonatal calves (<24 h old) showed that ingestion of as few as 17 *C. parvum* oocysts is sufficient to cause diarrhoea and oocyst shedding (Zambriski et al., 2013). Therefore, very few infective oocysts are needed to initiate infection in a susceptible host (Thomson et al., 2017). However, this varies according to parasite isolate and host susceptibility.

On reaching the small intestine, the *C. parvum* sporozoites invade the enterocytes and undergo replication. This results in morphological changes in the intestinal cytoskeleton, such as loss of microvilli and shortening of the epithelium, thereby causing severe villous atrophy. *C. parvum* infection is also known to induce disruption of epithelial barrier function by decreasing the expression of tight junction and adherens junction proteins (Priyamvada et al., 2021). The damage to the intestinal epithelium leads to malabsorption and fermentation of undigested milk and food, releasing large amount of water and exudates in the intestinal lumen (Cho et al., 2014). The calves may not exhibit symptoms in some cases, but nevertheless shed oocysts. Diarrhoea mostly occurs 3-4 days after ingestion of infective oocysts and lasts for approximately 1-2 weeks. Diarrheic calves are often lethargic and dehydrated, with loss of appetite; in some cases, death may occur. The faecal discharge is yellow-green and mostly watery (Thomson et al., 2017). In naturally infected calves, oocyst shedding can reach up to 10^6 - 10^8 per gram of faeces over a period of 6 days (Silverlås et al., 2013).

5.3.5 Immune response

The immune response against cryptosporidiosis has most commonly been studied in mouse models and there is limited knowledge regarding this in humans and livestock. *Cryptosporidium* being intracellular but extracytoplasmic might exert a more limited stimulation of host immune responses due to its unique location in the parasitophorous vacuole (Guérin and Striepen, 2020). The first line of innate immune response starts when the pathogen binds to PRRs the (Akira et al., 2006). Among several PRRs, the TLRs, specifically TLR2 and TLR4, were increased in *C. parvum*-infected bovine intestinal epithelial cells (Yang et al., 2015). The interaction between TLR2/TLR4 and *C. parvum* leads to activation of NF- κ B and subsequently, production of pro-inflammatory cytokines (e.g., TNF- α), chemokines (e.g., IL-8) and antimicrobial peptides (e.g., β defensins) (Chen et al., 2005). Activation of the NF- κ B signalling pathway also leads to release of Growth Regulated Oncogene-a (GRO-a) (Yang et al., 2015) and IL-8, which are key neutrophil chemoattractant molecules (Laurent et al., 1997). Similarly, infection of HCT-8 and HT-29 cells with *C. parvum* has shown to induce the expression of IL-18 (McDonald et al., 2006). The immune cell populations, such as natural killer (NK) cells and $\gamma\delta$ T cells, are thereby recruited to the site of infection. As primary T-cell mediated immune responses, antigen presenting cells (APCs), such as dendritic cells (DCs) and macrophages, engulf the antigen at the site of infection and migrate to mesenteric lymph nodes where the antigen is presented to the CD4⁺ T cells. DCs exposed to *C. parvum* secrete several cytokines such as IL-6, IL-1b, IL-12, IL-18, TNF- α , and INF-I through activation of TLR4 receptor (Barakat et al., 2009; Bedi et al., 2014; Perez-Cordon et al., 2014). Presentation of antigen, together with the presence of IL-12 and IFN- γ from APCs and NK cells/ $\gamma\delta$ T cells, respectively, results in the generation of a Th1 CD4⁺ T cell response. This is thought to be a vital immune response against *C. parvum* in humans, cattle, and mice (Thomson et al., 2017).

5.3.6 Diagnosis

Microscopy of faecal material from infected calves by faecal flotation, direct examination, and acid-fast stains are among the most common and cost-effective methods for veterinary diagnosis of cryptosporidiosis (Silverlås et al., 2010). Rapid

antigen tests such as dipstick tests, as mentioned in section 5.2.6, can be used for on farm diagnosis of *C. parvum* together with other pathogens (Wei et al., 2021). Immunofluorescent antibody testing (IFAT), with improved sensitivity and specificity, is the preferred method for detection of *Cryptosporidium* spp. in Europe and USA (Checkley et al., 2015). Molecular tools, such as PCR targeting small subunit (SSU) 18s rRNA for the speciation and gp60 genes for genotyping can be used in the research setting (Chalmers and Katzer, 2013), and multi-pathogen qPCR panels are often used for diagnosis in human medicine, particularly in wealthy countries such as Norway (Campbell et al., 2022).

5.3.7 Prevention and Treatment

Proper hygiene and herd management are the most effective ways to prevent or limit the spread of cryptosporidiosis in farmed animals. It is also recommended to feed new-born calves with an adequate amount of colostrum during their first 24 h of life. The practice of isolating sick calves in a clean, dry, and warm environment, keeping them separate from healthy ones, helps to limit the spread of infection.

Sick calves can be treated with supportive care such as fluid, glucose, and electrolytes with milk given in small quantities several times a day to ensure optimal digestion and reduce weight loss (Robertson et al., 2014). Halofuginone lactate is approved in Europe as the only licensed treatment in cases of severe diarrhoea in calves and has been shown to be beneficial, with milder clinical signs and lower shedding of oocysts (De Waele et al. 2010; Silverlås et al. 2009). A vaccination strategy could be useful to control many livestock diseases; however, as calves are often exposed to *Cryptosporidium* oocysts right after birth, this may be less likely to be successful against cryptosporidiosis. Theoretically, the most appropriate approach would be to immunize dams during late gestation and feed their colostrum to the new-born calves for passive immunization (Innes et al., 2020).

5.4 *In vitro* studies (2D and 3D cell-culture models) on BCoV and *C. parvum*

5.4.1 2D cell-culture models

Several two-dimensional (2D) cell-culture systems have been utilized to study BCoV and *C. parvum* individually. The 2D cell lines subject to genetic variation and most of them support asexual replication of *C. parvum* without continuation to the sexual cycle, and thus do not recapitulate the natural intestinal epithelium models (Feix et al., 2022; Bhalchandra et al., 2018).

2D cell-culture systems, such as human rectal tumour-18 (HRT-18G), human colon adenocarcinoma (HCT-8), Vero, Madin Darby bovine kidney (MDBK), Madin Darby canine kidney 1 (MDCK1) cell lines and primary bovine intestinal epithelial cells have previously been used to culture BCoV (Laporte et al., 1979; Kapil 1991; Dea et al., 1980; Schultze *et al.*, 1991). Cell lines such as THP-1, Bomac and HRT-18 have been used to study adaptation and mutation of BCoV in new host environments (Borucki et al., 2013). Similarly, HRT-18G cells have been utilized to study attachment and entry receptors used by BCoV (Szczepanski et al., 2019).

The first report of *C. parvum* culture was in avian embryos and the derived oocysts were infective to mice (Current and Long, 1983). The first culture of *C. parvum* asexual life cycle stages were performed in HRT-18 (Woodmansee and Pohlenz, 1983). Cryptosporidial sporozoite attachment to, and invasion of, MDCK cells was studied by Lumb and colleagues in 1988. Complete development (both sexual and asexual) in Caco-2 cells (HTB-37) was reported by Dattray et al., (1989). COLO-680N was suggested for long-term culture of *C. parvum* by Miller et al., (2018) while a recent finding by Vélez et al., (2022) contrasts this. Several gene expression studies on host response to *C. parvum* infection have also been conducted using MDBK, pig epithelial cells (IPEC-J2), and HT-29 (Matos et al., 2019; Heidarnejadi et al., 2018). Hollow-fibre systems as 3D models have also been utilized for continuous culture of *C. parvum* and have been reported to produce infective oocysts (Morada et al., 2016).

5.4.2 3D cell-culture: Organoids

Organoids are 3D cell-culture models with heterogenous cell populations derived from specific organs and grown as 3D structures inside extracellular matrixes supplemented with growth factors.

Enteroids are organoids that have been derived from intestinal tissue and consist of mixed populations of epithelial cells, including enterocytes, Paneth cells, goblet cells, enteroendocrine cells and intestinal stem cells (ISCs). The 3D structure of the enteroids, enclosed in a lumen with layers of different epithelial cells, provides an environment closer to the intestine and can serve as an effective model for the study of intestinal pathogens and their interactions with the gut epithelium (Barker et al., 2007; Hamilton et al., 2018). They can be passaged in the lab for a considerably longer duration than normal cell cultures due to the presence of ISCs. Their genome is more intact than carcinoma cells, and they retain their genomic stability over time, since DNA repair processes are still functional (Sato et al., 2011; Huch and Koo, 2015). With these features, enteroids are poised to fill the gap between traditional cell culture and animal models for studying intestinal pathogens.

There has been an upsurge in the use of human, murine and porcine enteroids to study host-pathogen interactions (Zou et al., 2019; Heo et al., 2018; Ettayebi et al., 2016; Li et al., 2019). The studies on bovine enteroids are relatively few with limited availability of bovine supplements/growth factors and reagents for bovine-specific markers such as M cells (Hamilton et al., 2018; Sutton et al., 2022). However, bovine enteroids are relevant for studying the interaction between enteric pathogens and the bovine intestinal epithelium as the mouse or the human models are not always translatable to large animals due to extensive differences in anatomy and physiology (Derricott et al., 2019).

BCoV has not been cultured in an organoid model to date. However, human and mouse intestinal and lung organoids support the complete life cycle of *C. parvum* and have been utilized to study transcripts regulated in different life cycle stages (Heo et al., 2018).

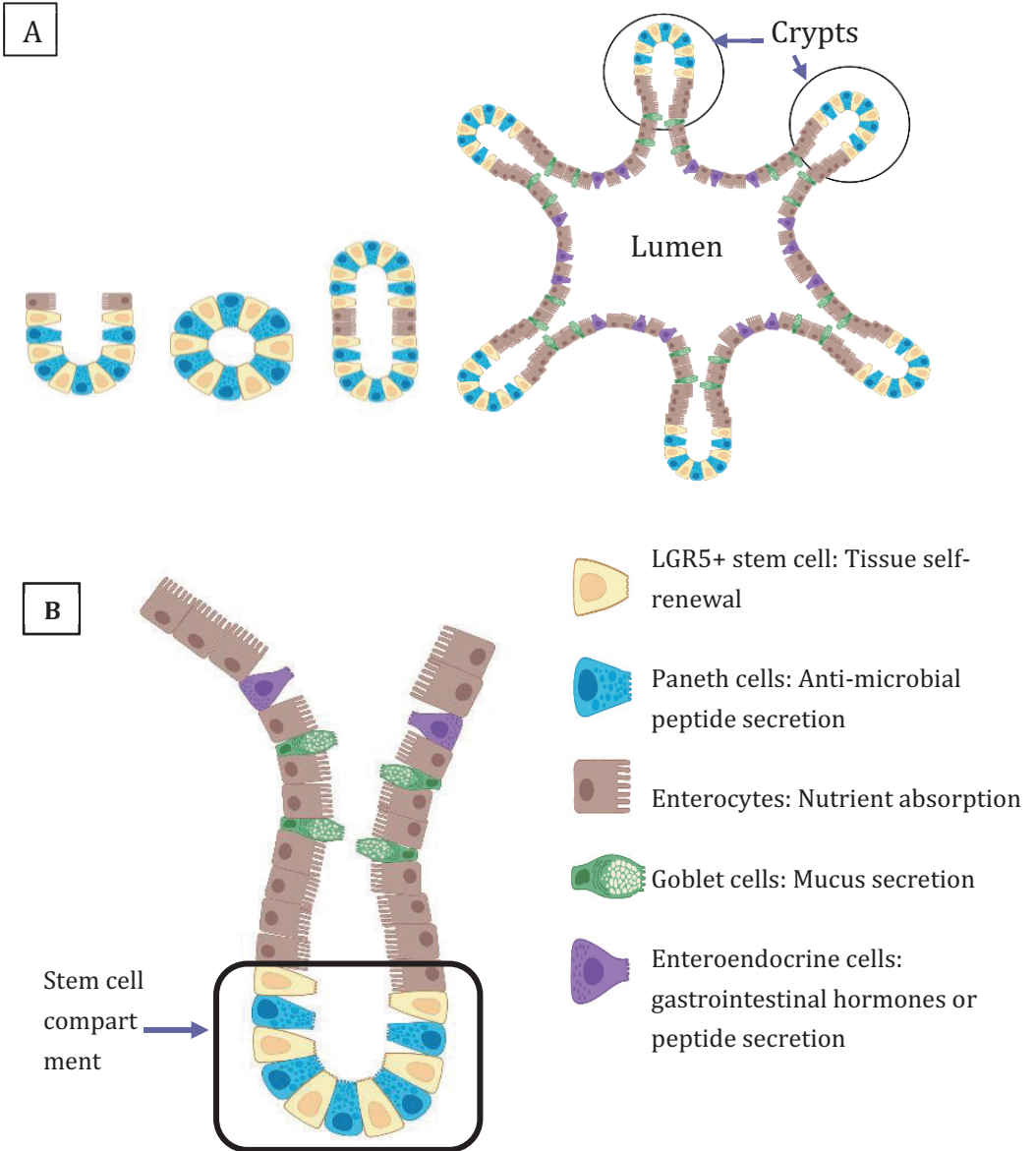


Figure 4: (A) Organoid structure with layers of different epithelial cells enclosed in a lumen with finger-like crypts at the tip. (B) Intestinal epithelium that is comprised of a diverse cell population with Paneth and stem cells localized at the bottom of the crypts. Other cells such as enterocytes, goblet cells, enteroendocrine cells are found towards the lumen upon differentiation, while tuft cells have not been detected in bovine epithelium (Source: Created in BioRender).

Credit: Ruchika Shakya

5.5 *In vivo* studies

Various animal experiments on cattle and mice have been carried out as natural models to study the pathogenesis of BCoV and *C. parvum*.

Replication and pathogenesis of BCoV diarrhoea have been studied in calves (Mebus et al., 1973; Saif et al., 1986; Tråvén, 2000; Oma et al., 2016). Aich et al., (2007) utilized the intestinal loops from BCoV-infected calves to study innate immune response. The pathogenicity of *C. parvum* has been studied in mice (Tyzzer, 1912; Hampton and Rosario, 1966). Mouse models, however, lack bovine-specific responses and mice are not the natural hosts of BCoV or *C. parvum*. *In vivo* models are essential to study clinical signs, shedding, and infectiousness to calves. Nevertheless, *in vivo* models are expensive, require larger facilities, and are labour intensive. At the same time, one must consider ethical and animal welfare aspects before proceeding with such experiments.

For the experimental study of BCoV and *C. parvum* in animals, calves are more commonly used than adult cattle. The reason for choosing calves is the pathogens predominantly infect young calves and makes it cost-efficient for the purchase and enclosure.

6 Knowledge gaps

Despite previous studies demonstrating the occurrence of bovine coronavirus and *Cryptosporidium parvum* as frequent enteropathogens in mixed/co-infections that result in calf diarrhoea, none have specifically addressed the potential interplay between these two enteric pathogens and the host cell during co-infections. To address this knowledge gap, we employed an *in vitro* system, utilizing HCT-8 cells and bovine enteroids as simplified models to examine pathogen-pathogen interactions, host-pathogen interactions, and potential mechanisms associated with pathogenicity. Additionally, although *in vitro* models have been utilized to study the host response to *C. parvum* infection, there are no such studies regarding BCoV infection. Hence, comparing the host response between single infection with BCoV and *C. parvum* and co-infection using *in vitro* models could elucidate any potential synergistic or antagonistic effects. Subsequent investigations that recapitulate the *in vitro* findings in a more intricate model (using the enteroid system with a heterogeneous cell population), could be relevant for studying the pathogenesis of calf diarrhoea during co-infection.

7 Aims of the study

General objectives: To use *in vitro* models to study the interplay between bovine coronavirus (BCoV) and *Cryptosporidium parvum* (*C. parvum*) during infection and their possible effects on the host.

Specific objectives:

1. To study BCoV and *C. parvum* interactions during infection of the HCT-8 cell line (Paper I)
2. To compare the host response during single and co-infections with BCoV and *C. parvum* in HCT-8 cells (Paper II)
3. To establish bovine enteroids as a culture system for BCoV (Paper III)
4. To characterize the enteroid cell population and compare expression of selected genes during BCoV infection in HCT-8 cells and bovine enteroids (Paper III).

8 Materials and methods

The materials and methods for papers I, II and III are described in detail within the respective papers and manuscripts and are discussed in the section methodological considerations of this thesis.

A brief overview of the materials and methods used in the different studies is provided below:

Paper I

Interactions between *Cryptosporidium parvum* and bovine corona virus during sequential and simultaneous infection of HCT-8 cells

Research question

Is there any interplay between BCoV and *C. parvum* during infection of HCT-8 cells?

Experimental study design

- HCT- 8 cells were inoculated with: (1) BCoV and *C. parvum* sequentially and simultaneously, (2) positive controls (BCoV or *C. parvum*), (3) negative controls (medium only).
- Samples were harvested at 1 hour post inoculation (hpi) and 24 hpi
- Relative numbers of BCoV or *C. parvum* genome copies were measured

Laboratory techniques

- Total RNA isolation
- (RT)-qPCR
- Flow cytometry
- Immunostaining

Data analysis and statistics

- Statistical methods: Two-sided Mann-Whitney U-test

Paper II

Gene expression profile of HCT-8 cells following single or co-infection with *Cryptosporidium parvum* and bovine coronavirus

Research question

How does the HCT-8 cell mRNA response to BCoV and *C. parvum* differ during single and co-infections?

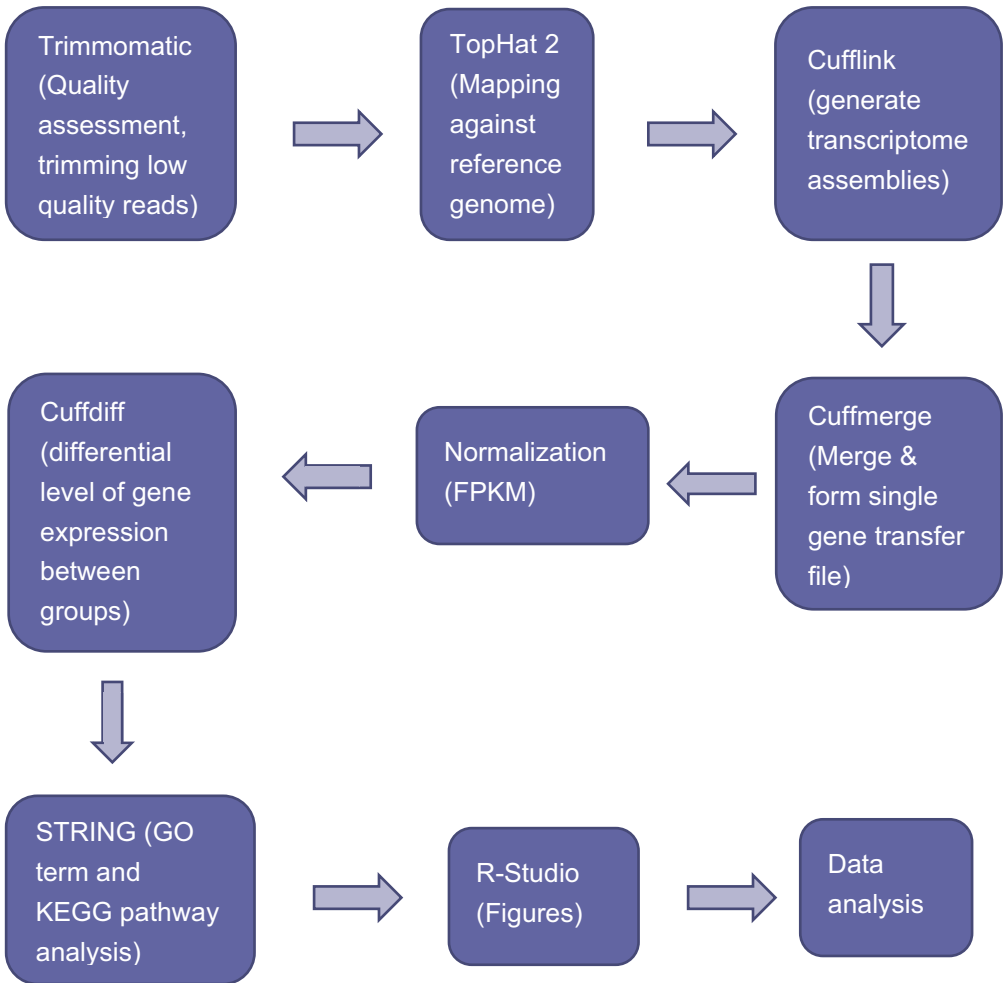
Experimental study design

- HCT- 8 cells were inoculated with (1) BCoV, (2) *C. parvum*, (3) BCoV and *C. parvum* (4) medium only
- Four experimental groups with 12 replicates
- Harvested at 24 and 72 hpi
- Analysis of mRNA expression

Laboratory techniques

- Total RNA isolation
- RNASeq: Illumina Novaseq 6000 with paired-end sequencing at 50 bp
- Immunostaining

➤ **RNASeq pipeline:**



Picture credit: Ruchika Shakya

Paper III

Bovine enteroids as an *in vitro* model for infection with bovine coronavirus

Research questions

Can bovine enteroids be used as an *in vitro* replication system for BCoV? What is the expression status of selected genes in bovine enteroids as compared to HCT-8 cells during BCoV infection?

Experimental study design

- Isolation of intestinal stem cells and culture of bovine enteroids
- Preparation of several media to test for differentiation of enteroids
- Enteroids inoculated with BCoV
- Analysed after 1 and 72 h for quantification of viral RNA
- Comparison of gene expression in the enteroids to the HCT-8 cell line (RNASeq results from Paper II)

Laboratory techniques

- Preparation of differentiation media
- Total RNA isolation
- One step TaqMan RT-qPCR (BCoV RNA quantification)
- Immunostaining for cell differentiation markers and BCoV S-protein
- cDNA synthesis and SYBRGreen qPCR (gene expression analysis)

Data analysis and statistics

- One-sided Mann-Whitney U-test, for BCoV RNA quantities
- Calculation of relative gene expression using the Pfaffl method
- Pair-wise fixed reallocation randomization test with at least 2000 randomizations performed using REST software 2009 for relative gene expression analysis.

9 Methodological considerations

9.1 2D cell culture

BCoV and *C. parvum* both infect the enterocytes of the small intestine and there are few available cell lines that support the growth of both. The HRT-18G cell line (human origin) has been recommended for the culture of BCoV as the cells have been selected for increased permissiveness for the virus (Da Silva et al, 1999). The viral strain used in papers I and II originated from a faecal sample and was already isolated in HRT-18G cell.

The HRT-18G cells, however, are less commonly used to study *C. parvum* as they support limited growth, and only the asexual cycle (Arrowood, 2002). The growth (asexual cycle) is nearly double for several *Cryptosporidium spp* in HCT-8 cell line and is preferable to several other cell lines (Hijawi, 2010). The two cell lines (HRT-18G and HCT-8) has a common origin as they were isolated from the colon of an adenocarcinoma patient (Vermeulen et al., 1998). We decided to use HCT-8 cells to optimize the conditions for *C. parvum* and adapt our BCoV by passing the virus on the HCT-8 cells. The MDBK cells, which are also permissive to both pathogens, gave a lower virus titre (personal communication).

The use of a human cell line in paper I and II, might not have been optimal. If commercial cell lines are preferred for future work, bovine cell lines permissive for both pathogens need further exploration.

9.2 3D cell culture – Bovine enteroids

Despite the informative insights into pathogen-pathogen interactions (Paper I) and host-pathogen interactions (Paper II) gained from the *in vitro* investigation using HCT-8 cells, this epithelial cell line is not a comprehensive representation of the composition and heterogeneity of intestinal epithelial cells. Enteroids with a heterogenous cell population were therefore included as a possibly better model to study host-pathogen interactions during infection with BCoV and *C. parvum*.

An extracellular matrix (such as Matrigel) encloses the 3D enteroids and is permeable to the supplied nutrients, but the apical surface of the epithelium lies inside a closed

unit making it inaccessible for added pathogens (Sutton et al., 2022; Derricott et al., 2019; Hamilton et al., 2018). Although we originally aimed to establish a protocol for infection of organoids with *C. parvum*, followed by a co-infection study, this could not be performed due to time constraints.

Although, we were successful in infecting the enteroids with BCoV, we encountered several other difficulties that have been discussed in detail in paper III.

The use of organoid systems is constrained by several factors, such as ensuring equal cell distribution among samples and the difficulty in enabling access of pathogens to the permissive cells' apical surface. To surmount these limitations, one possible strategy is growing the differentiated enteroids in 2D monolayers, as outlined in a recent investigation by Sutton et al. (2022).

To make 2D monolayers, organoids were disrupted by pipetting and seeded in 24-well plates coated with collagen I (bovine, Sigma Aldrich) or Matrigel (Fig 5). The enteroids grown using Matrigel formed confluent monolayers and survived for 7-10 days while those grown on collagen started to detach and degrade after 5-7 days of culture. The Matrigel sheets were further inoculated with BCoV, and we observed two rounds of successful viral replication. However, further attempts failed, and we did not manage to resolve the problem.

Another approach could be microinjection of the pathogen into the lumen of the enteroids. However, microinjection is laborious, time-consuming, and complicated, and requires specialised equipment. Another approach to increase access to target cells could be to use reverse polarization, where the apical surface is on the outside of the organoids and thus easily accessible (Co et al., 2021). Apical-out enteroids have a limited lifespan and therefore requires flipping them back again after exposure. The advantages include homogenous exposure of the apical part of the enteroids to the pathogen (Seeger, 2020). The apical-out approach has recently been performed on bovine enteroids (Blake et al., 2022).

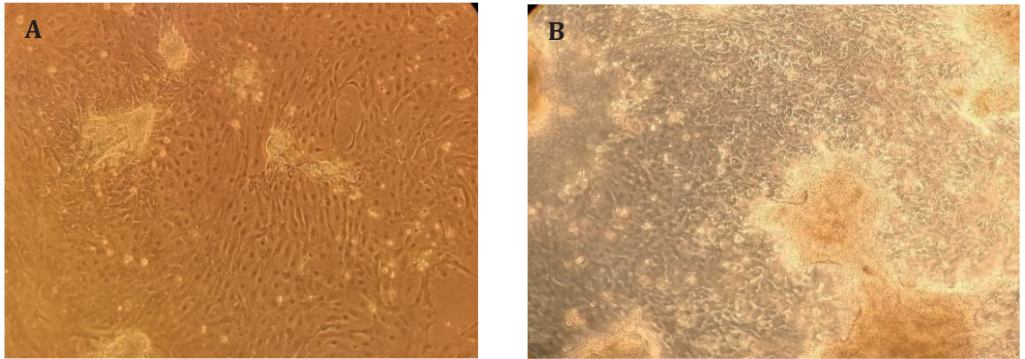


Figure 5: Epithelial sheets formed after 5 days in wells coated with: A. Collagen and B. Matrigel.

Picture credit: Alejandro Jimenez Meléndez and Ruchika Shakya

9.3 Nucleic acid extraction

There are several methods available to isolate nucleic acids. In Paper I, viral RNA and *C. parvum* DNA were co-extracted. The Nuclisens miniMag protocol, based on a silica bead magnetic-separation technique, can be used to isolate total nucleic acids. With this method the lysis buffer is added directly onto the infected cells and mixed well before the extraction procedure.

A treatment step to remove DNA is necessary for studying gene expression to eliminate amplification of genomic DNA (gDNA). In Paper II, total RNA was isolated from the cell lysates using QIAGEN RNeasy Mini Plus Kit, including a homogenization and gDNA elimination step. Similarly, DNase treatment of the RNA was incorporated in Paper III.

9.4 (RT)-qPCR

Realtime PCR (qPCR) is a method to detect and quantify specific nucleic acids. qPCR utilizes fluorescently labelled probes or dyes to measure the relative amounts of PCR products formed. It is highly sensitive, relatively fast as it avoids post-PCR analysis (electrophoresis), high-throughput, and multiplexable (Pestana et al., 2010, Csako, 2006). In reverse transcription quantitative PCR (RT-qPCR), RNA is reverse transcribed to cDNA before qPCR. It is routinely used in diagnosis of viral/parasitic infections, gene expression analysis, and genetic testing (Logan et al, 2009). The

fluorescently labelled methods of qPCR could be probe-based, such as TaqMan probe, a hydrolysis probe that emits fluorescence when the reporter dye is freed on cleavage by the 5' exonuclease activity of Taq-polymerase during elongation of the DNA strand (Dorak, 2006). In Paper I, TaqMan probe-based method was used for relative quantification of pathogen genomes. An alternative is SYBR green I that emits 1,000-fold greater fluorescence when bound to the minor groove of DNA than when it is free in solution (Valasek and Repa, 2005) but may generate false positives due to non-specific bindings. The specificity of the qPCR can be assessed by analysing the dissociation curve to find the specific melting temperature (T_m) of the amplicon. Primer design (e.g., intron-spanning primers) is considered in RT-qPCR-based assays aimed at gene expression analysis to eliminate amplification of gDNA. SYBR green RT-qPCR was used for the gene expression study in paper III as a simple and cost-effective approach, as it does not require the probes.

Limitations of (RT)-qPCR include the risk of false positive/negative results and end-point variations if the number of target molecules is very low. Therefore, to reduce false positive (cross contamination) or negative results, appropriate controls are included in each run.

9.5 Flow cytometry

Flow cytometry was carried out to study the proportion of cells infected with virus and/or Crypto (Paper I). It is recommended to use brighter fluorochromes for antigens with low or unknown expression. Also, one should be careful while choosing the fluorochromes to minimize spectral overlap. In the present study, cell aggregates were run through a 40 μ m strainer in order to obtain single cells. However, BCoV-infection leads to formation of cell syncytia, which are larger in size and some of these syncytia might have been retained in the strainer and lost for the flow analysis.

Flow results in Paper I revealed a low fraction of cells infected with BCoV and *C. parvum* of approximately 10-20% and 1-11%, respectively, and only 0.04% of cells that were double-infected.

9.6 Immunostaining

In Paper I and Paper II, HCT-8 cells infected with BCoV and *C. parvum* were stained to visualize single infected/co-infected cells. The cells were stained using anti-BCoV monoclonal antibodies raised against the spike (S) protein. Sporoglo™ is a commercially available antibody and consists of polyclonal rat IgG antibody that binds to sporozoites, merozoites, and all other intracellular reproductive stages of *C. parvum*. In Paper III, enteroids infected with BCoV were also stained for some cell differentiation markers as described in the paper. Furthermore, there are few commercially available cell-specific markers for bovine cells or that have been described so far.

9.7 Transmission electron microscopy

In experiments associated with Paper I, transmission electron microscopy (TEM) was carried out by Antje Hofgaard at University of Oslo (UiO). One intention was to utilize TEM to find any physical interaction between BCoV and *C. parvum* sporozoites following co-incubation. However, glutaraldehyde was necessary as a fixative, which creates adhesive properties (i.e., “sticky”) in the virus and sporozoites, thus posing a risk of creating spurious bindings that may result in false-positive outcomes. Therefore, we excluded this analysis, but used TEM to study infected cells.

At 24 hpi, we expected to see viruses that had replicated in the cytoplasm and trapped viruses inside the PV, and some trophozoites/meronts of *C. parvum* around the edges of the cell membrane. At 72 hpi, we anticipated to see different stages of *C. parvum* inside the infected cells near the cell membrane. While the identification of viral particles in the cytoplasm was relatively straightforward, the localization and identification of *C. parvum* proved challenging. The low proportion of infected cells may have contributed to this difficulty. The utilization of staining techniques or fluorescent markers could have been more effective for localizing parasite-infected cells. Nevertheless, we were able to identify *C. parvum* contained within the parasitophorous vacuole located at the periphery of HCT-8 cells at 24 hours post-infection (fig 6).

9.8 RNA sequencing (RNASeq)

In Paper II, RNASeq was utilized to explore the host response at the gene expression level, following single or co-infection with BCoV and *C. parvum*. These analyses were done in five steps: (i) design of experiment, (ii) sample preparation and library generation, (iii) next-generation sequencing of libraries, (iv) assembly, annotation, and determination of read count, and (v) assessment of RNASeq data quality, requiring a quality score greater than 30.

A proper experimental design with adequate number of replicates (six in our case), library type, and sequencing depth is essential to answer the biological question of interest. The greater number of replicates used in the experiment reduces the noise that may be introduced by technical variability between experiments, RNA extraction, and library preparation. This also provides a better opportunity to determine statistically significant differences in gene expression between experimental groups. Two different time points of 24- and 72-hours post inoculation (hpi) were part of the experimental design. By 24 h BCoV would have completed a replication cycle and there would be trophozoites/meront I of *C. parvum*. And, at 72 hpi there would be several asexual life cycle stages (merozoites, meront I, meront II) of *C. parvum*.

Most library preparations, as in our study, include a depletion step for ribosomal RNA (rRNA) which comprises 90% of the total RNA. Then fragmentation of RNA follows before cDNA synthesis. Library preparation can be strand-specific or non-directional or opposite-strand specific. In our case, it was strand-specific, which allows assignment of the reads to their original strand. One of the approaches is by attaching different adapter sequences in a known orientation relative to the 5' and 3' ends of the RNA transcript. The subsequent reverse transcription and amplification create a cDNA library flanked by two distinct adapter sequences, whereby the orientation of the adapters for the original mRNA is known. From now on it is possible to assign the produced reads for mapping.

One limitation of RNASeq is when few cells are infected, differential gene expression results are being lost among the background of a large population of uninfected cells. In such cases single-cell RNASeq could be a better approach. Given that RNASeq only confirms gene expression at the RNA-level it would be advantageous to perform a subsequent analysis at the proteomics level.

9.9 Bioinformatic analysis

In Paper II, bioinformatic analysis was performed by Shokouh Makvandi-Nejad on raw sequence reads. Trimmomatic was used for trimming the adapters, low quality

reads and quality assessment. The sequences were then mapped against the reference *Homo sapiens* genome using TopHat 2. It is essential to choose the most complete version of reference genome as the transcript assemblies are later generated based on it. Cufflinks was used to generate transcriptome assemblies from the mapped reads and Cuffmerge to merge the defined transcripts and form a single gene transfer file. Cuffdiff was used for differential gene expression. String version 11.5 (<https://string-db.org/>) was used for functional analysis including KEGG pathway and GO term enrichment analysis. The figures for the manuscript were plotted in R-studio. Although, some of the analysis showed more than 6000 differentially regulated genes, pathway analysis could only be performed with the top 2000 genes ranked by fold change due to the limitations in the software tool that was employed.

9.10 Statistical analysis

In Paper I, two-way Mann-Whitney test was chosen since we wanted to find any difference in viral/*C. parvum* copy numbers between single and co-inoculated cells. In Paper III, one-way Mann-Whitney test was used as the hypothesis was that enteroids inoculated with BCoV would show an increase in viral copy number from 1 to 72 hpi.

In Paper III, relative gene expression ratios were calculated using REST software (Pfaffl method) to assess whether there are statistically significant differences between BCoV-infected and the mock-infected samples by introducing randomization and bootstrapping techniques. The Pfaffl method considers the different reaction efficiencies where the targeted genes are normalized to multiple housekeeping genes. The hypothesis test performs many random reallocations of BCoV infected and mock-infected samples between the groups. It then counts the number of times the relative expression of the randomly assigned group is greater than the sample data.

In Paper II, the Cuffdiff method for normalization uses the t-test analogical method to test the changes in gene expression between different groups.

10 Results

All the results are discussed in detail in the papers, and the main findings from each article are presented here, together with some additional information that has not been included in the published articles.

10.1 Bovine coronavirus attaches to *C. parvum* during co-inoculation (Paper I and additional results)

Sequential inoculation of HCT-8 cells with the two agents did not show any effect of one pathogen on the other regarding replication. During simultaneous inoculation, entry of viral particles was higher at 1 hpi (approximately three-fold) in the presence of *C. parvum* sporozoites. However, the difference in viral RNA level (*w/wo* sporozoites) was no longer evident after 24 h. Two other viruses, equine herpes virus-1 (enveloped) and bovine norovirus (naked), were included in the study to investigate whether an attachment could be observed between these viruses and *C. parvum* sporozoites. There was no indication of any attachment for these two viruses. Immunostaining of co-inoculated cells showed an increase in foci of infection for both pathogens from 24 to 72 hpi, with a few double-infected cells. Flow cytometry corroborated a low percentage of double-infected cells. TEM results showed viral particles in the cytoplasm and the endoplasmic reticulum at 24 and 72 hpi, respectively (Fig 6A and B). *C. parvum* enclosed in parasitophorous vacuole was also detected at 24 hpi (Fig 6C).

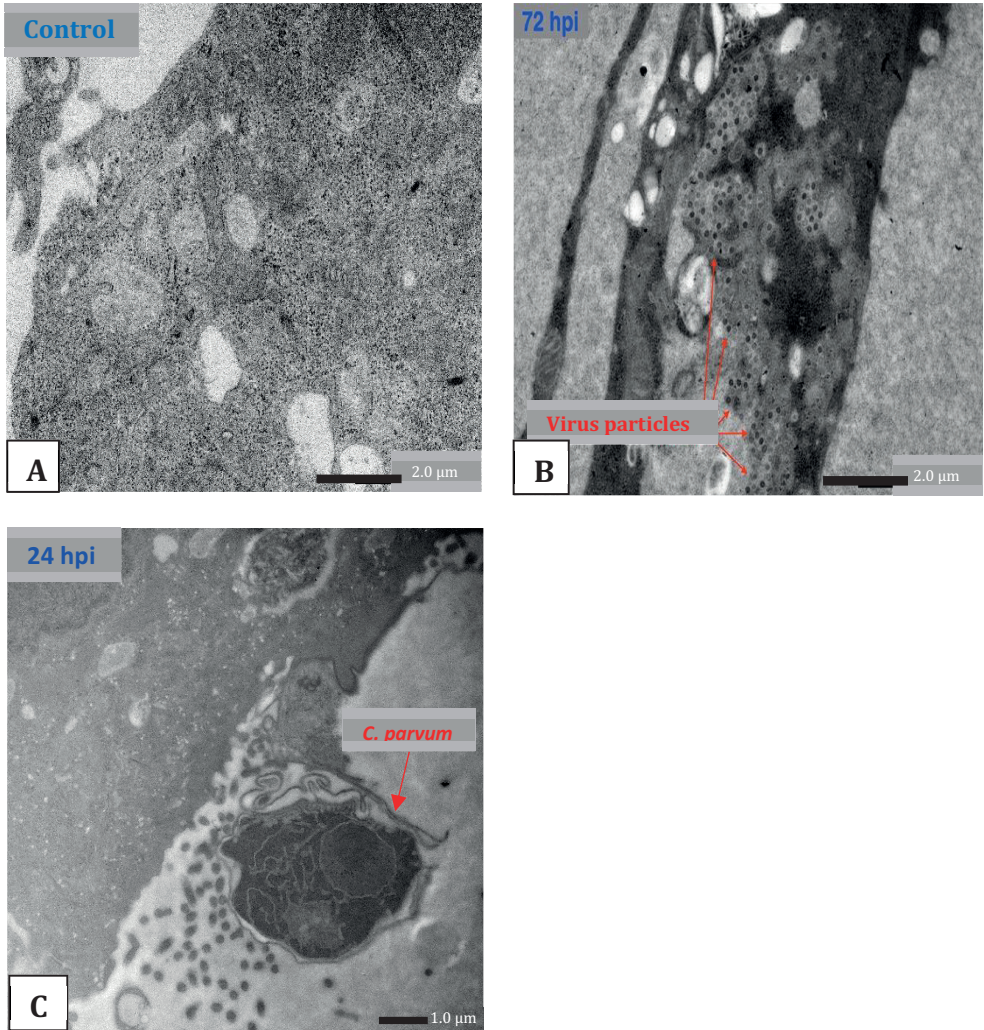


Figure 6: Transmission electron micrographs (TEMs) of HCT-8 cells: (A) Uninfected (Control). (B) infected with BCoV at 72 hpi. Arrows in (B) show virus particles in the endoplasmic reticulum. (C) *C. parvum* enclosed inside parasitophorous vacuole at 24 hpi and viral particles released from the cell. Scale bars in A and B = 2.0 μm ; C = 1.0 μm .

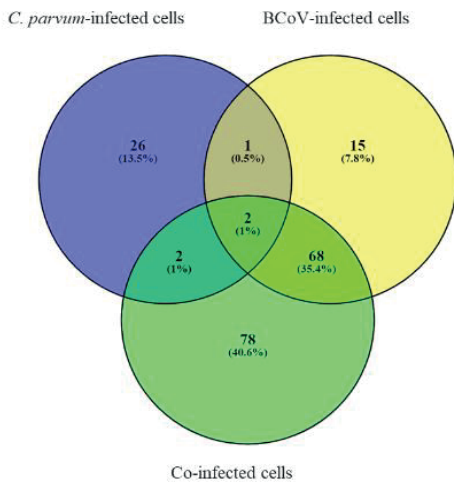
Picture credit: Antje Hofgaard, Lene Cecilie Hermansen and Ruchika Shakya

10.2 Marked pro-inflammatory response in BCoV- and co-infected HCT-8 cells (Paper II - Manuscript under review)

Around 40 million reads per sample were generated and 86% were mapped against the *Homo sapiens* reference genome indicating sequencing accuracy.

As shown in figure 7, the number of DEGs for BCoV, *C. parvum*, and co-infected cells at 24 hpi were 86, 31, and 150, respectively. The host response of BCoV- and co-infected cells at 72 hpi showed more than 6000 DEGs, whereas only 52 DEGs were identified in *C. parvum*-infected cells. Interestingly, 78 and 803 genes were uniquely expressed during co-infection, at 24 and 72 hpi, respectively.

A. 24 hpi



B. 72 hpi

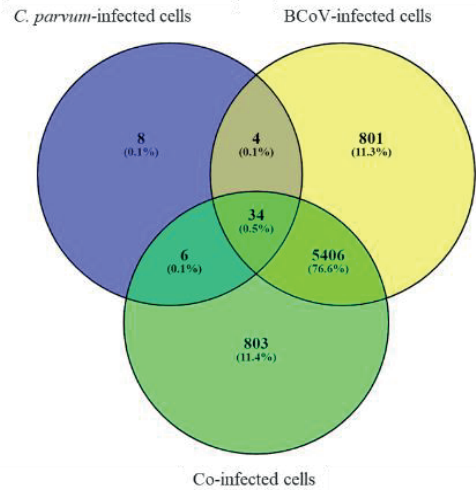


Figure 7: Venn diagrams with number of differentially expressed genes in the three infection setups at (A) 24 and (B) 72 hpi.

Picture credit: Shokouh Makvandi-Nejad

Genes with the highest fold change for BCoV-, *C. parvum*-, and co-infected cells, at 24 and 72 hpi are shown in Table 1.

Table 1. Differentially expressed genes with the highest fold change (FC) for BCoV, *C. parvum* and co-infected cells at 24- and 72-hours post inoculation (hpi).

Genes	BCoV (FC)		<i>C. parvum</i> (FC)		Co-infected (FC)	
	24 hpi	72hpi	24 hpi	72 hpi	24 hpi	72 hpi
<i>ANKRD1</i>	34.7	-	-	-	48.14	-
MTATP6P1	-	-	2.96	-	-	-
<i>IL-8</i>	-	323.8	-	-	-	268.5
<i>EGR-1</i>	-	-	-	6.22	-	-
<i>NR4A3*</i>	-	-	-	-	4.12	-
<i>DNAH17*</i>	-	-	-	-	-	55.2

*genes exclusively expressed during co-infection

At 24 hpi most GO-terms for BCoV-infected cells belonged to immune processes, such as cytokine-mediated signalling pathways, inflammatory response, cell chemotaxis, and response to IL-1. There was limited immune response against *C. parvum* as most of the GO terms belonged to metabolic categories, such as response to purine-containing compounds or hepxilin biosynthesis. For co-infected cells a notable similarity to that of BCoV-infected cells was found, with the majority of pathways belonging to the immune response category. At 72 hpi, there was enrichment of GO terms related to apoptotic processes and to immune responses for the BCoV-infection. For *C. parvum*-infected cells, the GO terms were still related to metabolic processes, along with cell death and responses to oxygen-containing compounds. Again, the co-infected cells had a pattern like that of BCoV-infected cells, with more enriched GOs associated with immune system processes, such as regulation of cytokine production, regulation of I-kappaB kinase/NF- κ B signalling and IL-1 mediated signalling pathway (shown in detail in Paper II). Regarding the enriched KEGG pathways, MAPK, TNF, NF- κ B, and IL-17 were assessed further based on the biological significance. Several components of the pathways (MAPK, TNF, NF- κ B, IL-17 and apoptosis) for BCoV-, *C. parvum*-, and co-infected cells, at 24 and 72 hpi as shown in Table 2, were modulated.

Table 2. Differentially expressed genes related to several pathways in BCoV-, *C. parvum*-, and co-infected cells at 24- and 72-hours post inoculation (hpi).

Pathways	Differentially expressed genes (DEGs)					
	BCoV infected	<i>C. parvum</i> infected	Co-infected	24 hpi	72 hpi	
MAPK	<p>24 hpi</p> <p><i>EREG, IL1A, GADD45A, DUSP2, MAP3K14, DUSP1, FOS, DDIT3</i></p> <p>upregulated.</p>	<p>72 hpi</p> <p>49 genes upregulated including <i>MAP3K8</i>.</p>	<p>24 hpi</p> <p><i>VEGFA, JUN</i></p> <p>upregulated.</p>	<p>72 hpi</p> <ul style="list-style-type: none"> <i>GADD45B, DUSP1, DUSP6, FOS, DUSP5, JUN</i> and <i>IGF2</i> upregulated. p38/Mapk, MAP kinase-activated protein kinase 2 (<i>MK2</i>), and <i>Mk3</i> genes downregulated. 	<p>24 hpi</p> <p><i>EPHA2, MAP3K8, DUSP4, JUNN</i></p> <p>upregulated.</p>	<p>72 hpi</p> <p>55 genes upregulated including <i>MAP3K8</i></p>
TNF	<p><i>MAPK3K14, FOS, CREB5, CXCL2, EDN1 PTGS2</i></p> <p>upregulated.</p>	<ul style="list-style-type: none"> Chemokines (<i>CXCL4, CXCL5</i>); genes responsible for the activation of immune cells (<i>CSF1</i>); surface receptors (<i>JAG1</i>); <i>MAPK; BIRC2; RIPK1</i> (necrosome); molecules responsible for cell adhesion: <i>ICAM1; TRAF3; CHUK; IKBKg; NF-κB1 / NF-κBIA</i> 	<p><i>MAPK12, JUN</i></p> <p>upregulated.</p>	<p><i>MAPK10</i> downregulated.</p>	<p><i>TNFAIP3</i></p> <p>upregulated.</p>	<ul style="list-style-type: none"> <i>TRAF2</i> and <i>CX3CL1</i> were upregulated. <i>RIPK3</i> was downregulated.

		<p>(NF-κB inhibitors); <i>ATF4</i>, <i>CEBPB</i>, <i>IRF1</i> upregulated.</p> <ul style="list-style-type: none"> Among downregulated genes, several genes involved in the MAPK pathway were found, such as <i>MAPK9</i>, <i>MAPK11</i>, <i>MAPK3</i>, <i>AKT1</i>, <i>DAB2IP</i>. 				
NF-κB	<p><i>MAPK3</i><i>K14</i>; <i>GADD45A</i>; <i>PTGS2</i>; <i>CXCL2</i> upregulated.</p>	<ul style="list-style-type: none"> sensors of DNA damage such as <i>IKBKg</i>, <i>UBE21</i> (sumoylation), <i>RIPK1</i>; inflammation (<i>DDX58</i>) and canonical and non-canonical pathways for hypoxia were upregulated. <i>EDA/EDAR</i>, which mediate the activation of NF-κB and JNK, 	-	-	<p><i>TNFAIP3</i> upregulated.</p>	<p><i>TRAF2</i> upregulated.</p>

		surface marker <i>CD14, TIRAP, PRKCQ</i> were downregulated.				
IL-17	<i>FOS, CXCL2, PTGS2</i> upregulated.	<ul style="list-style-type: none"> <i>FADD, TRAF3, 2TRAF6, NF-κB1, TBK1, USP25, HSP90AA1, TAB2, MAP3K7, IKBK, CHUK, NF-κBIA, CEBPB, CXCL1, CXCL5,</i> and matrix metalloproteases, such as <i>MMP1</i> and <i>MMP13</i> upregulated. <i>IL17RB, MAPK3, LCN2</i> downregulated. 	<i>JUN, MAPK12, TRAF4</i> upregulated.	<i>MAPK10</i> downregulated.	<i>TNFAIP3, FOSB</i> and <i>MAPK6</i> upregulated.	<i>TAB3, TRAF2</i> upregulated.
Apoptosis	<i>MAP3K14, DDIT3, EIF2AK3, FOS, GADD45A</i> upregulated.	<ul style="list-style-type: none"> Upregulation of pro-apoptotic genes (<i>BAK1, TNFSRF10B, PMAIP1</i>) and pro-survival genes (<i>GFLAR, BIRC-2</i>); key apoptotic genes- <i>CASP7, B-cell</i> 	-	<ul style="list-style-type: none"> <i>MAPK10</i> downregulated 	<i>MCL1</i> upregulated.	<ul style="list-style-type: none"> Upregulated: <i>CASP7, B-cell lymphoma (BCL) class genes: TRAF2, PIK3CA.</i> Downregulated: <i>CASP8AP2</i> (involved in the

		<p>lymphoma (BCL) class genes upregulated.</p> <ul style="list-style-type: none"> Downregulated: cellular tumour antigen <i>tp53</i>; <i>CASP2</i>, <i>CASP6</i>; <i>DAB2IP</i>, <i>MAPK9</i>; pro-apoptotic genes such as <i>BBC3</i>; <i>BCL7a</i>, <i>BCL11A</i>, <i>BCL2L15</i>, and <i>BCL2L14</i>. 			<p>TNF-α induced activation of NF-κB), <i>CASP5</i> (initiation of pyroptosis, regulation of antiviral innate immune activation), <i>CASP6</i>, <i>CASP2</i> (involved in the initiator phase), and <i>CASP4</i> (involved in inflammation); cellular tumour antigen <i>tp53</i>, <i>BCL7a</i>, <i>BCL11A</i>, <i>BCL2L15</i>, and <i>BCL2L14</i>.</p>
--	--	---	--	--	--

Numerous genes associated with **proinflammatory responses** were highly upregulated in BCoV- and co-infected cells at 24 and 72 hpi. For BCoV-infection some were associated with IFN-I induction and signalling. Interferon-stimulated gene 15 (*ISG-15*) was upregulated at 24 hpi in BCoV-infected cells. Most of the expression of ISGs was the same between BCoV and co-infected cells at 72 hpi except for *OAS3* and *ISG20L2* which were only expressed in co-infected cells. Also, interferon-responsive elements such as *IFITM1*, *IFITM2*, *IFITM3*, and *IFI27* were downregulated in both BCoV and co-infected cells. IL-1A, was also upregulated in virus and co-infected cells at both 24 and 72 hpi, together with tumour necrosis factor receptors (*TNFRs*), *TNFRSF12A*, *TNFRSF18*, and chemokines such as *CXCL2*, *CXCL8 (IL8)*, and *CXCL3*. At 72 hpi, there was modulation of both anti-inflammatory and proinflammatory genes to counteract BCoV infection. Meanwhile, toll-like receptors (TLRs) such as *TLR3* and *TLR5* were downregulated, whereas *TLR6* was upregulated in BCoV-infected cells at 72 hpi. Moreover, the expression of *DDX58*, *OASL*, and *ISG20* was increased in BCoV-infected cells at 72 hpi. *MT2A* (metallothioneins 2) and *GBP3* (guanylate-binding protein 3) were upregulated in co-infected cells at 24 hpi. Regarding the modulation of host cytoskeleton activities, there was upregulation of lectins, C-type lectin (*CLEC4*) and *IKBKG* in BCoV-infected cells at 24 hpi. Mucin-related genes were also modulated. *MUC5AC* was downregulated in *C. parvum*-infected cells at 72 hpi. In co-infected cells, heat -shock protein 90 (*hsp 90*) was upregulated, while keratin type I cytoskeletal was downregulated at 24 hpi. Similarly, in co-infected cells at 72 hpi, *CLEC4A*, *IKBKG*, and mucins (such as *MUC13*, *MUC20*, and *MUC4*) were upregulated.

10.3 Bovine enteroids are permissive for BCoV (Paper III and additional results)

Bovine organoids were cultured and maintained in IntestiCult media. Three other media as described in detail in Paper III were prepared for the differentiation of enteroids, but with no success. Differentiated enteroids supported viral replication, which was observed as a seven-fold increase in viral RNA and by immunostaining of the viral S-protein. Enteroid cultures comprised intestinal stem cells and differentiated populations of epithelial cells, including enterocytes, and enteroendocrine cells detected by immunostaining. The markers for stem cells (LGR5+) and enteroendocrine cells (ChrA) were upregulated, while the goblet cell marker (Muc-2) was downregulated during infection. The pro-inflammatory genes interleukin (IL)-8 and IL-1A, showed no differential expression in BCoV-infected enteroids while these genes were highly upregulated in infected HCT-8 cells (Paper

II). The immune genes matrix metalloprotease-13 (MMP13), chemokine ligand 3 (CXCL-3), and tumour necrosis factor alpha (TNF- α) were downregulated in the infected enteroids but upregulated in infected HCT-8 cells (Paper II).

In addition to the results described in paper III, enteroids were also grown as 2D epithelial sheets on collagen and Matrigel (Fig 5). The enteroids grown on Matrigel formed confluent monolayers and survived for 7-10 days, while on collagen they started to detach and degrade after 5-7 days of culture. The cells on Matrigel were further inoculated with BCoV and in two setups, there was a 4-fold increase in viral RNA after 72 h this approach was, however, discontinued after two additional repetitions as viral replication was no longer evident.

11 Discussion

Bovine coronavirus (BCoV) and *Cryptosporidium parvum* both infect enterocytes and cause severe diarrhoea in neonatal calves. In prior *in vitro* studies, HCT-8 cells were utilized to investigate these pathogens separately (Kapil 1991; Meloni and Thompson, 1996). Nevertheless, no exploration has been undertaken using *in vitro* tools to assess the interactions between these two pathogens.

Paper I explores interactions between BCoV and *C. parvum* using HCT-8 cells as an *in vitro* model. During sequential inoculation of the cells, prior inoculation with one pathogen did not have any effect on replication of the other or the difference was not statistically significant. Perhaps, incorporating more replicates could have made any difference clearer. For co-inoculation, the two pathogens were co-incubated at 37 °C for an hour before inoculating them onto the cells. We speculated that this would permit the pathogens to interact, as may occur in the intestinal tract of calves. It could be argued that such incubation step might have a negative effect on *C. parvum* sporozoites as the viability has been observed to decrease from 89 to 56% at 3h post-excystation (Matsubayasi et al., 2010). However, in the present study 85-90% of the excysted sporozoites were not stained with trypan blue and showed motility, prior to inoculation. When co-incubated with BCoV, the results at 1 hpi indicated an attachment of BCoV to the sporozoites meaning that more virus particles could enter the cells. Nevertheless, the higher level of viral RNA in the cells in presence of *C. parvum* sporozoites was no longer evident at 24 hpi suggesting that the mode of internalization was not beneficial for the virus. Co-incubation using a lower concentration of virus could have given a clearer indication of attachment showing a larger difference between controls and samples. We speculate that the attached viruses were trapped inside the parasitophorous vacuole, the location of *C. parvum* replication and development, and hence unable to reach the cytoplasm and replicate. To strengthen our hypothesis of BCoV attaching to *C. parvum* sporozoites, we intended to use TEM following co-incubation. However, we did not include this due to the possibility of getting false results. An alternative method for testing adherence could be to incubate a low concentration of virus with *C. parvum* sporozoites, filter the solution to retain the sporozoites, and check the filtrate for a possible reduction in viral RNA. To investigate whether the attachment between the BCoV and *C. parvum* sporozoites was specific to BCoV, two other viruses (Equine Herpesvirus-1, enveloped and Bovine Norovirus, naked) were co-incubated with *C. parvum*. As we

did not see an increase in viral RNA in presence of *C. parvum*, it seems likely that the binding of BCoV to the sporozoites is specific. Several studies have shown *C. parvum* sporozoites contain both O-linked and N-linked glycosylated proteins (mucins) such as GP900 (Cevallos et al., 2000), Gp40, Gp15 (Cevallos et al., 2000), and Muc4 (Paluszynski et al., 2014). Further studies are needed to identify any BCoV-binding molecules on the sporozoite surface, e.g., to stain or block, N-acetyl-9-O-acetylneuraminic acid (Neu5,9Ac2), which is the intestinal receptor for BCoV using, the *Cancer antennarius* (CCA) lectin (Ravindranath et al., 1985). We contemplated undertaking such investigations but were unsuccessful in identifying a vendor for this lectin.

Given that our findings indicated limited impact of co-infection on pathogen replication, we sought to explore the effect of single and co-infections on the host response (Paper II). Differential expression analysis revealed that the gene encoding for interleukin-8 (IL-8) had the highest fold change for BCoV- and co-infected cells at 72 hpi. A previous study on diarrhoeal calves supports our finding that IL-8 could also be used as a biomarker for intestinal injury (Ok et al., 2020), and its level has been observed to increase during other coronavirus infections (Mogensen and Paludan, 2001). On the other hand, *C. parvum*-infected cells showed that the highest FC was for gene encoding for Early Growth Response 1 (EGR1) at 72 hpi. The increase in EGR1 is considered a stress-induced specific response in epithelial cells against pathogens and induces apoptosis in *C. parvum*-infected cells (Liu et al., 2009). The gene expression profiles were quite similar between BCoV- and co-infected cells, however, 78 genes were only expressed in co-infected cells at 24 hpi, and this number increased to 803 at 72 hpi. At 24 hpi, *NR4A3* (FC = 4.12), had the highest FC, a transcriptional activator involved in regulating proliferation, survival differentiation, and inflammatory processes (Ok et al., 2020). At 72 hpi, the highest FC corresponds to *DNAH17* (FC=55.20), although the function of this dynein gene in our context is not obvious. The GO term analysis mostly showed an effect on cellular metabolic pathways and response to DNA damage both at 24 and 72 hpi. And there were no significantly enriched KEGG pathways with few immune genes among these DEGs. These genes need to be further explored as potential biomarkers for BCoV and *C. parvum* co-infection and their role in the pathogenesis in calf diarrhoea during co-infection should be addressed *in vivo*.

The gene ontology analysis in our study showed that GO terms associated with immune responses were mostly activated by BCoV-infection/co-infection, while for *C. parvum*-infection, the enriched GO terms were mainly associated with metabolic processes with few immune genes. One of the reasons for this could be that the *C.*

parvum residing in the parasitophorous vacuoles utilizes the host for its metabolites and is able to trigger host immune response to less extent as also described for other apicomplexan parasites such as *Toxoplasma gondii* (Guérin et al., 2020; Blume et al., 2009). On the other hand, viruses including coronaviruses replicating in the cytoplasm, exert a broader effect on host responses involving stimulation of immune responses mediated by IFN-I (Hoffman et al., 2015).

Among several enriched pathways, four of the major KEGG pathways (MAPK, TNF, NF- κ B, IL-17) were selected for detailed analysis (Table 3). The MAPK pathway was significantly modulated in all three experimental set ups (BCoV, *C. parvum*, and co-infected) as signalling from this pathway is generally generated when signalling molecules bind to the host receptors that activate the NF- κ B. *MAP3K8* was significantly upregulated in co-infected cells at 24 hpi which is required for lipopolysaccharide (LPS)-induced, TLR4-mediated activation of the MAPK/ERK pathway in macrophages, thus being critical for production of the proinflammatory cytokine, TNF- α during innate immune response (Schmid et al., 2014). The pathway is also involved in the regulation of T-helper cell differentiation and interferon gamma (IFNG) expression in T-cells. MAPK signalling pathways have been observed to be significantly modulated in other coronavirus infections, such as Middle East respiratory syndrome-related coronavirus (MERS) and SARS-CoV-2 (Islam et al., 2020) and therefore modulation of this pathway during BCoV infection could be further explored. None of the genes belonging to this pathway were significantly enriched in *C. parvum*-infected cells at 24 hpi; however, several genes were modulated at 72 hpi. Most of the key components of MAPK signalling pathways were not modulated in murine intestinal epithelial cells infected with *C. parvum* and the strategy was considered as a mechanism to evade host immune response (He et al., 2021).

The MAPK pathway is interlinked with TNF- α pathway, which was enriched in all our experimental setups (Paper II). TNF- α , a proinflammatory cytokine, is produced upon activation of the innate immune system and involved in various biological processes, including regulation of cell proliferation, differentiation, apoptosis, and immune responses (Zelová and Hošek, 2013). Activation of the nuclear factor kappa-light-chain-enhancer of activated B cells (NF- κ B) is implicated in the TNF- α pathway, inducing expression of genes that encode proinflammatory cytokines such as IL-6, as well as anti-apoptotic factors like *BIRC2*, *BIRC3*, and *BCL-2* homologue *BCL2L1*, thereby enabling the cell to remain inert to apoptotic stimuli (Farahani et al., 2022). The activated NF- κ B induces the expression of pro- and anti-apoptotic factors in *C. parvum*-infected cells (Liu et al., 2009) and proinflammatory cytokines (e.g., TNF- α ,

IL-8) (Lean et al., 2002). Similarly, NF- κ B has been considered to play a critical role in various viral and parasitic infections (Attiq et al., 2021; Chadha and Chadee, 2021). It has also been responsible in inducing Type I Interferon (IFN-1) e.g., IFN- β and other proinflammatory cytokines (e.g., IL-6 and IL-8) during RNA virus infections (Takeuchi et al., 2010, Cruz-Pulido et al., 2021). IFN-1 is considered as a first line of defence against viral infections; however, long-term production of IFN-1 can be deleterious for the host cells (Sa Ribero et al., 2020). In the present study, several components involved in IFN-1 pathways were upregulated at 24 and 72 hpi in BCoV infected cells. This contrasts with results from other studies where most of the coronaviruses are observed to be poor inducers of IFN-I response *in vitro* and in animal models (Blanco-Melo et al., 2020; Chu et al., 2020). At the same time, IFN-I responses are also considered to be variable among individual cells and cell populations.

Interleukin 17 (IL-17) acts synergistically with TNF and IL-1, with an increase in chemokine production in response to extracellular pathogens (Sahu et al., 2021), and has been extensively studied in other coronavirus infections such as SARS-CoV-2 (Sadeghi et al., 2019). Furthermore, its induction has also been studied in *C. parvum* infection in bovine and mice intestine (Drinkall et al., 2017; Zhao et al., 2016).

In the current study (Paper II), the BCoV-infected cells revealed upregulation of several chemokines and cytokines (*FOS*, *CXCL2*, *PTGS2*) at 24 hpi leading to autoimmune pathology, neutrophil recruitment, and immunity against extracellular pathogens. *C. parvum*-infected cells displayed upregulation of the *TRAF4* gene, which is associated with TNF receptor, connecting Il-1/Toll receptors with NF- κ B at 72 hpi. This inhibits activation of NF- κ B by *NOD2/RIP2* (inflammasome) and *JUN/MAPK12*. The co-infected cells showed upregulation of the gene *TNFAIP3*, which is induced by TNF- α inhibiting activation of NF- κ B and apoptosis mediated by TNF- α and thereby limiting inflammation. At 72 hpi, BCoV-infected cells exhibited greater modulation, involving multiple key genes including matrix metalloproteases (MMPs), compared to *C. parvum* or co-infected cells. The induction of MMPs contributes to an aggravated response by disruption of the barrier function of the epithelial intestinal cells and has been shown to be relevant in SARS-CoV-2 infections (Lee and Kim, 2022).

As for the apoptosis, there was a balance between the upregulation of pro-apoptotic genes (*BAK1*, *TNFSRF10B*, *PMAIP1*) and pro-survival genes (*BIRC-2*); in addition, there was downregulation of pro-apoptotic genes such as *BBC3* in BCoV-infected and co-infected cells at 72 hpi (Paper II). Caspases are considered crucial for apoptosis of which, caspase-7 (*CASP7*) was upregulated in BCoV- and co-infected cells at 72 hpi while other caspases such as *CASP2* and *CASP4* were downregulated at 72hpi in co-infected cells. Changes in expression of different caspases might explain some flow

results from work connected to Paper I (not included) where more dead cells were found in *C. parvum* infected cells than co-infected cells. During early phases of *C. parvum* infection, cells are expected to undergo apoptosis to prevent parasite invasion, as reported in previous studies (Chen et al., 1998; McCole et al., 2000). Nevertheless, for *C. parvum*-infected cells, there was downregulation of apoptotic genes such as *GADD45B*, *FOS*, and *JUN* at 72 hpi in our experimental setups. Overall, results from Paper II reflect that the proinflammatory responses, modifications in the host cell cytoskeleton and the protective mucus barrier, could be the molecular basis for *in vivo* damage to the epithelial barrier, leading to diarrhoea. Additionally, the results indicated the proinflammatory responses were much stronger at 72 hpi, mostly in BCoV and co-infected cells as compared with *C. parvum* infected cells. In co-infected cells, the host response was predominantly driven by the response to BCoV, likely due to higher susceptibility of HCT-8 cells to BCoV compared to *C. parvum*, as mentioned in Paper I, where the proportion of BCoV-infected cells was 10-20% and for *C. parvum* was 1-11%. The gene expression profile of the relatively small population of *C. parvum*-infected cells may have been overshadowed by the substantial majority of non-infected or virus-infected cells. It could have been a preferable strategy to lower the concentration of virus used for RNASeq based on the results from Paper I. A strategy for increasing the number of *C. parvum*-infected cells could be to increase the duration of exposure to *C. parvum*, or to add *C. parvum* immediately after pre-treatment (thereby bypassing the excystation stage). Alternatively, bovine enteroids (2D enteroids) need to be optimized that may exhibit high permissiveness to both pathogens to study a bovine-specific response. Another approach could be to utilize single-cell sequencing. In this study (Papers I and II) we utilized a human cell line that is likely less representative of the bovine intestine. To achieve a bovine-specific response to BCoV infection, a study was conducted on bovine enteroids that have a heterogeneous population of cells (Paper III). The bovine enteroids were successfully cultured and differentiated in this study using IntestiCult Organoid Growth Medium (Mouse media) based on the formulation by Hamilton et al., (2018). The enteroids were not fully differentiated, as only intestinal stem cells, enteroendocrine cells and enterocytes were detected. Perhaps, the use of IntestiCult Organoid Differentiation Medium (Human), which seems more efficient to induce differentiation of bovine enteroids could be explored (personal communication - Mathilde S. Varegg-PhD student at NMBU and David Smith-research fellow at Moredun Research Institute). This medium was not commercially available at the time of our experiment. We managed to infect the partially differentiated enteroids (IntestiCult) successfully with BCoV as demonstrated by a seven-fold increase in viral

RNA, which was lower than for HCT-8 cells (Paper I), where an approximately 40-fold increase occurred. This discrepancy might be the result of inoculating the enteroids with a lower dose of BCoV (6.32E+03 TCID₅₀) than in the HCT-8 cells (1.2E+06 TCID₅₀). Also, the virus was adapted to the HRT-18G cells, but not to the enteroids. Studies have indicated that adaptation to the culture system is usually necessary to increase the replication of viruses (Borucki et al., 2013). As the enteroid model is probably closer to the intestine, compared to a cell line, we should have tried passing an extract of a BCoV positive faecal sample directly on the enteroids.

Initially, when the intact or fragmented enteroids were inoculated with the BCoV, there was limited increase in viral RNA, which could be due to insufficient break down of the enteroids, limiting the exposure of the cells to the virus. Results using TrypL Xpress dissociated enteroids indicated that the enteroids were further opened, exposing the apical surface for the virus. One of the drawbacks of trypsinization could be that target cells might be lost, resulting in mainly non-differentiated stem cells at the time of infection. Therefore, further optimisation to break down the enteroids, minimizing loss of cells is necessary.

Gene expression analysis of BCoV-infected enteroids revealed upregulation of *LGR5+* at 72 hpi indicating self-renewal of intestinal stem cells. A similar result has been reported in porcine intestinal organoids infected with the coronavirus transmissible gastroenteritis virus (Yang et al., 2022). The BCoV-infected enteroids (at least passage 3) showed downregulation of *Muc2* at 72 hpi. On the other hand, staining results suggested limited production of *Muc2* protein by the goblet cells.

Although initially we aimed to infect the enteroids with *C. parvum* followed by co-infection (both BCoV and *C. parvum*), and compare the gene expression to the cell line, we were not able to due to time constraints. The pro-inflammatory cytokines, *IL-8* and *IL-1A*, were identified as being modulated as early immune response in viral infections (Mogensen and Paludan, 2001) and were unchanged in BCoV-infected enteroids, but significantly upregulated in BCoV-infected HCT-8 cells (Paper II). On the other hand, *CXCL-3*, *TNF- α* , and *MMP13* were significantly downregulated in the infected enteroids compared with the HCT-8 cells. Our results suggest that BCoV infection may be less damaging to enteroids than to HCT-8 cells, as other studies have associated *MMP13* and *TNF- α* with epithelial barrier function (Vandenbroucke et al., 2013; Crawford et al, 2022).

In general, the gene expression during BCoV infection differed between the enteroids and the HCT-8 cells. The bovine enteroid model with a heterogenous cell population is more complex and probably closer to the calf intestine than a traditional cell line. The presence of different cell types in the enteroids may have resulted in more

relevant gene expression and the ability to counteract pro-inflammatory responses. However, in real life scenario other factors such as the microbiome and immune cells also come into play. Besides, experimental differences between the studies include a lower BCoV dose used for enteroids compared to HCT-8 cells, infection of cells from different host species (human and bovine) and, the use of a BCoV strain that was already adapted to the cell line but not to the enteroids. However, the use of the same virus stock to infect both HCT-8 cell and enteroids was relevant for appropriate comparison.

12 Conclusions

The use of an *in vitro* model (HCT-8 cells) to study the interplay between bovine coronavirus and *Cryptosporidium parvum* revealed binding of viruses to the parasite. Extrapolating the results from an *in vitro* system to the intestine of calves with a microbiome is difficult. However, attachment of BCoV to *C. parvum* could possibly occur in real life scenario of co-infected calves and reduce the number of replicating virus. Although, human HCT-8 cells are not optimal to study bovine-specific responses, the host study response in case of single and co-infected HCT-8 cells revealed host transcriptome extensively modulated by BCoV with limited effect from *C. parvum* under our experimental settings. This could be different under natural settings due to the pathogen doses the animals are exposed to, the microbiome and the response of immune cells. However, quite a few genes were exclusively expressed during co-infection which could be used as potential biomarkers for BCoV and *C. parvum* co-infection. Bovine enteroids with a heterogenous cell population closer to the *in vivo* intestine was explored for host-pathogen interactions revealed successful establishment of differentiated enteroids as BCoV culture system. Expression of selected immune genes during BCoV infection in enteroids and HCT-8 cells were compared. The results indicate less damage to the enteroids, which demonstrates the importance of the model being used and that it requires comparative gene expression study between live animals and enteroids to determine whether enteroids are better models to recapitulate the pathogenesis of calf diarrhoea.

13 Future perspectives

- **Exploring molecule on *C. parvum*, which may serve as attachment sites for BCoV**

In Paper I, we were interested in looking at possible interactions between BCoV and *C. parvum*. The results from this study indicated specific attachment of BCoV to *C. parvum* sporozoites. However, we did not identify any molecules targeted by BCoV for attachment. Neu5Ac2 is the natural receptor for BCoV on epithelial cells. In lack of the specific lectin for staining, neuraminidase treatment could be tested.

- **Study apoptosis in single and co-infected cells**

Some flow results from work connected to Paper I (not included) revealed more dead cells in *C. parvum* infected cells as compared to BCoV- or co-infected cells. The gene expression study in Paper II indicated downregulation of apoptotic genes such as *CASP2* and *CASP4* in co-infected cells. These are interesting findings which should be followed up.

- **Exploring additional bovine cell lines to infect with BCoV and *C. parvum***

In Paper II, the aim was to enhance our comprehension of the host response to single and co-infection with BCoV and *C. parvum*. We employed human cell line HCT-8, which is composed of enterocytes (target cells for both pathogens) and is permissive to both pathogens. However, a bovine cell line would probably be more suitable for studying the host response to pathogens infecting the calf intestine. Furthermore, a proteomic analysis would bring knowledge a further step forward.

- **Optimization of infection protocol of bovine enteroid with BCoV**

In Paper III, while successful in infecting bovine enteroids with BCoV, the increase in viral RNA was limited and optimization of the infection protocol is required. This could perhaps be achieved by using a field strain of virus and adapt this to the enteroids. Other possible techniques such as apical-out approach that could increase viral access to luminal side of the enteroids should be further explored. It would be of interest to obtain fully

differentiated enteroids and investigate potential target cells for BCoV besides enterocytes.

- **Bovine enteroid as a replication system for *C. parvum***

Our initial aim was to infect the bovine enteroids with both BCoV and *C. parvum*, but time limit hindered us to work with *C. parvum*. It would be intriguing to be able to infect bovine enteroids with *C. parvum* and utilize the bovine model system to complete the life cycle of *C. parvum* and to do co-infections. Single-cell RNASeq on co-infected bovine enteroids could be conducted to study the host response.

- **Live animal study on infections with BCoV and *C. parvum***

Results in live animals could be compared with results obtained in bovine enteroids to clarify whether the *in vitro* model represents a good alternative to replace *in vivo* experiments. The infected enteroids together with the necropsy specimen of the intestine of the infected animal could be compared to look for any observable changes on the cell population, shortening of villi, barrier permeability etc. This could be followed up with transcriptomic study on infections in the enteroids and calves.

14 References

1. Abuelo A & Perez-Santos M. A winter dysentery (coronavirus infection) outbreak in a dairy herd in Galicia (northwestern Spain). *Vet. Rec. Case Rep.* 4(1): e000328. doi: 10.1136/vetreccr-2016-000328. (2016).
2. Aich P, Wilson HL, Kaushik RS, Potter AA, Babiuk LA & Griebel P. Comparative analysis of innate immune responses following infection of new-born calves with bovine rotavirus and bovine coronavirus. *J Gen Virol.* 88(Pt 10):2749-2761. doi: 10.1099/vir.0.82861-0. (2007).
3. Akira S, Uematsu S & Takeuchi O. Pathogen recognition and innate immunity. *Cell.* 124(4):783–801. doi: 10.1016/j.cell.2006.02.015. (2006).
4. Alenius, S, Niskanen, R, Juntti, N & Larsson, B. Bovine coronavirus as the causative agent of winter dysentery: serological evidence. *Acta Vet. Scand.* 32(2): 163-170. doi: <https://doi.org/10.1186%2FBF03546976>. (1991).
5. Amer, H. Bovine-like coronaviruses in domestic and wild ruminants. *Anim. Health. Res. Rev.* 19(2):113-124. doi:10.1017/S1466252318000117. (2018).
6. Arrowood MJ. *In vitro* cultivation of *Cryptosporidium* species. *Clin Microbiol Rev.* 15(3):390-400. doi: 10.1128/CMR.15.3.390-400.2002. (2002).
7. Asadi AH, Baghinezhad M & Asadi H. Neonatal calf diarrhoea induced by rotavirus and coronavirus. *Int. J. Biosci.* 6(2):230-236. doi: <http://dx.doi.org/10.12692/ijb/6.2.230-5>. (2015).
8. Attiq A, Yao LJ, Afzal S & Khan MA. The triumvirate of NF- κ B, inflammation and cytokine storm in COVID-19. *Int. Immunopharmacol.* 101(Pt B):108255. doi: 10.1016/j.intimp.2021.108255. (2021).
9. Balachandran S & Beg AA. Defining emerging roles for NF- κ B in antiviral responses: revisiting the interferon- β enhanceosome paradigm. *PLoS Pathog.* 7(10): e1002165. doi: <https://doi.org/10.1371/journal.ppat.1002165>. (2011).
10. Barakat FM, McDonald V, Di Santo JP & Korbelt DS. Roles for NK cells and an NK cell-independent source of intestinal gamma interferon for innate immunity to *Cryptosporidium parvum* infection. *Infect. Immun.* 77(11):5044–5049. doi: 10.1128/IAI.00377-09. (2009).
11. Barker N, Van Es JH, Kuipers J, Kujala P, Van den Born M, Cozijnsen M, Haeghebarth A, Korving J, Begthel H, Peters PJ & Clevers H. Identification of

- stem cells in small intestine and colon by marker gene Lgr5. *Nature*. 449(7165):1003–1007. doi: 10.1038/nature06196. (2007).
12. Bartels, CJ, Holzhauser, M, Jorritsma, R, Swart, WA & Lam, TJ. Prevalence, prediction, and risk factors of enteropathogens in normal and non-normal faeces of young Dutch dairy calves. *Prev. Vet. Med.* 93(2-3), 162-169 (2010).
 13. Bedi B, McNair NN & Mead JR. Dendritic cells play a role in host susceptibility to *Cryptosporidium parvum* infection. *Immunol Lett.* 158:42–51. doi: 10.1016/j.imlet.2013.11.015. (2014).
 14. Bhalchandra S, Cardenas D & Ward HD. Recent Breakthroughs and Ongoing Limitations in *Cryptosporidium* Research. *F1000Res.* 7:F1000 Faculty Rev-1380. doi: 10.12688/f1000research.15333.1. (2018).
 15. Bidokhti, MR, Trávén, M, Fall, N, Emanuelson, U & Alenius, S. Reduced likelihood of bovine coronavirus and bovine respiratory syncytial virus infection on organic compared to conventional dairy farms. *Vet. J.* 182, 436-440. doi: 10.1016/j.tvjl.2008.08.010. (2009).
 16. Blake R, Jensen K, Mabbott N, Hope J & Stevens J. The Development of 3D Bovine Intestinal Organoid Derived Models to Investigate *Mycobacterium Avium* ssp Paratuberculosis Pathogenesis. *Front Vet Sci.* 9:921160. doi: 10.3389/fvets.2022.921160. (2022).
 17. Blanchard PC. Diagnostics of dairy and beef cattle diarrhoea. *Vet Clin North Am Food Anim Pract.* 28(3):443–464. doi: 10.1016/j.cvfa.2012.07.002. (2012).
 18. Blanco-Melo D, Nilsson-Payant BE, Liu WC, Uhl S, Hoagland D, Møller R, Jordan TX, Oishi K, Panis M, Sachs D, Wang TT, Schwartz RE, Lim JK, Albrecht RA & tenOever BR. Imbalanced Host Response to SARS-CoV-2 Drives Development of COVID-19. *Cell.* 181(5):1036-1045.e9. doi: 10.1016/j.cell.2020.04.026. (2020).
 19. Blume M, Rodriguez-Contreras D, Landfear S, Fleige T, Soldati-Favre D, Lucius R & Gupta N. Host-derived glucose and its transporter in the obligate intracellular pathogen *Toxoplasma gondii* are dispensable by glutaminolysis. *Proc Natl Acad Sci U S A.* 106(31):12998-3003. doi: 10.1073/pnas.0903831106. (2009).
 20. Boileau, MJ & Kapil, S. Bovine coronavirus associated syndromes. *Vet. Clin. North Am. Food Anim. Pract.* 26, 123–146. doi: <http://dx.doi.org/10.1016/j.cvfa.2009.10.003>. (2010).
 21. Borucki MK, Allen JE, Chen-Harris H, Zemla A, Vanier G, Mabery S, Torres C, Hullinger P & Slezak T. The role of viral population diversity in adaptation

- of bovine coronavirus to new host environments. *PLoS One*. 8(1): e52752. doi: 10.1371/journal.pone.0052752. (2013).
22. Brandão AM, Villarreal LY, de Souza SL, Richtzenhain LJ & Jerez JA. Mixed infections by bovine coronavirus, rotavirus, and *Cryptosporidium parvum* in an outbreak of neonatal diarrhoea in beef cattle. *Arq Inst. Biol.* 74:33-4. doi: <https://doi.org/10.1590/1808-1657v74p0332007>. (2007).
 23. Brook E, Hart CA, French N & Christley R. Prevalence and risk factors for *Cryptosporidium* spp. infection in young calves. *Vet Parasitol.*152:46–52. doi: 10.1016/j.vetpar.2007.12.003. (2008).
 24. Brook EJ, Anthony Hart C, French NP & Christley RM. Molecular epidemiology of *Cryptosporidium* subtypes in cattle in England. *Vet J.* 179(3):378-82. doi: 10.1016/j.tvjl.2007.10.023. (2009).
 25. Brunauer M, Roch F-F & Conrady B. Prevalence of Worldwide Neonatal Calf Diarrhoea Caused by Bovine Rotavirus in Combination with Bovine Coronavirus, Escherichia coli K99 and *Cryptosporidium* spp.: A Meta-Analysis. *Animals*. 11(4):1014. doi: <https://doi.org/10.3390/ani11041014>. (2021).
 26. Cacciò S & Widmer G. *Cryptosporidium*: parasite and disease, (Ed.) Springer-Verlag, Wien XI:564. <http://www.springer.com/gp/book/9783709115619>. (2014).
 27. Campbell SM, Pettersen FO, Brekke H, Hanevik K & Robertson LJ. Transition to PCR diagnosis of cryptosporidiosis and giardiasis in the Norwegian healthcare system: could the increase in reported cases be due to higher sensitivity or a change in the testing algorithm? *Eur J Clin Microbiol Infect Dis*. 41(5):835-839. doi: 10.1007/s10096-022-04426-3. (2022).
 28. Centres for disease control and prevention. Available at: https://www.cdc.gov/dpdx/cryptosporidiosis/modules/Cryptosporidium_LifeCycle_lg.jpg (2015). (Accessed: 03 April 2023).
 29. Cevallos AM, Bhat N, Verdon R, Hamer DH, Stein B, Tzipori S, Pereira ME, Keusch GT & Ward HD. Mediation of *Cryptosporidium parvum* infection in vitro by mucin-like glycoproteins defined by a neutralizing monoclonal antibody. *Infect Immun*. 68(9):5167-75. doi: 10.1128/IAI.68.9.5167-5175.2000. (2000).
 30. Chadha A & Chadee K. The NF-κB Pathway: Modulation by *Entamoeba histolytica* and Other Protozoan Parasites. *Front Cell Infect Microbiol*. 11:748404. doi: 10.3389/fcimb.2021.748404. (2021).

31. Chalmers RM & Katzer F. Looking for *Cryptosporidium*: the application of advances in detection and diagnosis. *Trends Parasitol.* 29:237–251. doi: 10.1016/j.pt.2013.03.001. (2013).
32. Checkley, W, White, AC, Jaganath, D, Arrowood, MJ, Chalmers, RM, Chen, X-M & Houpt, ER. A review of the global burden, novel diagnostics, therapeutics, and vaccine targets for *Cryptosporidium*. *The Lancet Infect Dis.* 15 (1): 85-94. doi: 10.1016/S1473-3099(14)70772-8. (2015).
33. Chen XM, Levine SA, Tietz P, Krueger E, McNiven MA, Jefferson DM, Mahle M & LaRusso NF. *Cryptosporidium parvum* is cytopathic for cultured human biliary epithelia via an apoptotic mechanism. *Hepatology.* 28(4):906-13. doi: 10.1002/hep.510280402. (1998).
34. Chen XM, O'Hara SP, Nelson JB, Splinter PL, Small AJ, Tietz PS, Limper AH & LaRusso NF. Multiple TLRs are expressed in human cholangiocytes and mediate host epithelial defense responses to *Cryptosporidium parvum* via activation of NF-kappaB. *J Immunol.* 175:7447–7456. doi: 10.4049/jimmunol.175.11.7447. (2005).
35. Chigerwe M & Heller MC. Diagnosis and Treatment of Infectious Enteritis in Adult Ruminants. *Vet. Clin. North Am. Food Anim. Pract.* 34(1):119–131. doi: <https://doi.org/10.1016/j.cvfa.2017.10.004>. (2018)
36. Cho YI & Yoon KJ. An overview of calf diarrhoea-infectious etiology, diagnosis, and intervention. *J Vet Sci.*15(1):1-17. doi: <https://doi.org/10.4142/jvs.2014.15.1.1> (2014).
37. Chu H, Chan JFW, Wang Y, Yuen TTT, Chai Y, Hou Y, Shuai H, Yang D, Hu B, Huang X & Zhang X. Comparative replication and immune activation profiles of SARS-CoV-2 and SARS-CoV in human lungs: an ex vivo study with implications for the pathogenesis of COVID-19. *Clin Inf Dis.* 71(6):1400-1409. Doi: <https://doi.org/10.1093/cid/ciaa410>. (2020).
38. Clark MA. Bovine coronavirus. *Br Vet J.* 149(1):51-70. doi: 10.1016/S0007-1935(05)80210-6. (1993).
39. Co JY, Margalef-Català M, Monack DM & Amieva MR. Controlling the polarity of human gastrointestinal organoids to investigate epithelial biology and infectious diseases. *Nat Protoc.* 16(11):5171-5192. doi: 10.1038/s41596-021-00607-0. (2021).
40. Crawford CK, Lopez Cervantes V, Quilici ML, Armién AG, Questa M, Matloob MS, Huynh LD, Beltran A, Karchemskiy SJ, Crakes KR & Kol A. Inflammatory cytokines directly disrupt the bovine intestinal epithelial barrier. *Sci Rep.* 12(1):14578. doi: 10.1038/s41598-022-18771-y. (2022).

41. Cruvinel, LB, Ayres, H, Zapa, DMB, Nicaretta, JE, Couto, LFM, Heller, LM, Bastos, TSA, Cruz, BC, Soares, VE & Teixeira, WF. Prevalence and risk factors for agents causing diarrhoea (Coronavirus, Rotavirus, *Cryptosporidium* spp., *Eimeria* spp., and nematodes helminths) according to age in dairy calves from Brazil. *Trop. Anim. Health Prod.* 52(2):777-791. doi: 10.1007/s11250-019-02069-9. (2020).
42. Cruz-Pulido D, Boley PA, Ouma WZ, Alhamo MA, Saif LJ & Kenney SP. Comparative Transcriptome Profiling of Human and Pig Intestinal Epithelial Cells after Porcine Deltacoronavirus Infection. *Viruses.* 13(2):292. doi: 10.3390/v13020292. (2021).
43. Csako G. Present and future of rapid and/or high-throughput methods for nucleic acid testing. *Clin Chim Acta.* 363(1-2):6-31. doi: 10.1016/j.cccn.2005.07.009. (2006).
44. Current WL & Long PL. Development of human and calf *Cryptosporidium* in chicken embryos. *J. Infect. Dis.* 148(6):1108-1113. doi: <https://doi.org/10.1093/infdis/148.6.1108>. (1983).
45. Da Silva MR, O'Reilly KL, Lin X, Stine L & Storz J. Sensitivity comparison for detection of respiratory bovine coronaviruses in nasal samples from feedlot cattle by ELISA and isolation with the G clone of HRT-18 cells. *J Vet Diagn Invest.* 11(1):15-9. doi: 10.1177/104063879901100102. (1999).
46. Datry A, Danis M & Gentilini M. Complete Development Of *Cryptosporidium* In vitro-Applications. *Med Sci.* 5(10):762-766. (1989).
47. De Waele V, Speybroeck N, Berkvens D, Mulcahy G & Murphy TM. Control of cryptosporidiosis in neonatal calves: use of halofuginone lactate in two different calf rearing systems. *Prev Vet Med.* 96(3-4):143-51. doi: 10.1016/j.prevetmed.2010.06.017. (2010).
48. Dea S, Roy, RS & Begin ME. Bovine coronavirus isolation and cultivation in continuous cell lines. *Am. J. Vet. Res.* 41(1):30-8. (1980).
49. Derricott H, Luu L, Fong WY, Hartley CS, Johnston LJ, Armstrong SD, Randle N, Duckworth CA, Campbell BJ, Wastling JM, Coombes JL. Developing a 3D intestinal epithelium model for livestock species. *Cell Tissue Res.* 375(2):409-424. doi: 10.1007/s00441-018-2924-9. (2019).
50. Dorak, M. (Ed.). Real-time PCR (1st ed.). Taylor & Francis. doi: <https://doi.org/10.4324/9780203967317>. (2006).
51. Drinkall E, Wass MJ, Coffey TJ & Flynn RJ. A rapid IL-17 response to *Cryptosporidium parvum* in the bovine intestine. *Vet Immunol Immunopathol.* 191:1-4. doi: 10.1016/j.vetimm.2017.07.009. (2017).

52. Ellis J. What is the evidence that bovine coronavirus is a biologically significant respiratory pathogen in cattle? *Can. Vet. J.* 60(2):147–152. (2019).
53. Ettayebi K, Crawford SE, Murakami K, Broughman JR, Karandikar U, Tenge VR, Neill FH, Blutt SE, Zeng XL, Qu L, Kou B, Opekun AR, Burrin D, Graham DY, Ramani S, Atmar RL & Estes MK. Replication of human noroviruses in stemcell-derived human enteroids. *Science.* 353(6306):1387–1393. doi: 10.1126/science.aaf5211. (2016).
54. Farahani M, Niknam Z, Mohammadi Amirabad L, Amiri-Dashatan N, Koushki M, Nemati M, Danesh Pouya F, Rezaei-Tavirani M, Rasmi Y & Tayebi L. Molecular pathways involved in COVID-19 and potential pathway-based therapeutic targets. *Biomed Pharmacother.* 145:112420. doi: 10.1016/j.biopha.2021.112420. (2022).
55. Faubert GM & Litvinsky Y. Natural transmission of *Cryptosporidium parvum* between dams and calves on a dairy farm. *J Parasitol.* 86(3):495-500. doi: 10.1645/0022-3395(2000)086[0495:NTOCPB]2.0.CO;2. (2000).
56. Fayer R, Santín M & Trout JM. *Cryptosporidium ryanae* n. sp. (Apicomplexa: Cryptosporidiidae) in cattle (*Bos taurus*). *Vet Parasitol.* 156:191–198. doi: <https://doi.org/10.1016/j.vetpar.2008.05.024> (2008).
57. Fayer R, Santín M, Trout JM & Greiner E. Prevalence of species and genotypes of *Cryptosporidium* found in 1-2-year-old dairy cattle in the eastern United States. *Vet Parasitol.* 135:105–112. doi: 10.1016/j.vetpar.2005.08.003. (2006).
58. Fayer R, Santín M, Trout JM. Prevalence of *Cryptosporidium* species and genotypes in mature dairy cattle on farms in eastern United States compared with younger cattle from the same locations. *Vet Parasitol.* 145:260–266. doi: 10.1016/j.vetpar.2006.12.009. (2007).
59. Featherstone CA, Giles M, Marshall JA, Mawhinney IC, Holliman A & Pritchard GC. *Cryptosporidium* species in calves submitted for post-mortem examination in England and Wales. *Vet Rec.* 167(25):979–980. doi:10.1136/vr.c3948. (2010).
60. Feix AS, Cruz-Bustos T, Ruttkowski B & Joachim A. *In vitro* cultivation methods for coccidian parasite research. *Int. J. Parasitol.* doi: <https://doi.org/10.1016/j.ijpara.2022.10.002>. (2022).
61. Foster DM & Smith GW. Pathophysiology of diarrhoea in calves. *Vet. Clin. North Am. Food Anim. Pract.* 25:13–36 (2009).

62. Fulton, RW, Ridpath, JF & Burge, LJ. Bovine coronaviruses from the respiratory tract: Antigenic and genetic diversity. *Vaccine*. 31, 886–892. doi: 10.1016/j.vaccine.2012.12.006. (2013).
63. Göhring F, Moeller-Holtkamp P, Dausgshies A & Lendner M. Co-infections with *Cryptosporidium parvum* and other enteropathogens support the occurrence and severity of diarrhoea in suckling calves. *Tierärztliche Umschau*, 69(4), 112-120. (2014).
64. Gomez DE & Weese JS. Viral enteritis in calves. *Can Vet J*. 58(12):1267-74. (2017).
65. Guérin, A., & Striepen, B. The biology of the intestinal intracellular parasite *Cryptosporidium*. *Cell Host Microbe*. 28(4):509–515. doi: 10.1016/j.chom.2020.09.007. (2020).
66. Gulliksen SM, Jor E, Lie KI, Hamnes IS, Løken T, Akerstedt J & Osterås O. Enteropathogens and risk factors for diarrhea in Norwegian dairy calves. *J Dairy Sci*. 92(10):5057-66. doi: 10.3168/jds.2009-2080 (2009).
67. Gulliksen SM, Lie KI & Østerås O. Calf health monitoring in Norwegian dairy herds. *J Dairy Sci*. 92(4):1660-9. doi: <https://doi.org/10.3168/jds.2008-1518>. (2009).
68. Hägglund, S, Svensson, C, Emanuelson, U, Valarcher, JF & Alenius, S. Dynamics of virus infections involved in the bovine respiratory disease complex in Swedish dairy herds. *Vet. J*. 172. <https://doi.org/10.1016/j.tvjl.2005.04.029>. (2006).
69. Hamilton CA, Young R, Jayaraman S, Sehgal A, Paxton E, Thomson S, Katzer F, Hope J, Innes E, Morrison LJ & Mabbott NA. Development of in vitro enteroids derived from bovine small intestinal crypts. *Vet. Res*. 49, 1–15. doi: <https://doi.org/10.1186/s13567-018-0547-5>. (2018).
70. Hamnes IS, Gjerde B & Robertson L. Prevalence of *Giardia* and *Cryptosporidium* in dairy calves in three areas of Norway. *Vet Parasitol*. 140(3-4):204-16. doi: 10.1016/j.vetpar.2006.03.024. (2006).
71. Hampton JC & Rosario B. The attachment of protozoan parasites to intestinal epithelial cells of the mouse. *J Parasitol*. 52(5):939-49. (1966).
72. Hasoksuz M, Lathrop SL, Gadfield KL, Saif LJ. Isolation of bovine respiratory coronaviruses from feedlot cattle and comparison of their biological and antigenic properties with bovine enteric coronaviruses. *Am. J. Vet. Res*. 60(10):1227–1233. (1999).

73. Hayden, M. S., & Ghosh, Regulation of NF- κ B by TNF family cytokines. *Semin Immunol.* 26(3): 253-266. doi: <https://doi.org/10.1016/j.smim.2014.05.004>. (2014).
74. He W, Li J, Gong AY, Deng S, Li M, Wang Y, Mathy NW, Feng Y, Xiao L & Chen XM. Cryptosporidial Infection Suppresses Intestinal Epithelial Cell MAPK Signaling Impairing Host Anti-Parasitic Defense. *Microorganisms.* 9(1):151. doi: 10.3390/microorganisms9010151. (2021).
75. Heidarnejadi SM, Rafiei A, Makvandi M, Pirestani M, Saki J & Ghadiri A. Gene Profile Expression Related to Type I Interferons in HT-29 Cells Exposed to *Cryptosporidium parvum*. *Jundishapur J. Microbiol.* 11(7). doi: <https://doi.org/10.5812/jjm.63071>. (2018).
76. Heo I, Dutta D, Schaefer DA, Iakobachvili N, Artegiani B, Sachs N, Boonekamp KE, Bowden G, Hendrickx APA, Willems RJL, Peters PJ, Riggs MW, O'Connor R & Clevers H. Modelling *Cryptosporidium* infection in human small intestinal and lung organoids. *Nat Microbiol.* 3(7):814-823. doi: 10.1038/s41564-018-0177-8. (2018).
77. Hijjawi N. *Cryptosporidium*: new developments in cell culture. *Exp Parasitol.* 124(1):54-60. doi: 10.1016/j.exppara.2009.05.015. (2010).
78. Hodnik JJ, Ježek J & Starič J. Coronaviruses in cattle. *Trop. Anim. Health Prod.* 52(6):2809-2816. doi: 10.1007/s11250-020-02354-y. (2020).
79. Hoffmann, HH, Schneider, WM & Rice, CM. Interferons and viruses: an evolutionary arms race of molecular interactions. *Trends Immunol.* 36(3): 124-138. doi: <https://doi.org/10.1016/j.it.2015.01.004>. (2015).
80. Hofmann, MA, Sethna, PB & Brian, DA. Bovine coronavirus mRNA replication continues throughout persistent infection in cell culture. *J. Virol.* 64(9): 4108-14. doi: 10.1128/JVI.64.9.4108-4114.1990. (1990).
81. Huch M & Koo, BK. Modeling mouse and human development using organoid cultures. *Development.* 142(18): 3113-3125. doi: 10.1242/dev.118570. (2015).
82. ICTV (2019) Coronaviridae. EC 50, Washington, DC, July 2018. https://talk.ictvonline.org/ictv-reports/ictv_9th_report/positive-sense-rna-viruses-2011/w/posrna_viruses/222/coronaviridae.
83. Imre K, Lobo LM, Matos O, Popescu C, Genchi C & Darabus G. Molecular characterisation of *Cryptosporidium* isolates from pre-weaned calves in Romania: is there an actual risk of zoonotic infections? *Vet Parasitol.* 181(2-4):321-324. doi: <https://doi.org/10.21897/rmvz.1138>. (2011).

84. Innes EA, Chalmers RM, Wells B & Pawlowic MC. A One Health Approach to Tackle Cryptosporidiosis. *Trends Parasitol.* 36(3):290-303. doi: 10.1016/j.pt.2019.12.016. (2020).
85. Islam T, Rahman MR, Aydin B, Beklen H, Arga KY & Shahjaman M. Integrative transcriptomics analysis of lung epithelial cells and identification of repurposable drug candidates for COVID-19. *Eur J Pharmacol.* 887:173594. doi: 10.1016/j.ejphar.2020.173594. (2020).
86. Ismail MM, Cho KO, Ward LA, Saif LJ & Saif YM. Experimental bovine coronavirus in turkey poult and young chickens. *Avian Dis.* 45(1):157-63. doi: <https://doi.org/10.2307/1593023> (2001).
87. Izzo MM, Kirkland PD, Mohler VL, Perkins NR, Gunn AA & House JK. Prevalence of major enteric pathogens in Australian dairy calves with diarrhoea. *Aust. Vet. J.* 89(5):167-73. doi: 10.1111/j.1751-0813.2011.00692.x. (2011).
88. Joachim A, Krull T, Schwarzkopf J & Dausgchies A. Prevalence and control of bovine cryptosporidiosis in German dairy herds. *Vet Parasitol.* 112(4):277-288. doi: [https://doi.org/10.1016/S0304-4017\(03\)00006-2](https://doi.org/10.1016/S0304-4017(03)00006-2) (2003).
89. Kapil S, Pomeroy KA, Goyal SM & Trent, AM. Experimental infection with a virulent pneumoenteric isolate of bovine coronavirus. *J. Vet. Diagn. Invest.* 3(1):88-9. doi: 10.1177/104063879100300123. (1991).
90. Kienzle, T, Abraham, S, Hogue, BG & Brian DA. Structure and orientation of expressed bovine coronavirus hemagglutinin-esterase protein. *J. Virol.* 64(4): 1834-8. doi: 10.1128/jvi.64.4.1834-1838.1990. (1990).
91. Kunsch C & Rosen CA. NF- κ B subunit-specific regulation of the interleukin-8 promoter. *Mol. Cell Biol.* 13(10):6137-6146. doi: <https://doi.org/10.1128/mcb.13.10.6137-6146.1993>. (1993).
92. Laporte J, L'Haridon R & Bobulesco, P. In vitro culture of bovine enteric coronavirus (BEC). In: Bricout F., Pensaert M, Flewett TH, et al., compilers. Enterites virales chez l'homme et l'animal; viral Enteritis in humans and animals. Thiverval-Grignon, France: l'INSERM. 90:99-102. (1979).
93. Laurent, F, Eckmann L, Savidge TC, Morgan G, Theodos C, Naciri M & Kagnoff MF. *Cryptosporidium parvum* infection of human intestinal epithelial cells induces the polarized secretion of C-X-C chemokines. *Infect. Immun.* 65(12):5067-5073. doi: 10.1128/iai.65.12.5067-5073.1997. (1997).
94. Lean IS, McDonald V & Pollok RC. The role of cytokines in the pathogenesis of *Cryptosporidium* infection. *Curr. Op. Infect. Dis.* 15(3):229-234. doi: 10.1097/00001432-200206000-00003. (2002).

95. Lebbad, M, Winiecka-Krusnell, J, Stensvold, CR & Beser, J. High diversity of *Cryptosporidium* species and subtypes identified in cryptosporidiosis acquired in Sweden and abroad. *Pathogens*. 10(5): 1–23. doi: <https://doi.org/10.3390/pathogens10050523>. (2021).
96. Lee, H. S., & Kim, W. J. The Role of Matrix Metalloproteinase in Inflammation with a Focus on Infectious Diseases. *Int. J. Mol. Sci.* 23(18), 10546 (2022).
97. Leitch GJ & He Q. Cryptosporidiosis-an overview. *J Biomed Res.* 25(1):1-16. doi: 10.1016/S1674-8301(11)60001-8. (2011).
98. Li L, Fu F, Guo S, Wang H, He X, Xue M, Yin L, Feng L & Liu, P. Porcine intestinal enteroids: A new model for studying enteric coronavirus porcine epidemic diarrhea virus infection and the host innate response. *J. Virol.* 93(5), e01682-18. (2019).
99. Li, D., & Wu, M. Pattern recognition receptors in health and diseases. *Sig Transduct Target Ther.* 6(1): 291. doi: <https://doi.org/10.1038/s41392-021-00687-0>. (2021).
100. Libermann TA & Baltimore D. Activation of interleukin-6 gene expression through the NF-kappa B transcription factor. *Mol. Cell Biol.* 10(5):2327–2334. doi: <https://doi.org/10.1128/mcb.10.5.2327-2334.1990> (1990).
101. Liu J, Deng M, Lancto CA, Abrahamsen MS, Rutherford MS & Enomoto S. Biphasic modulation of apoptotic pathways in *Cryptosporidium parvum*-infected human intestinal epithelial cells. *Infect Immun.* 77(2):837-49. doi: 10.1128/IAI.00955-08. (2009).
102. Liu, J, Deng, M, Lancto, CA, Abrahamsen, MS, Rutherford, MS & Enomoto, S. Biphasic modulation of apoptotic pathways in *Cryptosporidium parvum*-infected human intestinal epithelial cells. *Infect. Immun.* 77(2): 837–849. doi: 10.1128/IAI.00955-08. (2009).
103. Logan JM, Edwards K & Saunders, N. Real-time PCR: current technology and applications. (2009).
104. Lumb J, Smith K, O'Donoghue PJ & Lanser JA. Ultrastructure of the attachment of *Cryptosporidium* sporozoites to tissue culture cells. *Parasitol. Res.* 74(6):531-536. doi: 10.1007/BF00531630. (1988).
105. Masters PS. The Molecular Biology of Coronaviruses. *Adv. Virus Res.* 66: 193-292. doi: [https://doi.org/10.1016/S0065-3527\(06\)66005-3](https://doi.org/10.1016/S0065-3527(06)66005-3). (2006).
106. Matos LVS, McEvoy J, Tzipori S, Bresciani KDS & Widmer G. The transcriptome of *Cryptosporidium* oocysts and intracellular stages. *Sci Rep.* 9(1):7856. doi: 10.1038/s41598-019-44289-x. (2019).

107. Matsubayashi M, Ando H, Kimata I, Nakagawa H, Furuya M, Tani H & Sasai K. Morphological changes and viability of *Cryptosporidium parvum* sporozoites after excystation in cell-free culture media. *Parasitol.* 137(13):1861-6. doi: 10.1017/S0031182010000685. (2010).
108. McCole DF, Eckmann L, Laurent F & Kagnoff MF. Intestinal epithelial cell apoptosis following *Cryptosporidium parvum* infection. *Infect Immun.* 68(3):1710-3. doi: 10.1128/IAI.68.3.1710-1713.2000. (2000).
109. McDonald V, McCrossan MV & Petry F. Localization of parasite antigens in *Cryptosporidium parvum*-infected epithelial cells using monoclonal antibodies. *Parasitol.* 110:259–268. (1995).
110. McDonald V, Pollok RC, Dhaliwal W, Naik S, Farthing MJ & Bajaj-Elliott M. A potential role for interleukin-18 in inhibition of the development of *Cryptosporidium parvum*. *Clin Exp Immunol.* 145:555–562. doi: 10.1111/j.1365-2249.2006.03159.x. (2006).
111. McGavin MD & Carlton W. Thomson Special Veterinary Pathology, 2nd ed, St. Louis: Mosby, p.48-58. (1995).
112. Mebus CA, Stair EL, Rhodes MB & Twiehaus MJ. Pathology of neonatal calf diarrhea induced by a coronavirus-like agent. *Vet. Pathol.* 10(1):45-64. doi: 10.1177/030098587301000105. (1973).
113. Meganck V, Hoflack G & Opsomer G. Advances in prevention and therapy of neonatal dairy calf diarrhoea: a systematical review with emphasis on colostrum management and fluid therapy. *Acta Vet Scand.* 56(1):75. doi: 10.1186/s13028-014-0075-x. (2014).
114. Meloni BP & Thompson RC. Simplified methods for obtaining purified oocysts from mice and for growing *Cryptosporidium parvum* *in vitro*. *J. Parasitol.* 82(5):757-762. (1996).
115. Miller CN, Jossé L, Brown I, Blakeman B, Povey J, Yiangou L, Price M, Cinatl J Jr, Xue WF, Michaelis M & Tsaousis AD. A cell culture platform for *Cryptosporidium* that enables long-term cultivation and new tools for the systematic investigation of its biology. *Int J Parasitol.* 48(3-4):197-201. doi: 10.1016/j.ijpara.2017.10.001. (2018).
116. Mogensen TH & Paludan SR. Molecular pathways in virus-induced cytokine production. *Microbiol Mol Biol Rev.* 65(1):131-50. doi: 10.1128/MMBR.65.1.131-150.2001. (2001).
117. Morada M, Lee S, Gunther-Cummins L, Weiss LM, Widmer G, Tzipori S & Yarlett N. Continuous culture of *Cryptosporidium parvum* using hollow fibre

- technology. *Int J Parasitol.* 46(1):21-9. doi: 10.1016/j.ijpara.2015.07.006. (2016).
118. Morenikeji OB, Strutton E, Wallace M, Bernard K, Yip E & Thomas BN. Dissecting Transcription Factor-Target Interaction in Bovine Coronavirus Infection. *Microorganisms.* 8(9):1323. doi: 10.3390/microorganisms8091323. (2020).
 119. Ohlson, A, Heuer, C, Lockhart, C, Tråvén, M, Emanuelson, U & Alenius, S. Risk factors for seropositivity to bovine coronavirus and bovine respiratory syncytial virus in dairy herds. *Vet. Rec.* 167, 201–206. doi: <http://dx.doi.org/10.1136/vr.c4119>. (2010).
 120. Ok, M, Yildiz, R, Hatipoglu, F, Baspinar, N, Ider, M, Üney, K, Ertürk, A, Durgut, M.K & Terzi, F. Use of intestine-related biomarkers for detecting intestinal epithelial damage in neonatal calves with diarrhea. *Am. J. Vet. Res.* 81: 139-146. doi: 10.2460/ajvr.81.2.139. (2020).
 121. Oma, VS, Tråvén, M, Alenius, S, Myrnel, M & Stokstad, M. Bovine coronavirus in naturally and experimentally exposed calves, viral shedding, and the potential for transmission. *Virol. J.* 13, 1–11. doi: <https://doi.org/10.1186/s12985-016-0555-x>. (2016).
 122. Østerås, O, Solbu, H, Refsdal, AO, Roalkvam, T, Filseth, O & Minsaas, A. Results and evaluation of thirty years of health recordings in the Norwegian dairy cattle population. *J. Dairy Sci.* 90(9):4483-4497. (2007).
 123. Paluszynski J, Monahan Z, Williams M, Lai O, Morris C, Burns P & O'Connor R. Biochemical and functional characterization of CpMuc4, a *Cryptosporidium* surface antigen that binds to host epithelial cells. *Mol Biochem Parasitol.* 193(2):114-21. doi: 10.1016/j.molbiopara.2014.03.005. (2014).
 124. Park, SJ, Kim, GY, Choy, HE, Hong, YJ, Saif, LJ, Jeong, JH, Park, SI, Kim, HH, Kim, SK, Shin, SS, Kang, MI & Cho, KO. Dual enteric and respiratory tropisms of winter dysentery bovine coronavirus in calves. *Arch. Virol.* 152: 1885–1900. doi: 10.1007/s00705-007-1005-2. (2007).
 125. Payne, HR, Storz, J & Henk, WG. Bovine coronavirus antigen in the host cell plasmalemma. *Exp. Mol. Pathol.* 53, (2) 152-9. doi: 10.1016/0014-4800(90)90039-g. (1990).
 126. Perez-Cordon G, Yang G, Zhou B, Nie W, Li S, Shi L, Tzipori S & Feng H. Interaction of *Cryptosporidium parvum* with mouse dendritic cells leads to their activation and parasite transportation to mesenteric lymph nodes. *Pathog Dis.* 70(1):17–27. doi: 10.1111/2049-632X.12078. (2014).

127. Pestana EA, Belák S, Diallo A, Crowther JR & Viljoen GJ. Early, rapid and sensitive veterinary molecular diagnostics - Real time PCR applications. ed. E. Pestana et al. (Springer Netherlands, Dordrecht) p. 27. doi: <http://dx.doi.org/10.1007/978-90-481-3132-7>. (2010).
128. Pinheiro, FA, Decaris, N, Parreño, V, Brandão, PE, Ayres, H, & Gomes, V. Efficacy of prepartum vaccination against neonatal calf diarrhea in Nelore dams as a prevention measure. *BMC Vet Res.* 18 (1):1-14. doi: <https://doi.org/10.1186/s12917-022-03391-5>. (2022).
129. Plutzer J & Karanis P. Genotype and subtype analyses of *Cryptosporidium* isolates from cattle in Hungary. *Vet Parasitol.* 146(3-4):357–362. doi: 10.1016/j.vetpar.2007.02.030. (2007).
130. Priyamvada S, Jayawardena D, Bhalala J, Kumar A, Anbazhagan AN, Alrefai WA, Borthakur A & Dudeja PK. *Cryptosporidium parvum* infection induces autophagy in intestinal epithelial cells. *Cell Microbiol.* 23(4): e13298. doi: 10.1111/cmi.13298. (2021).
131. Quílez J, Torres E, Chalmers RM, Robinson G, Del Cacho E & Sanchez-Acedo C. *Cryptosporidium* species and subtype analysis from dairy calves in Spain. *Parasitol.* 135(14):1613–20. doi: 10.1017/S0031182008005088. (2008).
132. Ravindranath MH, Higa HH, Cooper EL & Paulson JC. Purification and characterization of an O-acetyl sialic acid-specific lectin from a marine crab *Cancer antennarius*. *J Biol Chem.* 260(15):8850-6. (1985).
133. Renaud DL, Rot C, Marshall J & Steele MA. The effect of *Cryptosporidium parvum*, rotavirus, and coronavirus infection on the health and performance of male dairy calves. *J. Dairy Sci.*104(2):2151-2163. doi: 10.3168/jds.2020-19215 (2021).
134. Robertson LJ, Campbell AT & Smith HV. In vitro excystation of *Cryptosporidium parvum*. *Parasitol.* 106 (Pt 1):13-9. doi: 10.1017/s003118200007476x. (1993).
135. Robertson, LJ, Bjorkman, C, Axen, C & Fayer, R. Cryptosporidiosis in Farmed Animals. *Cryptosporidium: Parasite and Disease.* 17:149–235. (2014).
136. Robinson, G, Pérez-Cordón, G, Hamilton, C, Katzer, F, Connelly, L, Alexander, CL & Chalmers, RM. Validation of a multilocus genotyping scheme for subtyping *Cryptosporidium parvum* for epidemiological purposes. *Food Waterborne Parasitol.* 27: e00151. doi: <https://doi.org/10.1016/j.fawpar.2022.e00151>. (2022).

137. Ryan, U, Fayer, R & Xiao, L. *Cryptosporidium* species in humans and animals: Current understanding and research needs. *Parasitol.* 141(13): 1667–1685. doi: <https://doi.org/10.1017/S0031182014001085>. (2014).
138. Ryan, UM, Feng, Y, Fayer, R & Xiao, L. Taxonomy and molecular epidemiology of *Cryptosporidium* and *Giardia*—a 50-year perspective (1971–2021). *Int. J. Parasitol.* 51 (13-14):1099-1119. doi: <https://doi.org/10.1016/j.ijpara.2021.08.007>. (2021).
139. Sa Ribero, M, Jouvenet, N, Dreux, M & Nisole, S. Interplay between SARS-CoV-2 and the type I interferon response. *PLoS Pathog.* 16(7), e1008737. doi: <https://doi.org/10.1371/journal.ppat.1008737> (2020).
140. Sadeghi A, Tahmasebi S, Mahmood A, Kuznetsova M, Valizadeh H, Taghizadieh A, Nazemiyeh M, Aghebati-Maleki L, Jadidi-Niaragh F, Abbaspour-Aghdam S, Roshangar L, Mikaeili H & Ahmadi M. Th17 and Treg cells function in SARS-CoV2 patients compared with healthy controls. *J Cell Physiol.* 236(4):2829-2839. doi: 10.1002/jcp.30047. (2021).
141. Sahu U, Biswas D, Prajapati VK, Singh AK, Samant M & Khare P. Interleukin-17-A multifaceted cytokine in viral infections. *J Cell Physiol.* 236(12):8000-8019. doi: 10.1002/jcp.30471. (2021).
142. Saif LJ, Alhamo M. Bovine coronavirus infection. In Coetzer JAW, Thomson GR, Maclachlan NJ, Penrith ML (ed), *Infectious diseases of livestock*, 3rd ed. Oxford University Press, Oxford, United Kingdom. doi: <https://anipedia.org/resources/bovine-coronavirus-infection/1033>. (2018).
143. Saif LJ, Redman DR, Moorhead PD & Theil KW. Experimentally induced coronavirus infections in calves: viral replication in the respiratory and intestinal tracts. *Am. J. Vet. Res.* 47(7):1426-1432. (1986).
144. Saif, LJ & Jung, K. Comparative pathogenesis of bovine and porcine respiratory coronaviruses in the animal host species and SARS-CoV-2 in humans. *J. Clin. Microbiol.* 58, e01355-20. doi: <https://doi.org/10.1128/JCM.01355-20>. (2020).
145. Saif, LJ. Bovine respiratory coronavirus. *Vet. Clin. North Am. Food Anim. Pract.* 26(2): 349-364. doi: 10.1016/j.cvfa.2010.04.005. (2010).
146. Sato T, van Es JH, Snippert HJ, Stange DE, Vries RG, van den Born M, Barker N, Shroyer NF, van de Wetering M & Clevers H. Paneth cells constitute the niche for Lgr5 stem cells in intestinal crypts. *Nature.* 469(7330):415–418. doi: 10.1038/nature09637. (2011).

147. Schmid S, Sachs D & tenOever BR. Mitogen-activated protein kinase-mediated licensing of interferon regulatory factor 3/7 reinforces the cell response to virus. *J Biol Chem.* 289(1):299-311. doi: 10.1074/jbc.M113.519934. (2014).
148. Schultze B & Herrler G. Bovine coronavirus uses N-acetyl-9-O-acetylneuraminic acid as a receptor determinant to initiate the infection of cultured cells. *J Gen Virol.*73(4):901-6. doi: 10.1099/0022-1317-73-4-901. (1992).
149. Schultze B, Wahn K, Klenk HD & Herrler G. Isolated HE-protein from hemagglutinating encephalomyelitis virus and bovine coronavirus has receptor destroying and receptor-binding activity. *Virology.* 180:221-8. doi: 10.1016/0042-6822(91)90026-8. (1991).
150. Schwegmann-Wessels C & Herrler G. Sialic acids as receptor determinants for coronaviruses. *Glycoconj J.* 23(1-2):51-8. doi: 10.1007/s10719-006-5437-9. (2006).
151. Seeger B. Farm animal-derived models of the intestinal epithelium: recent advances and future applications of intestinal organoids. *Altern Lab An.* 48(5-6):215–233. doi: 10.1177/0261192920974026. (2020).
152. Seth RB, Sun LJ, Ea CK & Chen ZJJ. Identification and characterization of MAVS, a mitochondrial antiviral signalling protein that activates NF-kappa B and IRF3. *Cell.* 122(5):669–682. doi: <https://doi.org/10.1016/j.cell.2005.08.012>. (2005).
153. Shaw HJ, Innes EA, Morrison LJ, Katzer F & Wells B. Long-term production effects of clinical cryptosporidiosis in neonatal calves. *Int. J. Parasitol.* 50(5):371-376. doi: 10.1016/j.ijpara.2020.03.002 (2020).
154. Silverlås C, Björkman C & Egenvall. A Systematic review and meta-analyses of the effects of halofuginone against calf cryptosporidiosis. *Prev Vet Med.* 91(2-4):73-84. doi: 10.1016/j.prevetmed.2009.05.003. (2009).
155. Silverlås C, Bosaeus-Reineck H, Näslund K & Björkman C. Is there a need for improved *Cryptosporidium* diagnostics in Swedish calves? *Int J Parasitol.* 43:155–161. doi: 10.1016/j.ijpara.2012.10.009. (2013).
156. Silverlås C, de Verdier K, Emanuelson U, Mattsson JG & Björkman C. *Cryptosporidium* infection in herds with and without calf diarrhoeal problems. *Parasitol Res.* 107(6):1435-44. doi: 10.1007/s00436-010-2020-x. (2010).
157. Singh S, Singh R, Singh KP, Singh V, Malik YPS, Kamdi B, Singh R & Kashyap G. Immunohistochemical and molecular detection of natural cases of bovine

- rotavirus and coronavirus infection causing enteritis in dairy calves. *Microb Pathog.* 138:103814. doi: 10.1016/j.micpath.2019.103814. (2020).
158. Soba B & Logar J. Genetic classification of *Cryptosporidium* isolates from humans and calves in Slovenia. *Parasitol.* 135(11):1263–1270. doi: 10.1017/S0031182008004800. (2008).
159. Stokstad M, Klem TB, Myrmet M, Oma VS, Toftaker I, Østerås O, Nødtvedt A. Using Biosecurity Measures to Combat Respiratory Disease in Cattle: The Norwegian Control Program for Bovine Respiratory Syncytial Virus and Bovine Coronavirus. *Front Vet Sci.* 7:167. doi: 10.3389/fvets.2020.00167. (2020).
160. Sutton KM, Orr B, Hope J, Jensen SR & Vervelde L. Establishment of bovine 3D enteroid-derived 2D monolayers. *Vet Res.* 53(1):15. doi: 10.1186/s13567-022-01033-0. (2022).
161. Szczepanski A, Owczarek K, Bzowska M, Gula K, Drebot I, Ochman M, Maksym B, Rajfur Z, Mitchell JA & Pyrc K. Canine Respiratory Coronavirus, Bovine Coronavirus, and Human Coronavirus OC43: Receptors and Attachment Factors. *Viruses.* 11(4):328. doi: 10.3390/v11040328. (2019).
162. Szonyi B, Chang YF, Wade SE & Mohammed HO. Evaluation of factors associated with the risk of infection with *Cryptosporidium parvum* in dairy calves. *Am J Vet Res.* 73(1):76–85. doi: <https://doi.org/10.2460/ajvr.73.1.76>. (2012).
163. Takeuchi, O, & Akira, S. Pattern recognition receptors and inflammation. *Cell.* 140(6): 805-820. doi: <https://doi.org/10.1016/j.cell.2010.01.022>. (2010).
164. Thomson S, Hamilton CA, Hope JC, Katzer F, Mabbott NA, Morrison LJ & Innes EA. Bovine cryptosporidiosis: impact, host-parasite interaction, and control strategies. *Vet Res.* 48(1):42. doi: 10.1186/s13567-017-0447-0. (2017).
165. Thomson S, Innes EA, Jonsson NN & Katzer F. Shedding of *Cryptosporidium* in calves and dams: evidence of re-infection and shedding of different gp60 subtypes. *Parasitol.* 146(11):1404-1413. doi: 10.1017/S0031182019000829. (2019).
166. Toftaker I, Sanchez J, Stokstad M & Nødtvedt A. Bovine respiratory syncytial virus and bovine coronavirus antibodies in bulk tank milk - risk factors and spatial analysis. *Prev. Vet. Med.* 133:73-83. doi: 10.1016/j.prevetmed.2016.09.003. (2016).

167. Tråvén, M, Näslund, K, Linde, N, Linde, B, Silván, A, Fossum, C, Hedlund, KO & Larsson, B. Experimental reproduction of winter dysentery in lactating cows using BCV -- comparison with BCV infection in milk-fed calves. *Vet. Microbiol.* 81(2): 127-151. doi: [https://doi.org/10.1016/S0378-1135\(01\)00337-6](https://doi.org/10.1016/S0378-1135(01)00337-6). (2001).
168. Tråvén, M., 2000. Winter dysentery caused by bovine coronavirus; no rule without an exception: diagnostics, clinical picture, epidemiology, and herd immunology. Dissertation, Swedish University of Agricultural Science, Uppsala.
169. Trotz-Williams LA, Wayne Martin S, Leslie KE, Duffield T, Nydam DV & Peregrine AS. Calf-level risk factors for neonatal diarrhea and shedding of *Cryptosporidium parvum* in Ontario dairy calves. *Prev. Vet. Med.* 82(1):12-28. doi: 10.1016/j.prevetmed.2007.05.003. (2007).
170. Tyzzer EE. *Cryptosporidium parvum* (sp. nov.), a coccidium found in the small intestine of the common mouse. *Arch. Protistenkd.* 26:394-412. (1912).
171. Valasek MA & Repa JJ. The power of real-time PCR. *Adv Physiol Educ.* 29(3):151-9. doi: 10.1152/advan.00019.2005. PMID: 16109794. (2005).
172. Van Metre DC, Tennant BC, Whitlock RH. Infectious Diseases of the Gastrointestinal Tract. *Rebhun's Diseases of Dairy Cattle.* 200-94. doi: 10.1016/B978-141603137-6.50009-0. (2008).
173. Vandenbroucke RE, Dejonckheere E, Van Hauwermeiren F, Lodens S, De Rycke R, Van Wonterghem E, Staes A, Gevaert K, López-Otin C, Libert C. Matrix metalloproteinase 13 modulates intestinal epithelial barrier integrity in inflammatory diseases by activating TNF. *EMBO Mol Med.* 5(7):1000-16. doi: 10.1002/emmm.201202100. (2013).
174. Vélez J, Silva LMR, Kamena F, Dauschies A, Mazurek S, Taubert A & Hermosilla C. The Oesophageal Squamous Cell Carcinoma Cell Line COLO-680N Fails to Support Sustained *Cryptosporidium parvum* Proliferation. *Pathogens.* 11(1):49. doi: 10.3390/pathogens11010049. (2022).
175. Vermeulen SJ, Chen TR, Speleman F, Nollet F, Van Roy FM & Mareel MM. Did the four human cancer cell lines DLD-1, HCT-15, HCT-8, and HRT-18 originate from one and the same patient? *Cancer Genet Cytogenet.* 107(1):76-9. doi: 10.1016/s0165-4608(98)00081-8. (1998).
176. Vlasova AN & Saif LJ. Bovine Coronavirus and the Associated Diseases. *Front Vet Sci.* 8:643220. doi: 10.3389/fvets.2021.643220. (2021).

177. Wei, X, Wang, W, Dong, Z, Cheng, F, Zhou, X, Li, B, & Zhang, J. Detection of infectious agents causing neonatal calf diarrhea on two large dairy farms in Yangxin County, Shandong Province, China. *Front. Vet. Sci.* 7, 589126. doi: <https://doi.org/10.3389/fvets.2020.589126>. (2021).
178. Windeyer MC, Leslie KE, Godden SM, Hodgins DC, Lissemore KD & LeBlanc SJ. Factors associated with morbidity, mortality, and growth of dairy heifer calves up to 3 months of age. *Prev Vet Med.* 113(2):231-40. doi: [10.1016/j.prevetmed.2013.10.019](https://doi.org/10.1016/j.prevetmed.2013.10.019). (2014).
179. Woodmansee DB & Pohlenz JFL. Development of *Cryptosporidium* sp. in a human rectal tumour cell line, p. 306-319. In Proceedings of the Fourth International Symposium on Neonatal Diarrhea. Veterinary Infectious Disease Organization, University of Saskatchewan, Saskatoon, Canada. (1983).
180. Xiao L. Molecular epidemiology of cryptosporidiosis: an update. *Exp Parasitol.* 124(1):80-89. doi: <https://doi.org/10.1016/j.exppara.2009.03.018>. (2010).
181. Xiao, L, Fayer, R, Ryan, U & Upton, S. *Cryptosporidium* taxonomy: recent advances and implications for public health. *Clin. Microbiol. Rev.* 17:72-97. doi: <https://doi.org/10.1128/cmr.17.1.72-97.2004>. (2004).
182. Yang N, Zhang Y, Fu Y, Li Y, Yang S, Chen J & Liu G. Transmissible gastroenteritis virus infection promotes the self-renewal of porcine intestinal stem cells via Wnt/-Catenin pathway. *J. Virol.* 96(18): e0096222. doi: [10.1128/jvi.00962-22](https://doi.org/10.1128/jvi.00962-22). (2022).
183. Yang Z, Fu Y, Gong P, Zheng J, Liu L, Yu Y, Li J, Li H, Yang J & Zhang X. Bovine TLR2 and TLR4 mediate *Cryptosporidium parvum* recognition in bovine intestinal epithelial cells. *Microb Pathog.* 85:29-34. doi: [10.1016/j.micpath.2015.05.009](https://doi.org/10.1016/j.micpath.2015.05.009). (2015).
184. Zambriski JA, Nydam DV, Bowman DD, Bellosa ML, Burton AJ, Linden TC, Liotta JL, Ollivett TL, Tondello-Martins L & Mohammed HO. Description of fecal shedding of *Cryptosporidium parvum* oocysts in experimentally challenged dairy calves. *Parasitol Res.* 112(3):1247-54. doi: [10.1007/s00436-012-3258-2](https://doi.org/10.1007/s00436-012-3258-2). (2013).
185. Zelová H & Hošek J. TNF- α signalling and inflammation: interactions between old acquaintances. *Inflamm Res.* 62(7):641-51. doi: [10.1007/s00011-013-0633-0](https://doi.org/10.1007/s00011-013-0633-0). (2013).

186. Zhao GH, Fang YQ, Ryan U, Guo YX, Wu F, Du SZ, Chen DK & Lin Q. Dynamics of Th17 associating cytokines in *Cryptosporidium parvum*-infected mice. *Parasitol Res.* 115(2):879-87. doi: 10.1007/s00436-015-4831-2. (2016).
187. Zou WY, Blutt SE, Crawford SE, Ettayebi K, Zeng XL, Saxena K, Ramani S, Karandikar UC, Zachos NC & Estes MK. Human Intestinal Enteroids: New Models to Study Gastrointestinal Virus Infections. *Methods Mol Biol.* 1576:229-247. doi: 10.1007/7651_2017_1. (2019).

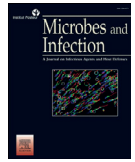
15 Papers

Paper I



Contents lists available at ScienceDirect

Microbes and Infection

journal homepage: www.elsevier.com/locate/micinf

Original article

Interactions between *Cryptosporidium parvum* and bovine coronavirus during sequential and simultaneous infection of HCT-8 cells

Ruchika Shakya*, Alejandro Jiménez Meléndez, Lucy J. Robertson, Mette Myrmel

Norwegian University of Life Sciences, Faculty of Veterinary Medicine, Department of Paraclinical Sciences, 1430 Ås, Norway



ARTICLE INFO

Article history:

Received 1 February 2021

Accepted 5 November 2021

Available online 20 November 2021

Keywords:

HCT-8

Cryptosporidium parvum

Bovine coronavirus

Co-infection

ABSTRACT

Neonatal diarrhoea in calves is one of the major health problems in the cattle industry. Although co-infections are often associated with greater severity of disease, there is limited information on any impact on the pathogens themselves. Herein, we studied *Cryptosporidium parvum* and bovine coronavirus (BCoV) in human HCT-8 cells, inoculated either sequentially or simultaneously, to investigate any influence from the co-infections. Quantitative results from (RT)-qPCR showed that prior inoculation with either of the two pathogens had no influence on the other. However, the results from simultaneous co-inoculation showed that entry of viral particles was higher when *C. parvum* sporozoites were present, although elevated virus copy numbers were no longer evident after 24 h. The attachment of BCoV to the sporozoites was probably due to specific binding, as investigations with bovine norovirus or equine herpes virus-1 showed no attachment between sporozoites and these viruses. Flow cytometry results at 72 h post inoculation revealed that *C. parvum* and BCoV infected 1–11% and 10–20% of the HCT-8 cells, respectively, with only 0.04% of individual cells showing double infections. The results from confocal microscopy corroborated those results, showing an increase in foci of infection from 24 to 72 h post inoculation for both pathogens, but with few double infected cells.

© 2021 The Author(s). Published by Elsevier Masson SAS on behalf of Institut Pasteur. This is an open access article under the CC BY license (<http://creativecommons.org/licenses/by/4.0/>).

Intestinal infections causing diarrhoea are major health problems in calves that may result in increased mortality rate and reduced weight gain [1]. According to the Norwegian Dairy Herd Recording System, diarrhoea accounts for almost 40% of calf diseases in Norway [2]. Multiple parameters are associated with the mechanism and characteristics (severity, persistence, etc.) of calf diarrhoea, including host, agent, and environmental factors [3,4]. Young calves are highly susceptible to gastroenteritis during their first month of life. Rotavirus (RoV), bovine coronavirus (BCoV) and *Cryptosporidium parvum* are the most prevalent (75–95%) enteropathogens among neonatal calves under 3 weeks of age [5,6]. In Spain, *C. parvum* was the most commonly detected enteropathogen in calves with diarrhoea (52%), and RoV and BCoV were detected in 87% and 11%, respectively, of the calves infected with *C. parvum* [6]. A two-year study in Norwegian dairy herds showed that RoV and *C. parvum* were the most common enteric pathogens responsible for diarrhoea, and that seropositivity in calves for BCoV (>72%) indicated active or newly introduced virus in the herd [7]. Mixed infections are more common among diarrhoeal calves than in

healthy calves, and co-infection with BCoV and *C. parvum* has been associated with reduced growth [1,8]. Anecdotal information indicates that co-infections with BCoV and *C. parvum* are associated with greater symptom severity [9,10].

Cryptosporidium spp. are intracellular protist parasites in the phylum Apicomplexa. There are more than 30 species of *Cryptosporidium*, some of which are host-specific, whereas others, in particular zoonotic *C. parvum*, are infectious to multiple species. Host infection occurs when *Cryptosporidium* oocysts (ca. 5 µm diameter) are ingested, excyst in the intestine, and the released sporozoites attach to, and invade, epithelial host cells [11].

Bovine coronavirus belongs to the family *Coronaviridae*, genus *Betacoronavirus*. They are enveloped viruses measuring about 120–160 nm in diameter with a positive sense, single-stranded RNA (+ssRNA) genome of 32 Kb [12]. Betacoronaviruses are highly variable and use several different attachment and entry receptors. The BCoV binds to the glycan layer, N-acetyl neuraminic acid (Neu5Ac), present on epithelial cells in the airways and the intestine [13,14] and causes respiratory and intestinal infections [15,16].

As both BCoV and *C. parvum* infect the enterocytes in the small intestine of calves [17,18], interactions between them and their host cells are of great interest. Field studies are unsuitable for

* Corresponding author.

E-mail address: ruchika.shakya@nmbu.no (R. Shakya).

investigating the mechanism and the severity of such co-infections but controlled experimental studies may provide useful knowledge. However, studies using experimentally infected animals are costly, time-consuming, require a high number of individuals, and have an ethical dimension. Experiments using *in vitro* models may be an alternative approach that enables investigation of specific questions [19], in a relatively less-complex format.

The main aim of the present study was to investigate the following question: Is there an influence from one pathogen on the other during co-infection?

To our knowledge, such *in vitro* studies have not previously been conducted but have the potential to provide information on relevant pathogen–pathogen interactions, host–pathogen interactions, and possible mechanisms associated with pathogenicity.

1. Materials and methods

1.1. Cell culture

The human ileocecal colorectal adenocarcinoma cell line (HCT-8, ATCC CCL-244) was kindly provided by Professor Elisabeth A. Innes and Alison Burrells (Moredun Research Institute, Scotland). The HCT-8 cells were grown in T75 flasks (Thermo Fisher Scientific, Grand Island, NY, USA) employing RPMI 1640 (Thermo Fisher Scientific) supplemented with 10% foetal bovine serum (FBS) (Thermo Fisher Scientific), 2% L-glutamine, and 1% Penicillin Streptomycin (PenStrep) (Life Technologies, Paisley, Scotland), and split every three to four days. After thorough re-suspension, approximately $8E+03$ and $4E+04$ cells were seeded per well in Nunc™ 96 and 24-well flat-bottom plates (Thermo Fisher Scientific), respectively, and incubated until 60% confluence before inoculation with pathogens. Culture of cells and pathogens was performed in a humidified incubator at 37 °C with 5% CO₂. A maintenance medium, consisting of RPMI 1640 with 2% FBS, 2% L-glutamine, and 1% PenStrep, was used during culture of the pathogens. The cells used in the experiment were from passages 16–20.

1.2. Excystation of *C. parvum*

C. parvum oocysts (Iowa-II strain) were obtained from Bunch Grass Farm (Deary, ID, USA). All oocysts were used for the *in vitro* assays within 3 months of arrival. Prior to excystation, the viability of each batch of oocysts was assessed by inclusion/exclusion of 4',6-diamino-2-phenylindole/propidium iodide (DAPI/PI) as previously described [20].

The oocysts were pre-treated with 6% sodium hypochlorite [21] and excysted as previously described [22]. The oocysts were washed four times and resuspended in phosphate-buffered saline (PBS). Once resuspended, 0.05% Trypsin-EDTA (Life Technologies) with 2% HCl (Merck Life Sciences, Darmstadt, Germany) was added, and the oocysts placed in a water bath at 37 °C for 30 min. The suspension was centrifuged at $4000\times g$ for 8 min at 4 °C and the pellet resuspended in PBS along with 2.2% sodium bicarbonate (Merck Life Sciences) and 1% sodium taurodeoxycholate (Sigma–Aldrich, St. Louis, MO, USA) and incubated in a 37 °C water bath for 1 h. The excysted sporozoites were resuspended in RPMI 1640 without FBS and passed through a 3 µm filter (Merck Millipore) to remove oocyst shells and non-excysted oocysts. The motility of the sporozoites was observed by microscopy, and intactness analysed by trypan blue exclusion. The excystation rate was estimated to be 85–90%.

1.3. Viruses

The BCoV strain originated from a calf faecal sample and had previously been isolated in our lab using the human rectal tumour

cell line HRT-18G [23]. This isolate was adapted to the HCT-8 cells during several passages, i.e., the virus was incubated on the cells for 1 h, before adding maintenance medium, and the supernatant was harvested after 5 days. The isolate was titrated on HCT-8 cells grown in a 96-well plate by ten-fold serial dilutions, using the Spearman-Kärber method [24] ($TCID_{50}/ml = 1.0E+07$). A clear cytopathic effect was observed in the cells after 3 days of culture.

For further investigation of some of the results in the present study, bovine norovirus (BNoV) and equine herpesvirus (EHV-1) were included in limited setups to compare with setups using BCoV.

The BNoV isolate, which originated from a calf faecal sample [25], was diluted 1:10 in PBS, vortexed for 30 s, and centrifuged ($1200\times g$ for 20 min). The supernatant was used in the experiment. To date, it has not been possible to culture BNoV in a commercial cell line.

The isolate of EHV-1 had previously been passaged in Madin–Darby bovine kidney cells (MDBK, ATCC CCL-22) in our lab.

All viruses were aliquoted and stored at –80 °C before use.

1.4. Study design

To study any influence of BCoV on *C. parvum* infection and replication in HCT-8 cells, and vice versa, various experimental set ups were included (Supplementary fig. 1). The HCT-8 cells were cultured with: (i) BCoV for 24 h, followed by introduction of *C. parvum* and further incubation of 24 h; (ii) *C. parvum* for 24 h, followed by introduction of BCoV and further incubation of 24 h, and (iii) BCoV and *C. parvum* simultaneously introduced in a mixed inoculum for 24 h. All experiments were carried out in 96-well plates, at least twice, and with three or more biological replicates. In all setups, BCoV ($1E+05$ $TCID_{50}$) and *C. parvum* sporozoites ($8E+04$), assuming each viable oocyst to contain 4 infective sporozoites, were added to each well with cells at 60% confluency. Over confluence was not observed, even after 72 h post inoculation (hpi). Pathogen suspensions were prepared in RPMI without FBS. All set ups included positive controls (i.e., cells inoculated with BCoV or *C. parvum* in same amounts as in test samples), and negative controls (cells inoculated with RPMI without FBS).

1.4.1. Sequential inoculations

HCT-8 cells were primarily inoculated with BCoV suspension. After 1 h incubation, the suspension was removed, the cells washed, and maintenance medium added. At 24 hpi, the suspension was removed, the cells washed once with PBS, and *C. parvum* sporozoite suspension added onto the cells. The cells were incubated for 1 h, the inoculum with any free sporozoites removed, the cells washed with PBS and incubated for another 24 h with maintenance medium prior to harvest. Positive controls were inoculations of same amounts of *C. parvum* in separate wells and harvested at the same time point (Supplementary fig 1A).

C. parvum inoculation followed by BCoV was carried out likewise with sporozoites inoculated per well, followed by inoculation with BCoV after 24 hpi. Positive controls were inoculations of same amounts of BCoV in separate wells and harvested at the same time point (Supplementary fig 1B).

1.4.2. Simultaneous inoculations

1.4.2.1. BCoV and *C. parvum*. The BCoV and the *C. parvum* sporozoite suspensions were mixed 1:1 and placed in a stirring water bath at 37 °C together with separate BCoV and *C. parvum* suspensions diluted 1:2 in medium (positive controls). After 1 h of incubation, the viability of the sporozoites was assessed by trypan blue exclusion and the suspensions were added onto the cells. After 1 h incubation, the suspension was removed, the cells washed once

with PBS, and maintenance medium was added. Samples for 1 hpi analysis were harvested after 1 h incubation, whereas the others were harvested after 24 h (Supplementary fig 1C).

1.4.2.2. C. parvum with BNoV or EHV-1. Suspensions of BNoV or EHV-1, together with excysted *C. parvum* sporozoites, were prepared and treated in a similar manner as described in section 2.4.2.1. After 1 h, the suspensions were added to wells containing a 60% confluent monolayer of HCT-8 cells. Positive controls were inoculations of same amounts of BNoV or EHV-1 in separate wells. The HCT-8 cells are not permissive for EHV-1 and BNoV. The intention was to investigate whether EHV-1 and/or BNoV would interact with the sporozoites.

1.5. Extraction of total nucleic acids

After the incubation period, media was removed, and the cells washed twice with PBS. NucliSENS miniMAG Lysis Buffer (350 µl) (Biomerieux, Marcy l'Etoile, France) was added to the cells and the lysate homogenized by pipetting several times. Total nucleic acids (NAs) were extracted from the lysates using the manufacturer's NucliSens miniMAG protocol. The NAs were eluted in 100 µl buffer and stored at -80 °C until analysis.

1.6. (RT)-qPCRs

Information on the primers, probes, and (RT)-qPCR conditions is provided in Supplementary Table 1.

RT-qPCR for BCoV and BNoV was performed using the RNA UltraSense™ One-Step Quantitative RT-PCR System kit (Invitrogen, MA, USA), as previously described [26].

Real-time PCR for *C. parvum* and EHV-1 was performed using TaqMan Environmental Master Mix 2.0 (Life Technologies), as previously described for *C. parvum* [27], and for EHV-1 [28].

All (RT)-qPCR reactions were carried out in a total volume of 20 µl with 2 µl of template NA, using a Stratagene AriaMx Real-Time PCR System (Agilent Technologies, Inc., USA), with Agilent Aria Software v1.5. All reactions were run in technical duplicates, with negative and positive controls included in each run.

The efficiencies of the BCoV and *C. parvum* (RT)-qPCRs were estimated from standard curves made on 10-fold and 4-fold serial dilution series of NAs from the respective pathogens (Supplementary fig 2A and B).

1.7. Flow cytometry

HCT-8 cells were grown to 60% confluency on 24-well plates and inoculated with BCoV (2.5E+05 TCID₅₀) and *C. parvum* sporozoites (1.6E+05) in separate wells or as mixed inoculum, in biological triplicates and in several setups.

After 1 h incubation, the suspension was removed, the cells washed once with PBS, and maintenance medium added. The plates were further incubated for 72 h and the cells washed once with PBS. After being dissociated by 1x TrypLE Express enzyme (Life Technologies) for 5–10 min, the cells were resuspended in medium with 2% FBS, and centrifuged (3400×g at 4 °C) for 8 min. Cells were held on ice after centrifugation and throughout the procedure. The cells were resuspended at ~2E+05 cells/ml in 1x flow buffer (Dulbecco's PBS with 0.05% sodium azide) with 2% bovine serum albumin (BSA) (Merck Life Sciences), transferred to a round-bottom 96-well flow plate and centrifuged for 5 min, 250 ×g at 4 °C. The supernatant was removed, and the pellet homogenized in a shaker at 1050 rpm for 30 s. The cells were fixed with IC Fixation buffer (eBioscience, 131 San Diego, CA, USA) at room temperature for

20 min, washed with permeabilization buffer (eBioscience), and blocked using PBS with 2% BSA and 0.1% Tween 20.

Antibodies were diluted in permeabilization buffer. For BCoV, monoclonal mouse anti-BCoV antibody (1:100) labelled with fluorescein isothiocyanate (FITC) (Bio-X Diagnostics, Rochefort, Belgium), and for *C. parvum*, 1x Sporoglo™ (Waterborne Inc, New Orleans, LA, USA), Cy3-labelled rat anti-*C. parvum* polyclonal antibodies (1:20) were used. After incubation in the dark for 1 h, the cells were washed with flow buffer, and R-phycoerythrin (RPE) tagged goat anti-rat IgG, (1:500) (Thermo Fisher Scientific) was added. After 20 min of incubation in the dark, cells were washed and resuspended in 1x flow buffer before filtration through Flowmi® Cell Strainers 40 µm (Merck Life Sciences) to break cell clumps. A minimum of 2E+04 cells per sample were analysed using the Gallios Flow Cytometer (Beckman Coulter, 135 Miami, FL, USA) and the data examined with the Kaluza software (Becton Dickinson).

1.8. Confocal microscopy

HCT-8 cells were grown to 60% confluency on 12 mm glass coverslips in 24-well plates and inoculated with BCoV (2.5E+05 TCID₅₀) and *C. parvum* sporozoites (1.6E+05) in triplicates, as previously described (Section 2.4.2.1). After 1 h incubation, the suspension was removed, the cells were washed once with PBS, and maintenance medium was added. The plates were further incubated for 24, 48, and 72 h. Following removal of media, the cells were washed twice with cold 1x flow buffer, fixed, permeabilized, and blocked as described in section 2.7. Anti-BCoV antibodies labelled with FITC (1:80) and 1x Sporoglo™ labelled with Cy3 (1:20) in permeabilization buffer were added to the cells and the plates incubated in the dark for 1 h. The cells were washed, counterstained with Hoechst 33342 (1:10,000) (Invitrogen), and the coverslips transferred onto slides with Fluoroshield (Sigma-Aldrich). The slides were examined using a confocal laser scanning microscope (Leica TCS SP5, Wetzlar, Germany), with several fields (at least 10) examined, and images captured at 40× magnification under oil immersion.

1.9. Relative enumeration of pathogens and statistical analysis

Based on Ct values and the efficiency (E) of the (RT)-qPCR reactions, relative quantification of BCoV and *C. parvum* copies was performed using the formula $Ns1 = Ns2 * (1+E)^{(Cts2-Cts1)}$ [29], where Ns1 and Ns2 represent sample copy numbers of BCoV or *C. parvum*, Cts1 and Cts2 are sample Ct values, and E the efficiency of the (RT)-qPCRs. For BCoV, E = 0.98 and for *C. parvum*, E = 0.93, based on the results from the standard curves. To compare the copy numbers of BCoV and *C. parvum* between groups of single and co-infected cells, the nonparametric Mann-Whitney U test was used for independent samples. Two-way analysis, to determine the influence of one pathogen on another, with a significance level of 0.05, was performed after visual inspection of the Ct-values.

2. Results

2.1. Viral and *C. parvum* copy number as determined by (RT)-qPCR

2.1.1. Sequential inoculations

The difference in *C. parvum* copy number was not statistically significant between cells with or without primary inoculation with BCoV (U = 28, p = 0.48) (Table 1).

Likewise, the difference in viral RNA copy number between cells with or without primary inoculation with *C. parvum* was not statistically significant (U = 25, p = 0.62) (Table 1).

Table 1
C. parvum and BCoV copy numbers during sequential and simultaneous infection of HCT-8 cells at 1 and 24 h post inoculation. Samples were analysed by (RT)-qPCR.

Inoculum	Harvest time point (hpi)	Median copy number (log ₁₀)		IQR (log ₁₀)	Number of replicates
		<i>C. parvum</i>	BCoV		
<i>C. parvum</i> (control) ^a	24	5.74	–	5.54–5.94	6
BCoV then <i>C. parvum</i> ^a	24	5.91	–	5.77–5.97	12
BCoV (control) ^b	24	–	6.95	6.91–7.10	6
<i>C. parvum</i> then BCoV ^b	24	–	7.07	6.91–7.32	10
<i>C. parvum</i> (control) ^c	1	5.02	–	4.53–5.16	9
<i>C. parvum</i> + BCoV ^c	1	4.79	–	4.41–5.13	9
<i>C. parvum</i> (control) ^c	24	5.82	–	5.42–5.87	9
<i>C. parvum</i> + BCoV ^c	24	5.65	–	5.16–5.82	9
BCoV (control) ^c	1	–	4.98*	4.76–5.23	27
<i>C. parvum</i> + BCoV ^c	1	–	5.48*	5.24–5.61	27
BCoV (control) ^c	24	–	7.10	6.92–7.16	27
<i>C. parvum</i> + BCoV ^c	24	–	7.12	6.83–7.27	27

Abbreviations, hpi: hours post inoculation, IQR = Inter quartile range, p = p-value.

*Statistically significant difference; p < 0.005.

^a Inoculation of cells with BCoV followed by *C. parvum*.

^b Inoculation of cells with *C. parvum* followed by BCoV.

^c Simultaneous inoculation of cells with *C. parvum* and BCoV.

2.1.2. Simultaneous inoculations

At 1 hpi and 24 hpi, the difference in *C. parvum* copy number between cells with or without co-inoculation with BCoV was not statistically significant (1h: U = 30.5, p = 0.40; 24h: U = 27, p = 0.25) (Table 1, Fig. 1A).

At 1 hpi, cells co-inoculated with BCoV and *C. parvum* had a statistically significantly higher (approximately threefold) number of viral RNA than cells inoculated with BCoV alone (U = 156.5, p = 0.00034) (Table 1, Fig. 1B).

At 24 hpi, the difference in viral RNA copies for cells with or without *C. parvum* co-inoculation was not statistically significant (U = 326, p = 0.51) (Table 1, Fig. 1B).

2.1.3. BNoV or EHV-1 during simultaneous inoculation with *C. parvum*

At 1 hpi, the Ct-value of both BNoV or EHV-1 was the same, regardless of whether the viruses were inoculated onto the cells alone or together with *C. parvum* (Table 2). The difference in Ct-values for BNoV (U = 11.5, p = 0.34) (n = 6) or EHV-1 (U = 15, p = 0.62) (n = 6) between cells with or without *C. parvum* was not statistically significant.

2.2. Estimate of proportions of infected cells by flow cytometry

The proportions of infected HCT-8 cells when inoculated with single pathogens, either *C. parvum* or BCoV, were 1–11% and (average 7%) 10–20% (average 16%), respectively. Fig. 2 shows representative results. Analyses of cells inoculated with both pathogens showed double infection in approximately 0.04% of cells (data not shown).

2.3. Confocal microscopy

The results from the confocal microscopy (Supplementary fig 3) showed an increase in foci of infection from 24 to 72 hpi for both pathogens. However, possible co-localization of both pathogens in the same cells was only noted in some areas (Fig. 3 and Supplementary fig 3), and large areas of cells were not infected with either BCoV or *C. parvum*.

3. Discussion

The most interesting finding from this study was that during simultaneous infection of HCT-8 cells with BCoV and *C. parvum*, at 1

hpi there was approximately three times more viral RNA copies than in cells inoculated with BCoV alone. As there is no virus replication at this early time point, this finding suggests an increased entry of BCoV into the cells in the presence of *C. parvum* sporozoites. We speculate that this increase is due to BCoV attaching to the sporozoites during co-incubation, and thereby gaining access to cells, along with the sporozoites. Given that the sporozoites are denser than free virus particles and probably settle more rapidly on the cells (Stokes' Law), and that sporozoites are independently motile and actively seek out cells to infect [30,31], any viral particles attached to them will likely enter cells more rapidly than free virus particles.

We chose to conduct a co-incubation (1 h at 37 °C) prior to the simultaneous inoculation in order to provide additional time for the two pathogens (BCoV and *C. parvum*) to interact, as could occur in vivo. The controls (single inoculum) were treated identically to our test samples. Any reduction in sporozoite infectivity during the co-incubation step might have reduced binding of BCoV to the sporozoites, as well as internalization of the sporozoites. This would have reduced, and not increased, the difference between samples and controls.

However, after 24 h of culture there was no difference in viral RNA copy numbers in cells inoculated with BCoV alone and cells inoculated with both pathogens. One explanation could be a general suppression of virus replication due to an antiviral effect induced by *C. parvum*. However, such an effect was not found in cells primarily inoculated with *C. parvum*. It is more likely that viral particles entering the cells while attached to sporozoites were prevented from replication. Firstly, the sporozoites could transport BCoV into cells less supportive of virus replication, reflecting a non-compatibility between BCoV and sporozoites due to different life cycles and replication requirements. Secondly, the attachment to sporozoites could have prevented BCoV from entering the cellular cytoplasmic compartment, which is crucial for virus replication [32]. Sporozoites have a unique location in the parasitophorous vacuole (PV), which is formed when the sporozoites enter the cell. Here, the sporozoites become enclosed by the host cell membrane, forming the PV, in which the replicating sporozoites have an intracellular, but extra-cytoplasmic, location [11]. Any BCoV that attaches to the sporozoites will probably be trapped in the PV, with no attachment to receptors, no fusion of the envelope with the cell membrane, and thus no access to the cell cytoplasm.

There are several possibilities for attachment of BCoV to *C. parvum* sporozoites; one of the most feasible is attachment

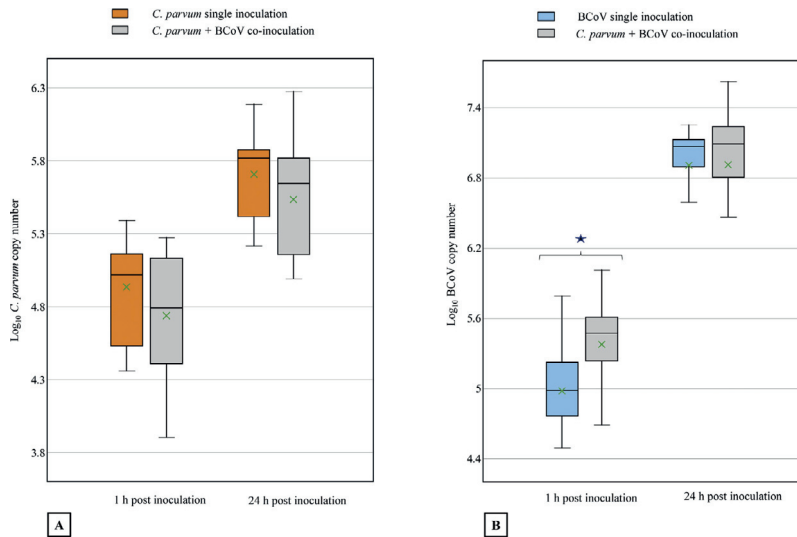


Fig. 1. A. *Cryptosporidium parvum* copy number for HCT-8 cells inoculated with either *C. parvum* or bovine coronavirus and *C. parvum*, simultaneously, at 1h and 24 h post inoculation. **B.** The viral RNA copy number for HCT-8 cells inoculated with either BCoV alone or BCoV and *C. parvum*, simultaneously, at 1h and 24 h post inoculation. On each box, the central mark indicates the median, x marks the mean, and the bottom and top edges of the box indicate the 25th and 75th percentiles, respectively.

Table 2

Ct-values for bovine norovirus RNA and equine herpes virus type-1 DNA. HCT-8 cells were inoculated with BNoV or EHV-1 (virus only) and with BNoV or EHV-1 and *C. parvum*. The cells were harvested at 1 h post inoculation.

Viruses	Average Ct-values ± SD			p-value	U-value	Z score
	Virus inoculum	Inoculated cells (Virus only)	Inoculated cells (Virus and <i>C. parvum</i>)			
BNoV	32.7	39.4 ± 0.7	39.8 ± 0.2	0.34	11.5	-0.96
EHV-1	25.4	32.1 ± 0.9	32.1 ± 1.3	0.62	15	0.40

Abbreviations: SD, standard deviation.

via carbohydrates on the sporozoite surface. Previous studies have suggested that viruses may bind to bacteria [33,34]. Human NoV was able to specifically bind to histo-blood group

antigens on extracellular polymeric substances of *Enterobacter cloacae* [35]. A similar study has also indicated bacterial–viral interaction with human NoV-like particles attaching to

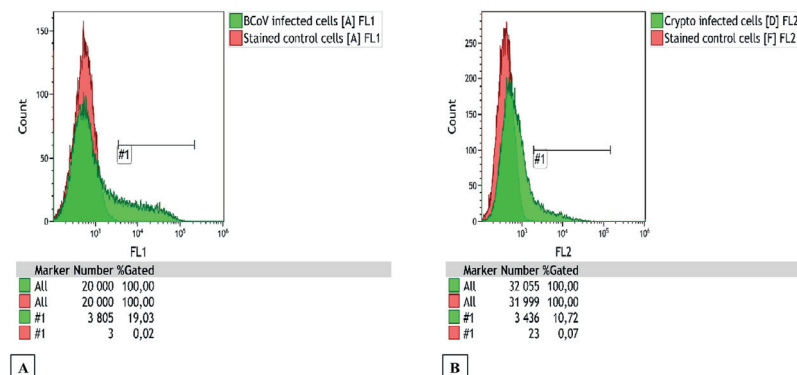


Fig. 2. Flow cytometry results showing stained control HCT-8 cells and cells inoculated with BCoV or *C. parvum* at 72 h post inoculation. The cells were permeabilized before staining with **A.** Fluorescein isothiocyanate (FITC)-labelled anti-BCoV antibodies, and **B.** primary anti-*C. parvum* antibodies and R-phycoerythrin (RPE)-labelled secondary antibodies. Histogram overlays show the fluorescence of infected (green) and uninfected cells (red). The tables present the number of cells analysed (Number) and the percentage of cells positive (#1, % Gated).

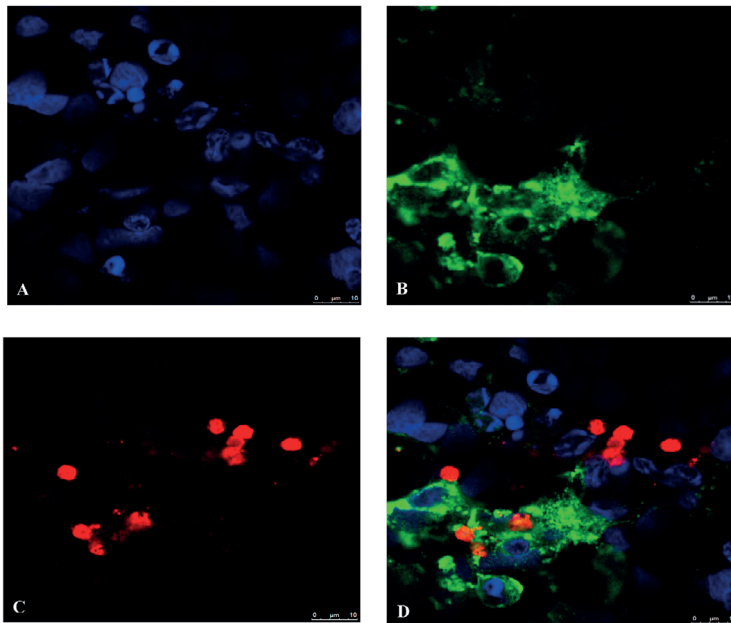


Fig. 3. Representative confocal images of HCT-8 cells co-infected with BCoV and *C. parvum* at 72 h post inoculation. Magnification = 40 x, Scale bar = 10 μ m. **A.** cell nuclei stained with Hoechst (blue), **B.** cells infected with BCoV (green), **C.** *C. parvum* merozoites in infected cells (red) and, **D.** overlaid image. Magnification = 40 x, Scale bar = 10 μ m.

Staphylococcus aureus, *Bacillus* spp., *Citrobacter* spp., and several other bacteria [33].

Viruses typically attach to target cells by binding to the glycan layer [36] that is present on the host cell membrane [37]. Neu5AC is the receptor for BCoV and is expressed on many mammalian cell surfaces. Although Neu5AC is essential for primary binding of BCoV to the cell surface, the human leukocyte antigen class I (HLA-I) could serve as entry receptor [38].

Several studies have shown that the *C. parvum* sporozoites contain both O-linked and N-linked glycosylated proteins (mucins) such as GP900 [39], Gp 40, Gp15 [40] and Muc4 [41]. Hence, there is a possibility that BCoV could attach to mucins on the surface of sporozoites. However, less specific attachment (for example, by Van der Waals forces) could also have been a possibility. To elucidate whether attachment of BCoV to *C. parvum* sporozoites was characteristic of this specific pathogen or could apply to viruses with either similar or different surface structures, the experiment was repeated with the sporozoites and two other viruses. Equine herpesvirus-1 has a morphology similar to BCoV, although it is larger, with a diameter of 150–250 nm. The virus belongs to *Herpesviridae*, and is covered by a lipid envelope, like BCoV [42]. The EHV-1 receptor is the MHC-1 protein complex on some equine cells [40]. BNoV is very different to BCoV in morphology, as it is a small (27–40 nm in diameter) naked virus, without a lipid envelope, and belongs to the *Caliciviridae*. Like BCoV, BNoV binds to carbohydrate receptors, but different ones, on enterocytes [43].

As our results provide no evidence of attachment between either BNoV or EHV-1 and the sporozoites, it seems likely that attachment of BCoV to the sporozoites is via a specific primary binding, rather than by non-specific attachment. Further studies are needed to identify the molecules behind such an attachment, e.g., to look for, or block, a possible Neu5AC receptor for BCoV on the sporozoite surface using, for example, the *Cancer antennarius* lectin [44].

One reason that we see no influence of BCoV on *C. parvum* replication and vice versa in this study could be due to low permissiveness of the HCT-8 cells to both pathogens. The flow cytometry results at 72 h revealed that *C. parvum* and BCoV infected between 1–11% and 10–20% of the HCT-8 cells, respectively. This low permissiveness might be explained by the different cell populations comprising the HCT-8 cell line [45]. Microscopy of the HCT-8 cells showed a heterogeneous population, which may present differences in permissiveness to BCoV and *C. parvum*. The confocal microscopy images indicated an increase over time in foci of infection for both pathogens, with some double-infected cells at later time points showing that both pathogens were able to infect the HCT-8 cells and proliferate with time (Supplementary fig 3). Although, some areas of the cells were positive for both pathogens, it is not possible to determine whether the same cells were infected in these instances. Nevertheless, a small number of co-infected individual cells was corroborated using flow cytometry.

Although cell cultures are cost-effective systems for studying co-infections, there are inherent limitations to these in vitro models. Most of the cell lines derived from tumour cells, particularly human cells, undergo genetic and morphological alterations after continuous or a long-term use [46]. Due to the absence of well-characterized bovine intestinal epithelial cell lines or primary cell cultures supporting the growth of both pathogens, the human ileocecal adenocarcinoma (HCT-8) cell line, [11,47], was used for investigation of the co-infections.

As with all in vitro studies, extrapolating from our results to in vivo infection is complicated due to a multitude of factors, including the host microbiome, host responses, and generally a more complex environment. However, the binding between BCoV and sporozoites seems to be specific and to result in BCoV particles getting trapped in PV and not being able to replicate as any attachment to sporozoites would reduce access to the cell cytoplasm.

Future studies should employ host cells of bovine origin, to obtain a more host-specific outcome and study of pathogenesis. A higher infection rate and better understanding of BCoV and *C. parvum* co-infections might also be obtained using bovine enteroids, comprising a mixed 3-dimensional population of cells [48]. Indeed, the complete lytic cycle of *C. parvum* has been achieved using human intestinal organoids [49], and such a model could provide a better reflection of the in vivo situation. However, to date, studies showing replication of BCoV or *C. parvum* in bovine organoids have not been published.

4. Conclusions

The present study demonstrated that, sequential inoculation of the HCT-8 cells with BCoV and *C. parvum* did not provide any advantage – or disadvantage – to either infectious agent. Although the results from simultaneous infection showed that more virus entered the cells when *C. parvum* sporozoites were also present, an increased virus copy number was not found after culture for 24 h. This is most likely due to the virus becoming trapped in the PV and thus unable to enter the cytoplasm for replication. Moreover, the attachment of BCoV to the *C. parvum* sporozoites seems to be specific as the EHV-1 and BNoV did not bind to the sporozoites.

Declaration of competing interest

The authors declare that they have no conflicts of interest.

Acknowledgements

This project was supported by internal funding from the Virology and Parasitology Unit, NMBU. We would like to thank Mamata Khatri for all the help in the laboratory. Preben Boysen for helping us with the gating for the flow set up. Hilde Raanaas Kolstad at Imaging Centre, NMBU for technical assistance on confocal microscopy. Britt Gjerset and Lars Austbø at the Norwegian Veterinary Institute for providing primers, probes, and qPCR protocol for the EHV-1.

Appendix A. Supplementary data

Supplementary data to this article can be found online at <https://doi.org/10.1016/j.micinf.2021.104909>.

References

- [1] Shaw HJ, Innes EA, Morrison LJ, Katzer F, Wells B. Long-term production effects of clinical cryptosporidiosis in neonatal calves. *Int J Parasitol* 2020;50(5):371–6.
- [2] Gulliksen SM, Jor E, Lie KI, Hammes IS, Løken T, Åkerstedt J, et al. Enteropathogens and risk factors for diarrhea in Norwegian dairy calves. *J Dairy Sci* 2009;92(10):5057–66.
- [3] Clement J, King M, Salman M, Wittum T, Casper H, Odde K. Use of epidemiologic principles to identify risk factors associated with the development of diarrhea in calves in five beef herds. *J Am Vet Med Assoc* 1995;207(10):1334–8.
- [4] Svensson C, Lundborg K, Emanuelson U, Olsson S-O. Morbidity in Swedish dairy calves from birth to 90 days of age and individual calf-level risk factors for infectious diseases. *Prev Vet Med* 2003;58(3–4):179–97.
- [5] Bendali F, Bicher H, Schelcher F, Sanaa M. Pattern of diarrhoea in newborn beef calves in south-west France. *Vet Res* 1999;30(1):61–74.
- [6] Garcia A, Ruiz-Santa-Quiteria J, Orden J, Cid D, Sanz R, Gómez-Bautista M, et al. Rotavirus and concurrent infections with other enteropathogens in neonatal diarrheic dairy calves in Spain. *Comp Immunol Microbiol Infect Dis* 2000;23(3):175–83.
- [7] Gulliksen SM, Lie KI, Østerås O. Calf health monitoring in Norwegian dairy herds. *J Dairy Sci* 2009;92(4):1660–9.
- [8] Renaud DL, Rot C, Marshall J, Steele MA. The effect of *Cryptosporidium parvum*, rotavirus, and coronavirus infection on the health and performance of male dairy calves. *J Dairy Sci* 2021;104(2):2151–63.
- [9] Gomez DE, Weese JS. Viral enteritis in calves. *Can Vet J* 2017;58(12):1267–74.
- [10] Trotz-Williams LA, Wayne Martin S, Leslie KE, Duffield T, Nydam DV, Peregrine AS. Calf-level risk factors for neonatal diarrhea and shedding of *Cryptosporidium parvum* in Ontario dairy calves. *Prev Vet Med* 2007;82(1):12–28.
- [11] Thomson S, Hamilton CA, Hope JC, Katzer F, Mabbott NA, Morrison LJ, et al. Bovine cryptosporidiosis: impact, host-parasite interaction and control strategies. *Vet Res* 2017;48(1):42.
- [12] ICTV. Coronaviridae. EC 50, Washington, DC, July 2018. 2019. https://talk.ictvonline.org/ictv-reports/ictv_9th_report/positive-sense-rna-viruses-2011/w/posrna_viruses/222/coronaviridae.
- [13] Schultze B, Herrler G. Bovine coronavirus uses N-acetyl-9-O-acetylneuraminic acid as a receptor determinant to initiate the infection of cultured cells. *J Gen Virol* 1992;73(4):901–6.
- [14] Schwegmann-Wessels C, Herrler G. Sialic acids as receptor determinants for coronaviruses. *Glycoconj J* 2006;23(1–2):51–8.
- [15] Saif IJ, Redman D, Moorhead P, Theil K. Experimentally induced coronavirus infections in calves: viral replication in the respiratory and intestinal tracts. *Am J Vet Res* 1986;47(7):1426–32.
- [16] Park SJ, Kim GY, Choy HE, Hong YJ, Saif IJ, Jeong JH, et al. Dual enteric and respiratory tropisms of winter dysentery bovine coronavirus in calves. *Arch Virol* 2007;152(10):1885–90.
- [17] Cho YI, Yoon KJ. An overview of calf diarrhoea-infectious etiology, diagnosis, and intervention. *J Vet Sci* 2014;15(1):1–17.
- [18] Foster DM, Smith GW. Pathophysiology of diarrhea in calves. *Vet Clin North Am Food Anim Pract* 2009;25(1):13–xi.
- [19] Blanchard PC. Diagnostics of dairy and beef cattle diarrhea. *Vet Clin North Am Food Anim Pract* 2012;28:22.
- [20] Campbell AT, Robertson LJ, Smith HV. Viability of *Cryptosporidium parvum* oocysts: correlation of in vitro excystation with inclusion or exclusion of fluorogenic vital dyes. *Appl Environ Microbiol* 1992;58(11):3488–93.
- [21] Woolsey ID, Blomstrand B, Øines Ø, Enemark HL. Assessment of differences between DNA content of cell-cultured and freely suspended oocysts of *Cryptosporidium parvum* and their suitability as DNA standards in qPCR. *Parasit Vectors* 2019;12(1):596.
- [22] Robertson LJ, Campbell AT, Smith HV. In vitro excystation of *Cryptosporidium parvum*. *Parasitology* 1993 Jan;106(Pt 1):13–9. <https://doi.org/10.1017/s003118200007476x>. PMID: 8479797.
- [23] Oma VS, Tråven M, Alenius S, Myrmet M, Stokstad M. Bovine coronavirus in naturally and experimentally exposed calves; viral shedding and the potential for transmission. *Virology* 2016;53(1):100.
- [24] Ramakrishnan MA. Determination of 50% endpoint titer using a simple formula. *World J Virol* 2016;5(2):85–6.
- [25] Jor E, Myrmet M, Jonassen CM. SYBR Green based real-time RT-PCR assay for detection and genotype prediction of bovine noroviruses and assessment of clinical significance in Norway. *J Virol Methods* 2010;169(1):1–7.
- [26] Christensen E, Myrmet M. Coagulant residues' influence on virus enumeration as shown in a study on virus removal using aluminium, zirconium and chitosan. *J Water Health* 2018;16(4):600–13.
- [27] Di Giovanni GD, LeChevallier MW. Quantitative-PCR assessment of *Cryptosporidium parvum* cell culture infection. *Appl Environ Microbiol* 2005;71(3):1495–500.
- [28] Manual OI. Manual of diagnostic tests and vaccines for terrestrial animals. Paris, France: OIE; 2018. <https://www.oie.int/standard-setting/terrestrial-manual/access-online/>.
- [29] Livak KJ, Schmittgen TD. Analysis of relative gene expression data using real-time quantitative PCR and the 2^{-ΔΔCT} method. *Methods* 2001;25(4):402–8.
- [30] Wetzel DM, Schmidt J, Kuhlenschmidt MS, Dubey JP, Sibley LD. Gliding motility leads to active cellular invasion by *Cryptosporidium parvum* sporozoites. *Infect Immun* 2005;73(9):5379–87.
- [31] Bouzid M, Hunter PR, Chalmers RM, Tyler KM. *Cryptosporidium* pathogenicity and virulence. *Clin Microbiol Rev* 2013;26(1):115–34.
- [32] Fehr AR, Perlman S. Coronaviruses: an overview of their replication and pathogenesis. In: Maier HJ, Bickerton E, Britton P, editors. *Coronaviruses: methods and protocols*. New York, NY: Springer New York; 2015. p. 1–23.
- [33] Almand EA, Moore MD, Outlaw J, Jaykus LA. Human norovirus binding to select bacteria representative of the human gut microbiota. *PLoS One* 2017;12(3):e0173124.
- [34] Neu U, Mainou BA. Virus interactions with bacteria: partners in the infectious dance. *PLoS Pathog* 2020;16(2):e1008234.
- [35] Miura T, Sano D, Suenaga A, Yoshimura T, Fuzawa M, Nakagomi T, et al. Histo-blood group antigen-like substances of human enteric bacteria as specific adsorbents for human noroviruses. *J Virol* 2013;87(17):9441–51.
- [36] Ströh LJ, Stehle T. Glycan engagement by viruses: receptor switches and specificity. *Annu Rev Virol* 2014;1(1):285–306.
- [37] Thompson AJ, de Vries RP, Paulson JC. Virus recognition of glycan receptors. *Curr Opin Virol* 2019;34:117–29.
- [38] Szczepanski A, Owczarek K, Bzowska M, Gula K, Drebót I, Ochman M, et al. Canine respiratory coronavirus, bovine coronavirus, and human coronavirus OC43: receptors and attachment factors. *Viruses* 2019;11(4).
- [39] Cevallos AM, Bhat N, Verdon R, Hamer DH, Stein B, Tzipori S, et al. Mediation of *Cryptosporidium parvum* infection in vitro by mucin-like glycoproteins defined by a neutralizing monoclonal antibody. *Infect Immun* 2000;68(9):5167–75.

- [40] Cevallos AM, Zhang X, Waldor MK, Jaison S, Zhou X, Tzipori S, et al. Molecular cloning and expression of a gene encoding *Cryptosporidium parvum* glycoproteins gp40 and gp15. *Infect Immun* 2000 Jul;68(7):4108–16. <https://doi.org/10.1128/IAI.68.7.4108-4116.2000>. PMID: 10858228; PMCID: PMC101706.
- [41] Paluszynski J, Monahan Z, Williams M, Lai O, Morris C, Burns P, et al. Biochemical and functional characterization of CpMuc4, a *Cryptosporidium* surface antigen that binds to host epithelial cells. *Mol Biochem Parasitol* 2014 Feb;193(2):114–21. <https://doi.org/10.1016/j.molbiopara.2014.03.005>. Epub 2014 Mar 29. PMID: 24690740; PMCID: PMC4073680.
- [42] Sasaki M, Hasebe R, Makino Y, Suzuki T, Fukushi H, Okamoto M, et al. Equine major histocompatibility complex class I molecules act as entry receptors that bind to equine herpesvirus-1 glycoprotein D. *Gene Cell* 2011;16(4):343–57.
- [43] Shirato H. Norovirus and histo-blood group antigens. *Jpn J Infect Dis* 2011;64(2):95–103.
- [44] Park SS. Post-glycosylation modification of sialic acid and its role in virus pathogenesis. *Vaccines (Basel)* 2019;7(4).
- [45] Barbat A, Pandrea I, Cambier D, Zweibaum A, Lesuffleur T. Resistance of the human colon carcinoma cell line HCT-8 to methotrexate results in selection of cells with features of enterocytic differentiation. *Int J Cancer* 1998 Mar 2;75(5):731–7. [https://doi.org/10.1002/\(sici\)1097-0215\(19980302\)75:5<731::aid-ijc11>3.0.co;2-9](https://doi.org/10.1002/(sici)1097-0215(19980302)75:5<731::aid-ijc11>3.0.co;2-9). PMID: 9495241.
- [46] Kleensang A, Vantangoli MM, Odwin-DaCosta S, Andersen ME, Boekelheide K, Bouhifd M, et al. Genetic variability in a frozen batch of MCF-7 cells invisible in routine authentication affecting cell function. *Sci Rep* 2016;6(1):28994.
- [47] Park SJ, Jeong C, Yoon SS, Choy HE, Saif IJ, Park S-H, et al. Detection and characterization of bovine coronaviruses in fecal specimens of adult cattle with diarrhea during the warmer seasons. *J Clin Microbiol* 2006;44(9):3178–88.
- [48] Hamilton CA, Young R, Jayaraman S, Sehgal A, Paxton E, Thomson S, et al. Development of in vitro enteroids derived from bovine small intestinal crypts. *Vet Res* 2018;49(1):54.
- [49] Heo I, Dutta D, Schaefer DA, Jakobachvili N, Arteghiani B, Sachs N, et al. Modelling *Cryptosporidium* infection in human small intestinal and lung organoids. *Nat Microbiol* 2018;3(7):814–23.

Paper II

Gene expression profile of HCT-8 cells following single or co-infections with *Cryptosporidium parvum* and bovine coronavirus

Alejandro JIMENEZ-MELENDZ (✉ Alejandro.jimenez.melendez@nmbu.no)

Norwegian University of Life Sciences (NMBU)

Ruchika SHAKYA

Norwegian University of Life Sciences (NMBU)

Turhan MARKUSSEN

Norwegian University of Life Sciences (NMBU)

Lucy J. ROBERTSON

Norwegian University of Life Sciences (NMBU)

Mette MYRMEL

Norwegian University of Life Sciences (NMBU)

Shokouh MAKVANDI-NEJAD


Norwegian Veterinary Institute

Article

Keywords: Bovine coronavirus, *Cryptosporidium parvum*, RNA-Seq, Neonatal diarrhoea

Posted Date: March 23rd, 2023

DOI: <https://doi.org/10.21203/rs.3.rs-2673942/v1>

License:  This work is licensed under a Creative Commons Attribution 4.0 International License. [Read Full License](#)

Abstract

Among the causative agents of neonatal diarrhoea in calves, two of the most prevalent are bovine coronavirus (BCoV) and the intracellular parasite *Cryptosporidium parvum*. Although several studies indicate that co-infections are associated with greater symptom severity, the host-pathogen interplay remains unresolved. Here, our main objective was to investigate the modulation of the transcriptome of HCT-8 cells during single and co-infections with BCoV and *C. parvum*. For this, HCT-8 cells were inoculated with (1) BCoV alone, (2) *C. parvum* alone, (3) BCoV and *C. parvum* simultaneously. After 24 and 72 h, cells were harvested and analyzed using high-throughput RNA sequencing. Following differential expression analysis, over 6000 differentially expressed genes (DEGs) were identified in virus and co-infected cells at 72 hpi, whereas only 52 DEGs were found in *C. parvum*-infected cells at the same time point. Pathway (KEGG) and gene ontology (GO) analysis showed that DEGs in the virus-infected and co-infected cells were mostly associated with immune pathways (such as NFK β , TNF α or, IL-17), apoptosis and regulation of transcription, with a more limited effect exerted by *C. parvum*. Although the modulation observed in the co-infection was apparently dominated by the virus, over 800 DEGs were uniquely expressed in co-infected cells at 72 hpi. Our findings provide insights on possible biomarkers associated with co-infection, which could be further explored using *in vivo* models.

1. Introduction

Neonatal diarrhoea affects calves worldwide [1, 2], adversely impacting animal welfare and leading to vast economic losses. Although calf diarrhoea can be attributed to non-infectious factors (e.g., diet and environment) [3, 4], several enteric pathogens may also be involved, such as enterotoxigenic *Escherichia coli*, *Cryptosporidium* spp., bovine rotavirus, and bovine coronavirus (BCoV) [5]. *Cryptosporidium parvum* is responsible for severe profuse diarrhoea in calves, which can lead to dehydration and death and can also have long-term health effects, such as reduced weight gain and respiratory disease later in life [6, 7]. BCoV, a β -coronavirus, is another prevalent cattle pathogen [8], causing respiratory and diarrhoeal diseases in calves and winter dysentery in adult cattle [9, 10].

Both BCoV and *C. parvum* infect enterocytes in the small intestines of calves [11, 12]. Pathogens involved in the calf neonatal diarrhoea complex frequently occur as co-infections [3, 13, 14]. Although several studies indicate that BCoV and *C. parvum* co-infections are associated with greater symptom severity [15, 16], the host-pathogen and pathogen-pathogen interplays remain mainly unknown. For exploration of the pathogenesis in such infections and the host-pathogen interplay, *in vitro* models offer several advantages over costly and cumbersome *in vivo* models; environmental factors can be controlled, and several experimental replicates are easily achievable. *In vitro* transcription studies of *C. parvum*, investigating its pathogenicity at early stages of infection, have revealed modulation of pathways such as cell cycle [17] and interferon type I (IFN-I) responses [17, 18, 19, 20, 21]. However, compared with other apicomplexan parasites, *Cryptosporidium* might exert a more limited stimulation of host immune responses due to its unique location, being intracellular but extracytoplasmic [22]. Furthermore, *C. parvum*, depends on the host-cell carbon metabolism cycle for nutrient acquisition, as previously described for other related Apicomplexa, such as *Toxoplasma gondii* [23, 24, 25]. In comparison with other apicomplexan parasites, *C. parvum* has a more restricted metabolism, lacking functional mitochondria and with various metabolic pathways lost during evolution, relying entirely on host glycolysis for nutrient acquisition [26]. In contrast, viruses, including coronaviruses, are known to exert a broad effect on host cellular responses, involving, among others, stimulation of immune mechanisms mediated by IFN-I. However, they have also evolved mechanisms to counteract the host antiviral responses [27]. To our knowledge, there have been no *in vitro* studies on the host transcriptome in response to BCoV infection. Despite the prevalence of co-infections with *C. parvum* and BCoV, there is only one *in vitro* study on the co-infection. In that study, interactions between the two pathogens were reported, with increased entry of the virus into host HCT-8 cells when the pathogens were co-inoculated [28]. However, the host immune response to the co-infection was not investigated.

Here, our aim was to compare the differential gene expression profiles of HCT-8 cells following single and co-infections with *C. parvum* and BCoV by means of high-throughput RNA sequencing.

2. Materials & Methods

2.1 Cell culture

A human ileocecal colorectal adenocarcinoma cell line (HCT-8, ATCC CCL-244) was kindly provided by Professor Elisabeth A. Innes and Alison Burrells (Moredun Research Institute, Scotland). The cells were grown in T75 Nunc flasks (Thermo Fisher Scientific, Grand Island, NY, USA) in RPMI 1640 culture medium (Thermo Fisher Scientific) supplemented with 10% foetal bovine serum (FBS) (Thermo Fisher Scientific), 2% L-glutamine, and 1% Penicillin Streptomycin (PenStrep) (Life Technologies, Paisley, Scotland). Culture of cells and incubation/culture of pathogens were performed in a humidified incubator at 37°C with 5% CO₂. After inoculation, a maintenance medium, consisting of RPMI 1640 with 2% FBS, 2% L-glutamine and 1% PenStrep, was employed. The HCT-8 cells used in the experiments were from passage 16–20 and certified as free from *Mycoplasma* spp. by PCR at a commercial facility (Eurofins Genomics).

2.2 Bovine coronavirus (BCoV)

The BCoV strain used in this study was originally isolated from a calf faecal sample and adapted to the human rectal tumour cell line, HRT-18G [9]. This isolate was further adapted to HCT-8 cells during several passages [28], and the supernatant titrated in a 96-well plate by ten-fold serial dilutions, using the Spearman-Kärber method [29] (TCID₅₀/mL = 1.0E + 07), aliquoted and stored at -80°C.

2.3 Excystation of *Cryptosporidium parvum*

C. parvum oocysts (Iowa-II strain) were obtained from Bunch Grass Farm (Deary, ID, USA) and used within one month of receipt. Prior to excystation, the viability was assessed by inclusion/exclusion of 4',6-diamino-2-phenylindole/propidium iodide (DAPI/PI), as previously described by Campbell et al., [30].

The oocysts were pre-treated with 6% sodium hypochlorite and excysted as previously described [28, 31]. Briefly, oocysts were washed, treated with 0.05% trypsin-EDTA (Life Technologies) with 2% HCl (Merck Life Sciences, Darmstadt, Germany), then placed in a water bath at 37°C for 30 min. After washing, the pellet was resuspended in PBS with 2.2% sodium bicarbonate (Merck Life Sciences) and 1% sodium taurodeoxycholate (Sigma-Aldrich, St. Louis, MO, USA). After incubation in a 37°C water bath for 1 h, the excysted sporozoites were resuspended in RPMI 1640 medium without FBS and passed through a 3 µm filter (Merck Millipore) to remove oocyst shells and non-excysted oocysts. The excystation rate was determined by relating the number of oocyst shells plus partially excysted oocysts to the total number of oocysts and calculated to be 85–90%. The motility of the sporozoites was observed by microscopy, and intactness analysed by trypan blue exclusion.

2.4 Cell inoculation

Inoculation of HCT-8 cells was performed in T25 flasks (Sarstedt, Nümbrecht, Germany) seeded with 3E + 05 cells. The cells were grown to 60% confluency, washed with PBS, and inoculated with: i) RPMI without FBS (uninfected control), ii) BCoV, iii) *C. parvum* sporozoites, and iv) *C. parvum* sporozoites together with BCoV. The inocula were kept on the cells for 2 h in a 37°C humidified incubator before washing and adding maintenance medium. The selected multiplicity of infection (MOI) was four for *C. parvum* sporozoites (1.12E + 06 oocysts, assuming one viable oocyst contains 4 sporozoites), and one for BCoV (1.2E + 06 TCID₅₀).

Each of the four experimental groups consisted of 12 replicates, of which six were harvested at 24 hours post inoculation (hpi) and six at 72 hpi, giving a total of 48 samples. Harvesting for RNA-Seq was by direct lysis of the cells

by addition of 1.2 mL of RLT buffer plus DTT (2M) after washing with cold PBS. Lysates were kept at -80°C until RNA extraction.

In parallel, HCT-8 cells grown on 12 mm glass coverslips in 24-well plates were inoculated in the same way to visualize infected cells by immunostaining.

2.5 Immunostaining

Following removal of media, the cells were washed twice with cold Dulbecco's PBS with 0.05% sodium azide and 2% bovine serum albumin (BSA) (Merck Life Sciences). The cells were fixed with IC Fixation buffer (eBioscience, 131 San Diego, CA, USA) at room temperature for 20 min, washed with permeabilization buffer (eBioscience), and blocked using PBS with 2% BSA and 0.1% Tween 20. To stain for BCoV or *C. parvum*, monoclonal mouse anti-BCoV antibodies (1:80) labelled with fluorescein isothiocyanate (FITC; Bio-X Diagnostics, Rochefort, Belgium) or 1x Cy3-labelled polyclonal Sporoglo™ antibody (Waterborne Inc., New Orleans, LA, USA), (1:20) in permeabilization buffer (eBioscience) were used, with co-exposed cells receiving both primary antibodies. After 1 h incubation in the dark, the cells were washed, counterstained with Hoechst 33342 (1:10.000) (Invitrogen, Waltham, MA, USA), and the coverslips transferred onto slides with Fluoroshield (Sigma-Aldrich, St. Louis, MO, USA). The slides were examined using a Leica Inverted Confocal SP5 equipped with a White Light Laser, a Leica HyD Detector (Leica microsystems GmbH, Mannheim, Germany). A minimum of 10 fields were examined per slide, and images were captured at 40 x magnification under oil immersion using the Leica Application Suite software.

2.6 Isolation of total RNA

Total RNA was isolated from the cell lysates using QIAGEN Rneasy Mini Plus Kit (Qiagen, Hilden, Germany), following the manufacturer's instructions, including a gDNA elimination step. RNA concentration was determined using NanoDrop ND-1000 spectrophotometer (ThermoFisher Scientific, Waltham, Massachusetts, USA). The RNA integrity number (RIN) and size distribution were assessed using Bioanalyzer 2100 (Agilent Technologies, Santa Clara, CA, USA). Samples with concentrations of RNA between 0.5 and 5 µg/mL, RINs higher than 9, and 260/280 absorbance ratios higher than 2.0 were included in the study. Samples were normalized to 400 ng/µL before library synthesis.

2.7 Transcriptome sequencing, assembly, annotation, and statistical analysis

Transcriptome libraries were prepared by the Norwegian Sequencing Center (<https://www.Sequencing.uio.no/>) using a TruSeq® Stranded mRNA Library Prep kit, following the manufacturer's protocol. Stranded sequencing was performed on Novaseq 6000 with paired end sequencing at 50 bp, using a Novaseq S1 full flow cell. Following read quality assessment by FastQC (www.bioinformatics.babraham.ac.uk/projects/fastqc/), Trimmomatic was used for quality assessment and trimming low quality bases in order to retain high quality [32]. Reads of low quality (Phred score < 30), low complexity, containing adapter sequences, or with sequences matching ribosomal or mitochondrial RNA, were discarded. Reads were mapped to the CRGh38/hg38 assembly using TopHat (version 2.0.13) [33] and reads with more than a single hit in the genome were discarded. Cufflinks [34, 35] was used to generate transcriptome assemblies for each sequenced sample and merged by Cuffmerge to construct a single gene transfer file. Expression data were normalized via the median of geometric means of fragment counts across all samples, where relative expressions are expressed as fragments per kilobase of exon per million mapped reads (FPKM) values. Cuffdiff was then used to estimate the expression abundances of the assembled genes and transcripts and to test for differential levels of expression between groups (exposed vs non-exposed and single-exposed vs co-exposed). Transcripts with > 1.5-fold difference in expression and corrected *p*-values (*q*-values, false discovery rate (FDR) adjusted) of < 0.05 were assigned as differentially expressed (DE). The heatmaps illustrating the differentially expressed genes (DEGs) were plotted in

RStudio (Version 1.4.1103). For further analysis, only genes that showed no overlapping in infected and uninfected cells replicates were considered.

To assess reproducibility and experimental variation among biological replicates, RNA-Seq data were subjected to principal component analysis (PCA).

2.8 Functional enrichment and network analysis: gene ontology and pathway enrichment

Functional enrichment was performed by assessing gene ontology (GO) terms and pathway analysis, Kyoto Encyclopaedia of Genes (KEGG), and was carried out on our list of DEGs by the online tool String version 11.5 (<https://string-db.org/>) [36] and plotted in RStudio. The analysis was performed against human reference genome with $q\text{-value} < 0.005$ (FDR Benjamini and Hochberg method).

Due to the large number (> 6000) of DEGs in some of the comparisons and limitations of the software employed, further enrichment analyses (GO, KEGG) were performed with the 2000 genes that appeared to be most significantly regulated, either up or down, according to their fold change (FC) and p-adjusted value.

3. Results And Discussion

3.1 Generation of RNA-Seq data and mapping against *Homo sapiens* genome

Using high throughput RNA-Seq, we generated approximately 40 million reads per sample. After alignment, an average of 86% of the high-quality reads were mapped against the reference *Homo sapiens* genome, providing a global indicator of sequencing accuracy (Table 1).

Table 1

RNA-sequencing and genome mapping statistics (million reads) from HCT-8 cells that were uninfected, or infected with bovine coronavirus (BCoV), *Cryptosporidium parvum* or both agents.

	Uninfected (Controls)		BCoV		C. parvum		Co-infected (BCoV + C. parvum)	
	24	72	24	72	24	72	24	72
Post infection timepoint (hpi)	24	72	24	72	24	72	24	72
Raw reads	39.883	40.364	41.346	45.148	47.200	47.672	46.339	39.948
Trimmed reads	38.905	39.453	40.034	43.703	46.070	46.652	45.294	39.046
Mapped reads (<i>Homo sapiens</i>) (%)	97	97	79	72	97	97	78	73

The PCA plot showed that, except for a few anomalies, samples belonging to different biological groups clustered together. The virus-infected and co-infected cells clustered similarly at both 24 and 72 hpi. Uninfected cells clustered with virus-infected and co-infected cells at 24 hpi, and clearly differed from *C. parvum*-infected cells. However, at 72 hpi, uninfected cells clustered more closely with *C. parvum*-infected cells (Fig. 1).

In addition, volcano plots illustrated the higher number of DEGs identified in virus and co-infected cells at 72 hpi (Supplementary Fig. 1). It is important to note that, for both the single and co-infections, immunostaining (Supplementary Fig. 2) showed that the proportion of cells infected with *C. parvum* was lower than those infected with

BCoV. This might have biased the results, as the gene expression profile from fewer *C. parvum*-infected cells might have been diluted by the presence of a significant majority of uninfected or virus-infected cells.

3.2 Host cell transcriptome modulation by bovine coronavirus and *C. parvum*

3.2.1 Single infection with bovine coronavirus and co-infection with *C. parvum* produced stronger modulation of host cell transcriptome than the single infection with *C. parvum*.

The host gene expression profiles for the different biological groups are reflected in the hierarchical analysis (Fig. 2). *C. parvum*-infected cells at 24 hpi showed the lowest number of DEGs (Table 2, Supplementary table 1), whereas the number of DEGs and the general gene expression profile for the BCoV-infected cell were similar to those of the co-infected cells at 24 hpi (Table 2; Supplementary table 1; Figs. 2–3). However, at 72 hpi, a more pronounced effect on the host responses was observed when the cells were infected with BCoV or co-infected, with over 6000 DEGs (Supplementary table 1), visualized by the expression patterns in the cluster heatmaps (Fig. 2). In contrast, only 52 DEGs were identified in *C. parvum*-infected cells (Fig. 3). The highest FC in BCoV-infected cells at 72 hpi was for the gene coding for interleukin-8 (IL-8) (FC = 323.8), which was also the gene with the highest fold change in co-infected cells (FC = 268.5). IL-8 (also termed CXCL-8) is a potent chemoattractant for neutrophils [37, 38] and levels increase in infections with other coronaviruses, such as SARS-CoV-2 [39]. In *C. parvum*-infected cells, the highest FC in expression was displayed by the gene encoding the Early Growth Response 1 (EGR1) (FC = 6.22) at 72 hpi. Increased EGR1 expression in epithelial cells has been associated with stress-induced specific response to pathogens [40] and has been reported to induce apoptosis in *C. parvum*-infected cells [41].

Table 2
Summary of Differential Expressed Genes (DEGs) after single or co-infections of HCT-8 cells.

	BCoV		<i>C. parvum</i>		Co-infected (BCoV + <i>C. parvum</i>)		BCoV vs Co-infected		<i>C. parvum</i> vs co-infected	
	24	72	24	72	24	72	24	72	24	72
Post infection time (hpi)	24	72	24	72	24	72	24	72	24	72
Differentially expressed genes (DEGs)	86	6246	31	52	150	6252	14	26	197	6252
Upregulated genes	80	3197	26	26	141	3085	5	16	165	3234
Downregulated genes	6	3049	5	26	9	3167	9	10	32	3058

When co-infected cells were compared to single infections, there were more similarities in the gene expression profiles between BCoV-infected and co-infected cells than between the *C. parvum*-infected and co-infected cells, as indicated by the higher number of DEGs on the later comparison ($n = 197$ and 6292 at 24 and 72 hpi respectively) (Supplementary table 2). *ANKRD1* (FC = 42) was identified to be expressed with the highest FC in co-infected cells at 24 hpi. At 72 hpi, the gene displaying the highest FC, and overexpressed in co-infected cells, was the one encoding IL-8 (FC = 268.5). Moreover, when DEGs from co-infected cells were compared to those from BCoV-infected, 14 and 26 DEGs were identified in BCoV-infected cells at 24 and 72 hpi, respectively. The highest FC in transcript levels at 24 hpi in BCoV-infected cells was for RP11-211C9.1 (FC = 1.92), and, at 72 hpi, CTC-534B23.1 (FC = 2.3). These findings strongly suggest that BCoV infection was the main contributor to the transcriptome differences observed in the co-infection when compared to the uninfected cells. Despite the similarities shown between only virus-infected and co-infected cells, 78 genes were identified that were only expressed in co-infected cells at 24 hpi, and this number increased to 803 at 72 hpi (Fig. 3), as further described in section 3.2.5.

3.2.2 Gene ontology (GO) analyses show extensive modulation of host cell biological processes after infection

Among the GO terms enriched in our subset of DEGs, it is noteworthy that most of those enriched in BCoV-infected cells at 24 hpi are involved in immune processes, such as cytokine-mediated signalling pathways, inflammatory response, cell chemotaxis, and response to IL-1 (Fig. 4a, Table 3, Supplementary table 4). In contrast, and as reflected in the number of DEGs, the effect of *C. parvum* infection on the host cell immune responses was more limited; the most enriched GO terms *C. parvum*-infected cells at 24 hpi belong to metabolic categories, such as response to purine-containing compounds or hepxilin biosynthesis (Fig. 4b, Table 3, supplementary table 5). The pattern seen in co-infected cells is again more like that seen in BCoV-infected cells, with several GO terms related to immune processes. It should be noted that the GO term “regulation of IL-6 production” appears in co-infected cells and is absent from cells infected only with BCoV at 24 hpi, which could indicate additional immune regulation (Fig. 4c, Table 3). IL-6 has been described as presenting a proinflammatory effect but can also function as a regulatory cytokine [42, 43].

Table 3
Gene Ontology (GO) terms associated with single-infected and co-infected cells.

Comparison	BCoV-infected		<i>C. parvum</i> -infected		Co-infected (BCoV + <i>C. parvum</i>)	
	24 hpi	72 hpi	24hpi	72 hpi	24 hpi	72 hpi
Number of GO terms among upregulated genes (Biological process)	243	273	45	96	269	332
Examples	regulation of signal transduction, cellular response to stress, positive regulation of cell death	regulation of cellular metabolic process, regulation of nitrogen compound metabolic process, regulation of NF-κB signalling	oxidative phosphorylation, respiratory electron transport chain	regulation of nitrogen compound metabolic process, regulation of MAPK cascade	regulation of metabolic process, response to ER stress	regulation of cellular metabolic process, NF-κB signalling
Number of GO terms downregulated genes (Biological process)	-	73	-	9	-	91
Examples	-	SRP-dependent co-translational protein targeting to membrane, protein targeting to ER, etc	-	regulation of nucleobase-containing compound metabolic process , nucleosome assembly, etc	-	Lipid metabolic process, Oxidative phosphorylation, etc

At 72 hpi, the number of GO terms relating to immune responses was enriched, and the number of DEGs associated with them was higher than at 24 hpi for all set ups (Table 3). For BCoV-infected cells at 72 hpi, there was enrichment of GO terms related to apoptotic processes, but also many GO terms associated with immune responses. This could indicate a later effect on the host cells after the initial proinflammatory response (Fig. 4d, Supplementary table 5). These GO terms reflect a positive regulation of several signalling cascades, including IL-6 production, inflammatory responses, or the signalling pathway of NF-κB. The fact that the inflammatory response occurs at both time points, but with an increased number of genes involved at 72 hpi, indicates a broadening and strengthening of the inflammatory response. For *C. parvum*-infected cells at 72 hpi, the enriched GO terms remained associated with metabolic processes, but other GO terms, such as cell death and responses to oxygen-containing compounds, also occur (Fig. 4e). Production of reactive oxygen species (ROS) is one of the key mechanisms that host cells have evolved to counteract intracellular parasites [44], but *C. parvum* is extremely resistant to oxidants [45]. However, GO terms associated with immune processes were also enriched in the *C. parvum*-infected cells, such as “positive regulation of myeloid leukocyte differentiation”.

Interestingly, when the host response from *C. parvum*-infected cells was compared with BCoV-infected cells, fewer immune genes were found as regulated; this could be due to *C. parvum* residing in the parasitophorous vacuole, thus evading the host response [22]. However, as mentioned previously, this could also result from fewer host cells being infected by the parasite than by the virus. At 72 hpi, the pattern is similar in co-infected and BCoV-infected cells, with more GOs enriched that are associated with immune system processes (Fig. 4), such as “regulation of cytokine production”; “regulation of I-kappaB kinase/NF-kappaB signalling” and “interleukin-1 mediated signalling pathway” (Fig. 4f). Among the down-regulated DEGs, for both co-infected and virus-infected cells at 72 hpi, most of the GO terms belong to metabolic processes, processes involved in lipid metabolism, protein-DNA complex organization, or carboxylic acid metabolism.

3.2.3 Infected HCT-8 cells show a marked proinflammatory profile after BCoV or co-infection with BCoV and *C. parvum*, whereas *C. parvum* has a more limited effect

From the enrichment, four KEGG pathways (MAPK, TNF, NF-κB, and IL-17) were selected for exploration in further detail, based on the number of DEGs and the biological significance of the pathways (Table 4, Supplementary tables 4–9, Supplementary Fig. 3).

Table 4
KEGG pathways associated with single-infected and co-infected cells.

Comparison	BCoV-infected	<i>C. parvum</i> -infected	Co-infected	Co-infected vs BCoV-infected	Co-infected vs <i>C. parvum</i> -infected
Post infection time (hpi)	24 hpi				
Total N pathways enriched	34 (34 for upregulated genes)	9 (11 for upregulated genes)	19 (22 for upregulated genes)	0 for up; 5 for downregulated genes	4 for up; 9 for down
Pathways selected	MAPK, IL-17, TNF, NF-κB		MAPK, IL-17, TNF, NF-κB	NA	IL-17, TNF, MAPK Oxidative Phosphorylation
Pathways selected	MAPK, IL-17, TNF, NF-κB		MAPK, IL-17, TNF, NF-κB	NA	IL-17, TNF, MAPK Oxidative Phosphorylation
Post infection time (hpi)	72 hpi				
Total N pathways enriched	28 (first 2000 genes upregulated); 15 (first 2000 downregulated genes)	17 (35 for upregulated genes)	42 (first 2000 upregulated genes); 13 for the first 2000 downregulated genes	NA	25 for upregulated genes, 30 for downregulated genes
Pathways selected	MAPK, IL-17, TNF, NF-κB	MAPK, IL-17	MAPK, IL-17	NA	TNF, IL-17, NF-κB

The Mitogen Associated Protein Kinases (MAPK) pathway is involved in many key cellular processes, with variable outcomes such as cell proliferation, differentiation, development, inflammatory responses, and apoptosis. Generally,

signalling from this pathway starts when a signalling molecule binds to a receptor in the cell surface and the signalling cascade affects transcription in the nucleus [46]. In the present study, various components of the MAPK signalling pathway were modulated in all experimental set ups. In co-infected cells, the gene encoding MAP3K8 was upregulated at 24 hpi. MAP3K8 has been shown to be required for lipopolysaccharide-induced, toll-like receptor-4 (TLR4)-mediated activation of the MAPK/ extracellular signal-regulated kinase (ERK) pathway in macrophages and is thus critical for production of the proinflammatory cytokine TNF- α (TNF α) during immune responses [47]. It is also involved in the regulation of T-helper cell differentiation and interferon gamma (IFN γ) expression in T-cells. Studies on cells in the lungs of ferrets infected with SARS-CoV-2 and in primary human microvascular endothelial cells infected with Middle East respiratory syndrome-related coronavirus (MERS) demonstrated a remarkable decrease in MAP3K8 expression within 12–24 h of infection [48], although the specific viral genes involved have not been identified yet. Therefore, MAP3K8 may be involved in the cellular response or host cell vulnerability to coronaviruses. In the current study, more genes belonging to MAPK pathway were modulated at 72 hpi (n = 49 and 55) for BCoV-infected and co-infected cells, respectively; Table 4). Among these, MAP3K8 is upregulated for both, in contrast to the aforementioned β -coronaviruses. The relevance and other possible differences in the modulation of this pathway between BCoV and other coronaviruses such as MERS or SARS-CoV-2 remain to be explored. As a pleiotropic pathway, several of the potential outcomes from upregulation of the MAPK pathway is proliferation/differentiation/inflammation and apoptosis through the transcription factor FOS, which was upregulated in both BCoV and *C. parvum* single infections. In our study, MAPK modulations were not seen in *C. parvum*-infected cells, and the pathway was not found to be significantly enriched at 24 hpi. Nevertheless, at 72 hpi, the pathway was enriched, and several genes involved in this pathway, such as GADD45B, DUSP1, DUSP6, FOS, DUSP5, JUN and IGF2, were upregulated. Dual specificity phosphatases (DUSPS) have been described as anti-cancer molecules, being inhibitors of cell proliferation and MAPK activation [49]. A study on murine intestinal epithelial cells infected with *C. parvum* showed that most of the genes encoding the key components of the MAPK signalling pathway were not modulated. However, a significant downregulation of *p38/Mapk*, MAP kinase-activated protein kinase 2 (*Mk2*), and *Mk3* genes was found. This suppression of MAPK signalling activity in *C. parvum*-infected intestinal epithelial cells was postulated as a strategy to evade host immune response [50].

Interlinked with the MAPK signalling cascade, it is worth noting that the pathway for tumour necrosis factor alpha (TNF α) was enriched in all our experimental setups. TNF α is a proinflammatory cytokine produced upon activation of the immune system and involved in various biological processes, including regulation of cell proliferation, differentiation, apoptosis, and immune responses [51]. One of the signalling cascades after TNF α involves the nuclear factor kappa-light-chain-enhancer of activated B cells (NF- κ B) activation. In turn, NF- κ B activation induces transcription and expression of genes encoding proinflammatory cytokines, such as IL-6, but also anti-apoptotic factors such as BIRC2, BIRC3, and BCL-2 homologue BCL2L1, enabling the cell to remain inert to apoptotic stimuli [52].

The importance of NF- κ B in several viral and parasitic diseases has been extensively reported [53, 54]. It has been shown to be responsible for the rapid induction of type I IFNs (such as IFN- β) and other proinflammatory cytokines (e.g., IL-6 and IL-8) during infections with RNA virus [55, 56]. It has been suggested that several TLRs, such as TLR2, TLR3, TLR4, TLR7/8, and TLR9, contribute to antiviral responses against infections caused by coronaviruses, both located in the cell membrane and intracellular [57]. Amongst them, TLR3 and TLR7 are capable to sense ssRNA in the endosomes, and dsRNA can be also recognised by cytosolic RIG-like receptors (RLRs) in human epithelial cells [58]. This activates the interferon regulatory factor (IRF) IRF3, IRF7, and NF- κ B, which are key regulators of proinflammatory response and innate immunity [59]. Several genes involved in TNF and NF- κ B signalling were modulated in our experiments. At 24 hpi, several genes were upregulated in BCoV-infected cells, including MAP3K14, FOS, and CREB5. It is noteworthy that several chemokines, such as CXCL2, also, termed GRO β (Growth-regulated protein beta) were also upregulated; this is involved in immunoregulatory and inflammatory processes acting as a chemotactic for neutrophils. PTGS2 was also upregulated;

this is an inducible prostaglandin-endoperoxide synthase involved in inflammatory processes by regulating the synthesis of prostaglandins [60].

In *C. parvum*-infected cells, activation of NF- κ B, induces the expression of pro- and anti-apoptotic factors (Liu et al., 2009) and proinflammatory cytokines (e.g., TNF- α , IL-8) [62–65]. TNF- α and TGF- β play roles in providing the host protective immunity and tissue repair effects against infection [66]. In conjunction with ERK1/2 and p38 MAPK pathways, host cells attempt to destroy the parasite by inducing formation of the neutrophil extracellular traps (NETosis) [67]. In addition, multiple genes, such as heat-shock genes, chemokines (such as CXCL8, CCL5, CXCL10, SCYB5), host actin and tubulin, are known to be upregulated in *C. parvum* infection in human epithelial cells, presumably in an attempt to eliminate the pathogen [68–69]. However, none of these chemokines were found to be modulated in *C. parvum*-infected cells in our study.

In co-infected cells, TNFAIP3 was upregulated at 24 hpi. This transcription factor is involved in immune and inflammatory responses signalled by cytokines, such as TNF- α and IL-1 beta, or pathogens via TLRs through termination of NF- κ B activity, ensuring the transient nature of inflammatory signalling pathways [70].

At 72 hpi, the modulation was more evident, with more genes belonging to inflammatory pathways being differentially expressed. In BCoV-infected cells, several genes were upregulated that are responsible for leukocyte recruitment and activation, such as chemokines (CXCL4, CXCL5), genes responsible for the activation of immune cells (CSF1); surface receptors (JAG1); MAPK; BIRC2; RIPK1 (necrosome); molecules responsible for cell adhesion: ICAM; Vascular factors: EDN1; TRAF3; CHUK; IKKKG; NF- κ B1/ NF- κ BIA (NF- κ B inhibitors); ATF4; CEBPB; IRF1. Among downregulated genes, several genes involved in the MAPK pathway were found, such as MAPK9, MAPK11, MAPK3, AKT1, DAB2IP (with functions in several pathways implicated on metabolism, proliferation, cell survival, growth, and angiogenesis). In *C. parvum*-infected cells, MAPK10 was downregulated. In co-infected cells, TRAF2 and CX3C were upregulated, whereas RIPK3 was downregulated.

In BCoV-infected cells, several genes were upregulated at 24 hpi, such as MAPK3K14; PTGS2; CXCL2; GADD45A. At 72 hpi, a more extensive modulation of the pathway was evident, as several genes belonging to the NF- κ B signalling cascades were upregulated. For example, sensors of DNA damage such as IKKKG, UBE21 (sumoylation), RIPK1; inflammation (DDXS8) and canonical and non-canonical pathways for hypoxia. Several of these genes converge in the degradation of the inhibitor NF- κ BIA, activating the transcription of target genes. Downregulated genes in BCoV-infected cells at 72 hpi included EDA/EDAR, which mediate the activation of NF- κ B and JNK; surface marker CD14, which acts via MyD88, TIRAP and TRAF6, leading to NF- κ B activation, cytokine secretion, and the inflammatory response [71]. In addition, TIRAP was downregulated. This is an adapter involved in TLR2 and TLR4 signalling pathways in the innate immune response, resulting in cytokine secretion and inflammatory response, positively regulating the production of TNF- α and IL-6.

Interleukin 17 is a family of proinflammatory cytokines that act as potent mediators in delayed-type reactions by increasing chemokine production in various tissues in response to extracellular pathogens, acting synergistically with TNF and IL-1 [72]. Its relevance has been recently explored in other viral diseases, including COVID-19 [73]. Furthermore, a few studies have shown that it is important in cryptosporidiosis, with a rapid induction in the intestine of mice and bovines [74, 75]. At 24 hpi, the genes that were upregulated in BCoV-infected cells included FOS, CXCL2, PTGS2. These chemokines and cytokines may lead to autoimmune pathology, neutrophil recruitment, and immunity against extracellular pathogens. In *C. parvum*-infected cells, the TRAF4 gene, which is associated to TNF receptor, connecting IL-1/Toll receptors with NF- κ B, was upregulated at 72 hpi. This inhibits activation of NF- κ B by the inflammasome NOD2/RIP2 and JUN/MAPK12. In the co-infected cells, the gene TNFAIP3 was upregulated, which is induced by TNF- α . This mechanism could inhibit NF- κ B activation and apoptosis mediated by TNF- α and limit inflammation. Two other

genes, FOSB and MAPK6, were also upregulated in co-infected cells at 24 hpi, but were not differentially expressed in either of the single infections for the same time point.

More extensive modulation was evident in BCoV-infected cells at 72 hpi, where several genes were upregulated, including FADD, TRAF3, 2TRAF6, NF- κ B1, TBK1, USP25, HSP90AA1, TAB2, MAP3K7, IKBKG, CHUK, NF- κ BIA, CEBPB, CXCL1, CXCL5, and matrix metalloproteases, such as MMP1 and MMP13, which are important for the remodelling of extracellular matrix. Matrix metalloproteases, induced after the expression of proinflammatory cytokines, contribute to pathogenesis by disrupting the barrier function of cells, and have been shown to be relevant in SARS-CoV-2 [76]. The damage to the barrier function of enterocytes and intestinal cells could lead to diarrhoea, the clinical sign most associated with both BCoV and *C. parvum* infection *in vivo*.

Apoptosis is characterized by a series of dramatic perturbations to the cellular architecture that contribute not only to cell death, but also prepare cells for their removal by phagocytes. This prevents the occurrence of unwanted immune responses and is commonly associated with both viral infections and parasitic infections [77, 78]. During the execution phase of apoptosis, several mechanisms are orchestrated by the caspase family of cysteine proteases. Caspases (CASP) target proteins for restricted proteolysis in a controlled manner, minimizing damage and the release of immunostimulatory molecules [79]. Interestingly, in our experimental setup, BCoV-infected and co-infected cells at 72 hpi show a balance between the upregulation of pro-apoptotic genes (BAK1, TNFSRF10B, PMAIP1) and pro-survival genes (BIRC-2); in addition, there was downregulation of pro-apoptotic genes such as BBC3. Among the key apoptotic genes, CASP7 was upregulated in BCoV and co-infected cells at 72 hpi. This caspase has been shown to have a role in inflammation, being activated by caspases-8 and -9 and presenting the same function as CASP3 [80]. Other caspases, such as CASP8AP2 (involved in the TNF- α induced activation of NF- κ B), CASP5 (initiation of pyroptosis, regulation of antiviral innate immune activation), CASP6, CASP2 (involved in the initiator phase), and CASP4 (involved in inflammation) were downregulated after 72 hpi in co-infected cells. Also, B-cell lymphoma (BCL) class genes were mostly upregulated, while cellular tumour antigen p53 was downregulated in both BCoV-infected and co-infected cells at 72 hpi. Other genes, such as BCL7a, BCL11A, BCL2L15, and BCL2L14, were also downregulated in both these set ups. Cellular apoptosis has also been described to occur as a host response to evade parasite invasion in the early phase of *C. parvum* infection [81, 82]. A microarray analysis of infected host intestinal mucosa has revealed overexpression of TNF-superfamily receptor osteoprotegerin (OPG), which inhibits the TNF- α -related-apoptosis-inducing ligand (TRAIL)-mediated apoptosis [83]. This helps the parasite to escape the host defences and complete its life cycle. However, in our experiments, only GADD45B, FOS, and JUN were modulated at 72 hpi in *C. parvum*-infected cells.

3.2.4 The proinflammatory modulation found in vitro could indicate the basis for the molecular pathogenesis and intestinal damage in vivo

As hinted before, several upregulated genes following BCoV and co-infection are involved in proinflammatory responses. Some of these genes are implicated in IFN-I induction and signalling at 24 and 72 hpi in BCoV-infected cells. At 24 hpi, ISG15 (Interferon-stimulated gene 15), an interferon-inducible gene, was upregulated. ISG15 is a crucial component of the immune response to viral infections [84]. The pattern of expression of other ISGs was almost identical in BCoV-infected and co-infected cells, with only two differences: OAS3 and ISG20L2, which were found in co-infected cells, but not in BCoV-infected cells at 72 hpi. ISG20 is an interferon-induced antiviral exoribonuclease that acts on single-stranded RNA and exhibits antiviral activity against RNA viruses, including hepatitis C virus (HCV), hepatitis A virus, and yellow fever virus, in an exonuclease-dependent manner [85, 86]. In contrast, other interferon-responsive elements, such as IFITM1, IFITM2, IFITM3, and IFI27, were downregulated in both set ups. IL-1A, considered as one of the endogenous pyrogens and a potent proinflammatory protein, was also upregulated at both 24 and 72 hpi, together with tumour necrosis factor receptors (TNFRs), TNFRSF12A, TNFRSF18, and chemokines such as CXCL2, CXCL8 (IL8), and CXCL3.

At 72 hpi, we found a modulation of both anti-inflammatory and proinflammatory genes, which might represent an attempt of the host cells to counteract BCoV infection. TLRs showed a mixed expression profile, since TLR3 and TLR5 were downregulated, while TLR6 was upregulated. TLR3 is a nucleotide-sensing TLR that is activated by double-stranded RNA, a sign of viral infection, associating endosomal recognition of viruses to IFN-I responses and leading to NF- κ B activation, cytokine secretion, and the inflammatory response [87, 88]. However, this receptor probably does not have a function during the initial steps of infection with BCoV, but later during the replication. In addition, DDX58, OASL, and ISG20 were upregulated. DDX58 (also known as RIG-1) is an immune receptor that senses cytoplasmic viral nucleic acids and activates a downstream signalling cascade leading to the production of type I IFNs and proinflammatory cytokines [89]. OASL (2'-5'-oligoadenylate synthetase-like protein) displays antiviral activity against encephalomyocarditis virus and HCV via an alternative antiviral pathway independent of RNase L [90]. Also, MT2A (metallothioneins 2) and GBP3 (guanylate-binding protein 3) were upregulated in co-infected cells at 24 hpi. Furthermore, modulation of host cytoskeleton activities was found, with upregulation of lectins (CLEC4) and IKBKG in BCoV-infected cells at 24 hpi. Also, mucin genes were modulated. In *C. parvum*-infected cells at 72 hpi, MUC5AC was downregulated. In co-infected cells at 24 hpi, heat shock protein 90 (hsp 90) was upregulated, while keratin type I cytoskeletal was downregulated. Similarly, in co-infected cells at 72 hpi, CLEC4A (C-type lectin), IKBKG, and mucins (such as MUC13, MUC20, and MUC4) were upregulated. Pathogens damaging the gastrointestinal tract cause damage to the mucus barrier, which can worsen mucus quality and reduce mucus production, potentially leading to chronic inflammation and disease [91].

Taking all our findings together, the proinflammatory modulation, in concert with the alterations in the host cell cytoskeleton and the protective mucus barrier, could suggest the molecular basis *in vivo* for damage to the epithelial barrier, leading to diarrhoea. *In vivo*, both BCoV and *C. parvum* replicate in enterocytes, causing morphological changes in the intestinal cytoskeleton, such as loss of microvilli and shortening of columnar epithelium, thereby causing severe villous atrophy. This leads to reduced digestion of feed and decreased absorptive capacity of the intestine, causing an osmotic imbalance that could be exacerbated by changes in the permeability of the epithelial cells [92, 93]. Additionally, it has been recently shown that concentrations of IL-8 in serum from BCoV infected calves increased from 0 to 24 hpi, indicating intestinal injury and diarrhoea [94]. However, our results provide no indication of a greater severity when both pathogens are present, as the host expression profiles between single BCoV-infection and co-infection are very similar. The possible relevance and influence on pathogenesis need to be explored by using more complex *in vitro* models or by *in vivo* approaches.

3.2.5 Genes exclusively expressed in co-infected cells as potential biomarkers for BCoV and *C. parvum* co-infection.

At 24 hpi, 78 DEGs were identified in co-infected cells, with the highest FC corresponding to NR4A3 (FC = 4.12), a transcriptional activator involved in regulating proliferation, survival differentiation, and inflammatory processes [94]. At 72 hpi, 803 DEGs were uniquely expressed in co-infected cells (Fig. 3). The highest FC corresponds to DNAH17 (FC = 55.20), although the function of this dynein gene in our context is not obvious. GO term analysis mostly showed an effect on cellular metabolic pathways and response to DNA damage both at 24 and 72 hpi (Supplementary table S10). Strikingly, we found no significantly enriched KEGG pathways and few immune genes among these DEGs. Despite this, the high fold change shown by some of the genes could imply that they represent interesting targets as biomarkers for co-infections, and their putative role in the pathogenesis of these intestinal infections should be addressed in *in vivo* models.

Conclusion

Our work demonstrates extensive modulation of the host-cell transcriptome by BCoV, influencing immune processes and metabolic pathways, and a more limited effect from *C. parvum* under our experimental settings. The co-infection is thus dominated by BCoV, although there is a possible bias due to the difference in infection success shown by the pathogens. Nevertheless, our findings provide insights into the molecular pathogenesis of these intestinal infections and suggest possible biomarkers associated with co-infection that could be explored further using novel *in vitro* models (such as bovine intestinal organoids) or *in vivo*.

Declarations

Acknowledgements:

The authors would like to acknowledge Mamata Khatri for her help with lab work and Stanislav Iakhno for providing input on the RNA-Seq pipeline.

Funding: This project was supported by internal funding from the Virology and Parasitology Units, Department of Paraclinical Sciences (PARAFAG), Faculty of Veterinary Sciences, NMBU.

Author contributions statement: Conceptualization, M.M, S.M.N, L.J.R.; methodology, data curation, and formal analysis, R.S., A.J.M., T.M., S.M.N.; writing—original draft preparation, R.S., A.J.M; writing—review and editing, A.J.M, R.S, T.M, L.J.R, M.M, S.M.N.; funding acquisition, L.J.R., M.M and project administration, M.M. All authors have reviewed and agreed to the current version of the manuscript.

Data availability

The RNA sequencing data used and analysed in the current study are available from GEO, under the accession number GSE223548.

References

1. C Björkman 1, C Svensson, B Christensson, K de Verdier. *Cryptosporidium parvum* and *Giardia intestinalis* in calf diarrhoea in Sweden. *Acta Vet. Scand.* 44 (3–4):145 – 52. doi: 10.1186/1751-0147-44-145 (2003).
2. USDA. Dairy. Part II: *Changes in the U.S. Dairy Cattle industry, 1991–2007*. Fort Collins: USDA-APHIS-VS, CEAH; 2008. pp. 57–61 (2007).
3. Bartels, C.J., Holzhauser, M., Jorritsma, R., Swart, W.A., Lam, T.J. Prevalence, prediction and risk factors of enteropathogens in normal and non-normal faeces of young Dutch dairy calves. *Prev. Vet. Med.* 93(2–3), 162–169 (2010).
4. Izzo MM, Kirkland PD, Mohler VL, Perkins NR, Gunn AA, House JK. Prevalence of major enteric pathogens in Australian dairy calves with diarrhoea. *Aust. Vet. J.* 89(5):167–73. doi: 10.1111/j.1751-0813.2011.00692.x. (2011)
5. García A, Ruiz-Santa-Quiteria JA, Orden JA, Cid D, Sanz R, Gómez-Bautista M, de la Fuente R. Rotavirus and concurrent infections with other enteropathogens in neonatal diarrheic dairy calves in Spain. *Comp. Immunol. Microbiol. Infect. Dis.* 23(3):175–83. doi: 10.1016/s0147-9571(99)00071-5 (2000).
6. Renaud DL, Rot C, Marshall J, Steele MA. The effect of *Cryptosporidium parvum*, rotavirus, and coronavirus infection on the health and performance of male dairy calves. *J. Dairy Sci.*104(2):2151–2163. doi: 10.3168/jds.2020-19215 (2021).
7. Shaw HJ, Innes EA, Morrison LJ, Katzer F, Wells B. Long-term production effects of clinical cryptosporidiosis in neonatal calves. *Int. J. Parasitol.* 50(5):371–376. doi: 10.1016/j.ijpara.2020.03.002 (2020).

8. Boileau MJ, Kapil S. Bovine coronavirus associated syndromes. *Vet. Clin. North. Am. Food Anim. Pract.* 26(1):123 – 46, table of contents. doi: 10.1016/j.cvfa.2009.10.003 (2010).
9. Oma VS, Trávén M, Alenius S, Myrnel M, Stokstad M. Bovine coronavirus in naturally and experimentally exposed calves; viral shedding and the potential for transmission. *Virolog. J.* 13;13:100. doi: 10.1186/s12985-016-0555-x (2016).
10. Hodnik JJ, Ježek J, Starič J. Coronaviruses in cattle. *Trop. Anim. Health Prod.* 52(6):2809–2816. doi: 10.1007/s11250-020-02354-y (2020).
11. Y.I. Cho, K.J. Yoon. An overview of calf diarrhea - infectious etiology, diagnosis, and intervention. *J. Vet. Sci.*, 15, 1–17 (2014).
12. Foster DM, Smith GW. Pathophysiology of diarrhea in calves. *Vet. Clin. North Am. Food Anim. Pract.* 25:13–36 (2009).
13. Naciri M, Lefay MP, Mancassola R, Poirier P, Chermette R. Role of *Cryptosporidium parvum* as a pathogen in neonatal diarrhoea complex in suckling and dairy calves in France. *Vet. Parasitol.* 85(4):245–57. doi: 10.1016/s0304-4017(99)00111-9 (1999).
14. Gulliksen SM, Jor E, Lie KI, Hamnes IS, Løken T, Akerstedt J, Osterås O. Enteropathogens and risk factors for diarrhea in Norwegian dairy calves. *J. Dairy Sci.* 92(10):5057–66. doi: 10.3168/jds.2009-2080 (2009).
15. Gomez DE, Weese JS. Viral enteritis in calves. *Can. Vet. J.* 58(12):1267–1274 (2017).
16. Trotz-Williams LA, Wayne Martin S, Leslie KE, Duffield T, Nydam DV, Peregrine AS. Calf-level risk factors for neonatal diarrhea and shedding of *Cryptosporidium parvum* in Ontario dairy calves. *Prev Vet Med.* 15;82(1–2):12–28. doi: 10.1016/j.prevetmed.2007.05.003 (2007).
17. Mirhashemi ME, Noubary F, Chapman-Bonofiglio S, Tzipori S, Huggins GS, Widmer G. Transcriptome analysis of pig intestinal cell monolayers infected with *Cryptosporidium parvum* asexual stages. *Parasit. Vectors.* 11(1):176. doi: 10.1186/s13071-018-2754-3 (2018).
18. Heo I *et al.* Modelling *Cryptosporidium* infection in human small intestinal and lung organoids. *Nat. Microbiol.* 3(7):814–823. doi: 10.1038/s41564-018-0177-8 (2018).
19. Heidamejadi, S. M., Rafiei, A., Makvandi, M., Pirestani, M., Saki, J., & Ghadiri, A. (2018). Gene Profile Expression Related to Type I Interferons in HT-29 Cells Exposed to *Cryptosporidium parvum*. *Jundishapur J. Microbiol.* 11(7) (2018).
20. Barakat, F. M., McDonald, V., Foster, G. R., Tovey, M. G., & Korbel, D. S. (2009). *Cryptosporidium parvum* infection rapidly induces a protective innate immune response involving type I interferon. *J. Infect. Dis.*, 200(10), 1548–1555 (2009).
21. Relat, R. M. B., & O'Connor, R. M.. *Cryptosporidium*: host and parasite transcriptome in infection. *Curr. Opin. Microbiol.* <background-color:#FFCC66;ivertical-align:baseline;>58</background-color:#FFCC66;ivertical-align:baseline;>, 138–145 (2020).
22. Guérin, A., & Striepen, B. (2020). The biology of the intestinal intracellular parasite *Cryptosporidium*. *Cell Host Microbe*, 28(4), 509–515 (2020).
23. Blume, M., *et al.* Host-derived glucose and its transporter in the obligate intracellular pathogen *Toxoplasma gondii* are dispensable by glutaminolysis. *Proc. Natl. Acad. Sci. U.S.A.*, 106(31), 12998–13003 (2009).
24. Nitzsche, R., Zagoriy, V., Lucius, R., & Gupta, N. Metabolic cooperation of glucose and glutamine is essential for the lytic cycle of obligate intracellular parasite *Toxoplasma gondii*. *J. Biol. Chem.*, 291(1), 126–141(2016).
25. Krishnan, A., *et al.* Functional and computational genomics reveal unprecedented flexibility in stage-specific *Toxoplasma* metabolism. *Cell Host Microbe*, 27(2), 290–306 (2020).

26. Mogi, T., & Kita, K. (2010). Diversity in mitochondrial metabolic pathways in parasitic protists *Plasmodium* and *Cryptosporidium*. *Parasitol. Int.* 59(3), 305–312 (2010).
27. Hoffmann, H. H., Schneider, W. M., & Rice, C. M. Interferons and viruses: an evolutionary arms race of molecular interactions. *Trends Immunol.* 36(3), 124–138 (2015),
28. Shakya, R., Meléndez, A. J., Robertson, L. J., & Myrmel, M. Interactions between *Cryptosporidium parvum* and bovine corona virus during sequential and simultaneous infection of HCT-8 cells. *Microbes Infect.* 24(3), 104909 (2022).
29. Ramakrishnan MA. Determination of 50% endpoint titer using a simple formula. *World J. Virol.* 5(2):85e6 (2016).
30. Campbell, A. T., Robertson, L. J., & Smith, H. Viability of *Cryptosporidium parvum* oocysts: correlation of *in vitro* excystation with inclusion or exclusion of fluorogenic vital dyes. *Appl. Environ. Microbiol.*, 58(11), 3488–3493 (1992).
31. Robertson, L. J., Campbell, A. T., & Smith, H. V. *In vitro* excystation of *Cryptosporidium parvum*. *Parasitology*, 106(1), 13–19 (1993).
32. Bolger, A. M., Lohse, M., & Usadel, B. Trimmomatic: a flexible trimmer for Illumina sequence data. *Bioinformatics*, 30(15), 2114–2120 (2014).
33. Kim, D., Pertea, G., Trapnell, C., Pimentel, H., Kelley, R., & Salzberg, S. L. TopHat2: accurate alignment of transcriptomes in the presence of insertions, deletions and gene fusions. *Genome Biol.* 14(4), 1–13 (2013).
34. Trapnell, C., *et al.* Transcript assembly and abundance estimation from RNA-Seq reveals thousands of new transcripts and switching among isoforms. *Nat. Biotech.* 28(5), 511 (2010).
35. Trapnell, C., *et al.* Differential gene and transcript expression analysis of RNA-seq experiments with TopHat and Cufflinks. *Nat. Protoc.* 7(3), 562–578 (2012).
36. Szklarczyk, D., *et al.* STRING v11: protein–protein association networks with increased coverage, supporting functional discovery in genome-wide experimental datasets. *Nucleic acids Res.*, 47(D1), D607–D613 (2019).
37. Grimm, M. C., Elsbury, S. K., Pavli, P., & Doe, W. F. Interleukin 8: cells of origin in inflammatory bowel disease. *Gut*, 38(1), 90–98 (1996)-
38. Cotton, J. A., Platnich, J. M., Muruve, D. A., Jijon, H. B., Buret, A. G., & Beck, P. L. Interleukin-8 in gastrointestinal inflammation and malignancy: induction and clinical consequences. *Int. J. Interferon, Cytokine Mediat. Res.*, 8, 13 (2016).
39. Roy, K., Agarwal, S., Banerjee, R., Paul, M. K., & Purbey, P. K. COVID-19 and gut immunomodulation. *World J. Gastroenterol.* 27(46), 7925 (2021).
40. Banerji, R., & Saroj, S. D. Early growth response 1 (EGR1) activation in initial stages of host–pathogen interactions. *Mol. Biol. Rep.* 48(3), 2935–2943 (2021).
41. Liu, J., Deng, M., Lancto, C. A., Abrahamsen, M. S., Rutherford, M. S., & Enomoto, S. Biphasic modulation of apoptotic pathways in *Cryptosporidium parvum*-infected human intestinal epithelial cells. *Infect. Immun.* 77(2), 837–849 (2009).
42. Diehl, S., & Rincón, M. The two faces of IL-6 on Th1/Th2 differentiation. *Mol. Immunol.* 39(9), 531–536 (2002).
43. Velazquez-Salinas, L., Verdugo-Rodriguez, A., Rodriguez, L. L., & Borca, M. V. The role of interleukin 6 during viral infections. *Front. Microbiol.*, <background-color:#FFCC66;ivertical-align:baseline;>10</background-color:#FFCC66;ivertical-align:baseline;>, 1057 (2019).
44. Lee, J., & Song, C. H. Effect of reactive oxygen species on the endoplasmic reticulum and mitochondria during intracellular pathogen infection of mammalian cells. *Antiox.* 10(6), 872. (2021).
45. Hong, *et al.* Expression of *Cryptosporidium parvum* thioredoxin peroxidase in COS-7 cells confers radioprotection. *Exp. Parasitol.* 163, 8–15. doi: 10.1016/j.exppara.2016.01.012 (2016).

46. Braicu, C. *et al.* A comprehensive review on MAPK: a promising therapeutic target in cancer. *Cancers*, 11(10), 1618 (2019).
47. Schmid, S., & Sachs, D. (2014). Mitogen-activated protein kinase-mediated licensing of interferon regulatory factor 3/7 reinforces the cell response to virus. *J. Biol. Chem.* 289(1), 299–311 (2014).
48. Islam, T. *et al.* Integrative transcriptomics analysis of lung epithelial cells and identification of repurposable drug candidates for COVID-19. *Eur. J. Pharmacol.* 887, 173594 (2020).
49. Nunes-Xavier, C., *et al.* (2011). Dual-specificity MAP kinase phosphatases as targets of cancer treatment. *Anticancer Agents Med. Chem.* 11(1), 109–132 (2011).
50. He, W. *et al.* Cryptosporidial infection suppresses intestinal epithelial cell MAPK signaling impairing host anti-parasitic defense. *Microorganisms*, 9(1), 151 (2021).
51. Zelová, H., & Hošek, J. TNF- α signalling and inflammation: interactions between old acquaintances. *Inflamm. Res.* 62(7), 641–651 (2013).
52. Farahani, M., *et al.* Molecular pathways involved in COVID-19 and potential pathway-based therapeutic targets. *Biomed. Pharmacother.* 145, 112420 (2022).
53. Attig, A., Yao, L. J., Afzal, S., & Khan, M. A. The triumvirate of NF- κ B, inflammation and cytokine storm in COVID-19. *Int. Immunopharmacol.* 101, 108255 (2021).
54. Chadha, A., & Chadee, K. The NF- κ B pathway: modulation by *Entamoeba histolytica* and other Protozoan parasites. *Front. Cell. Infect. Microbiol.* 11, 748404 (2021).
55. Takeuchi, O., & Akira, S. Pattern recognition receptors and inflammation. *Cell*, 140(6), 805–820. (2010).
56. Cruz-Pulido, D., *et al.* (2021). Comparative transcriptome profiling of human and pig intestinal epithelial cells after porcine deltacoronavirus infection. *Viruses*, 13(2), 292 (2021).
57. Liu ZM, Yang MH, Yu K, Lian ZX, Deng SL. Toll-like receptor (TLRs) agonists and antagonists for COVID-19 treatments. *Front. Pharmacol.* 7, 13:989664. doi: 10.3389/fphar.2022.989664 (2022).
58. Seth, R. B., Sun, L., & Chen, Z. J. Antiviral innate immunity pathways. *Cell Res.* 16(2), 141–147 (2006).
59. Hayden, M. S., & Ghosh, Regulation of NF- κ B by TNF family cytokines. In *Seminars in immunology* (Vol. 26, No. 3, pp. 253–266). Academic Press (2014).
60. Kirkby, N.S., *et al.* Differential COX-2 induction by viral and bacterial PAMPs: Consequences for cytokine and interferon responses and implications for anti-viral COX-2 directed therapies. *Biochem. Biophys. Res. Commun.* 438, 249–56. doi: 10.1016/j.bbrc.2013.07.006 (2013).
61. Liu, J. *et al.* Biphasic modulation of apoptotic pathways in *Cryptosporidium parvum*-infected human intestinal epithelial cells. *Infect. Immun.* 77, 837–849 (2009).
62. Laurent, F. *et al.* *Cryptosporidium parvum* infection of human intestinal epithelial cells induces the polarized secretion of C-X-C chemokines. *Infect. Immun.* 65, 5067–5073 (1997).
63. Laurent, F. *et al.* Human intestinal epithelial cells respond to *Cryptosporidium parvum* infection with increased prostaglandin H synthase 2 expression and prostaglandin E2 and F2 α production. *Infect. Immun.* 66, 1787–1790 (1998).
64. McDonald, V., Korbil, D. S., Barakat, F. M., Choudhry, N., & Petry, F. Innate immune responses against *Cryptosporidium parvum* infection. *Parasite Immunol.* 35(2), 55–64 (2013).
65. Wang, Y., *et al.* Induction of inflammatory responses in splenocytes by exosomes released from intestinal epithelial cells following *Cryptosporidium parvum* infection. *Infect. Immun.* 87(4), e00705-18 (2019).
66. Lean, I. S., McDonald, V., & Pollok, R. C. The role of cytokines in the pathogenesis of *Cryptosporidium* infection. *Curr. Op. Infect. Diseases*, 15(3), 229–234 (2002).

67. Muñoz-Caro, T., Lendner, M., Dauschies, A., Hermosilla, C., & Taubert, A. NADPH oxidase, MPO, NE, ERK1/2, p38 MAPK and Ca²⁺ influx are essential for *Cryptosporidium parvum*-induced NET formation. *Dev. Comp. Immunol.* 52, 245–254 (2015).
68. Deng, M., Lancto, C.A., Abrahamsen, M.S. *Cryptosporidium parvum* regulation of human epithelial cell gene expression. *Int. J. Parasitol.* 34, 73–82 (2004).
69. Maillot, C., et al. *Cryptosporidium parvum* infection stimulates the secretion of TGF- β , IL-8 and RANTES by Caco-2 cell line. *Parasitol. Res.*, 86, 947–949 (2000).
70. Parvatiyar K, Harhaj EW. Regulation of inflammatory and antiviral signaling by A20. *Microbes Infect.* 13(3):209–15. doi: 10.1016/j.micinf.2010.11.003 (2011).
71. Haziot, A. et al. Resistance to endotoxin shock and reduced dissemination of gram-negative bacteria in CD14-deficient mice. *Immunity*, 4(4), 407–414 (1996).
72. Sahu, U., Biswas, D., Prajapati, V. K., Singh, A. K., Samant, M., & Khare, P. Interleukin-17—A multifaceted cytokine in viral infections. *J. Cell. Physiol.* 236(12), 8000–8019 (2021).
73. Sadeghi, A. et al. Th17 and Treg cells function in SARS-CoV2 patients compared with healthy controls. *J. Cell. Physiol.*, 236(4), 2829–2839 (2021).
74. Drinkall, E., Wass, M. J., Coffey, T. J., & Flynn, R. J. A rapid IL-17 response to *Cryptosporidium parvum* in the bovine intestine. *Vet. Immunol. Immunopathol.* 191, 1–4 (2017).
75. Zhao, G. H., et al. Dynamics of Th17 associating cytokines in *Cryptosporidium parvum*-infected mice. *Parasitol. Res.* 115(2), 879–887 (2016).
76. Lee, H. S., & Kim, W. J. The Role of Matrix Metalloproteinase in Inflammation with a Focus on Infectious Diseases. *Int. J. Mol. Sci.* 23(18), 10546 (2022).
77. Yapasert, R., Khaw-On, P., & Banjerdpongchai, R. Coronavirus infection-associated cell death signaling and potential therapeutic targets. *Molecules*, 26(24), 7459 (2021).
78. Kapczuk, P., et al. The influence of selected gastrointestinal parasites on apoptosis in intestinal epithelial cells. *Biomolecules*, 10(5), 674 (2020).
79. Taylor, R. C., Cullen, S. P., & Martin, S. J. Apoptosis: controlled demolition at the cellular level. *Nat. Rev. Mol. Cell Biol.* 9(3), 231–241 (2008).
80. Lamkanfi, M., & Kanneganti, T. D. Caspase-7: a protease involved in apoptosis and inflammation. *Int. J. Biochem. Cell Biol.* 42(1), 21–24 (2010).
81. Chen, X. M., et al. *Cryptosporidium parvum* is cytopathic for cultured human biliary epithelia via an apoptotic mechanism. *Hepatology*, 28(4), 906–913 (1998).
82. McCole, D. F., Eckmann, L., Laurent, F., & Kagnoff, M. F. Intestinal epithelial cell apoptosis following *Cryptosporidium parvum* infection. *Infect. Immun.*, 68(3), 1710–1713 (2000).
83. Di Genova, B. M., & Tonelli, R. R. Infection strategies of intestinal parasite pathogens and host cell responses. *Front. Microbiol.*, 7, 256 (2016).
84. Zhang, M., et al. ISGylation in Innate Antiviral Immunity and Pathogen Defense Responses: A Review. *Front Cell Dev Biol* <background-color:#FFCC66;vertical-align:baseline;>9</background-color:#FFCC66;vertical-align:baseline;>:788410. doi: 10.3389/fcell.2021.788410 (2021).
85. Zhou, Z., et al. Antiviral activities of ISG20 in positive-strand RNA virus infections. *Virology*, 409(2), 175–188 (2011).
86. Deymier, S., Louvat, C., Fiorini, F., & Cimarelli, A. ISG20: an enigmatic antiviral RNase targeting multiple viruses. *FEBS Open Bi*- (2022).

87. Bonjardim, C. A., Ferreira, P. C., & Kroon, E. G. Interferons: signaling, antiviral and viral evasion. *Immunol. Lett.*, 122(1), 1–11 (2009).
88. Sa Ribero, M., Jouvenet, N., Dreux, M., & Nisole, S. Interplay between SARS-CoV-2 and the type I interferon response. *PLoS Pathog.*, 16(7), e1008737 (2020).
89. Onomoto K, Onoguchi K, Yoneyama M. Regulation of RIG-I-like receptor-mediated signaling: interaction between host and viral factors. *Cell Mol. Immunol.* 18(3):539–555. doi: 10.1038/s41423-020-00602-7 (2021).
90. Lin, R. J., Yu, H. P., Chang, B. L., Tang, W. C., Liao, C. L., & Lin, Y. L. Distinct antiviral roles for human 2', 5'-oligoadenylate synthetase family members against dengue virus infection. *J. Immunol.* 183(12), 8035–8043 (2009).
91. Kang Y, Park H, Choe BH, Kang B. The Role and Function of Mucins and Its Relationship to Inflammatory Bowel Disease. *Front Med* 9, 848344. doi: 10.3389/fmed.2022.848344 (2022).
92. White, C. *Cryptosporidium* species. In: Mandell GL, Bennett JE, Dolin R (eds) *Principles and practice of infectious diseases*, 7th edn. Churchill Livingstone, Elsevier, Philadelphia (2010).
93. Cho YI, Yoon KJ. An overview of calf diarrhea - infectious etiology, diagnosis, and intervention. *J. Vet. Sci.* 15(1):1–17. doi: 10.4142/jvs.2014.15.1.1 (2014).
94. Ok, M.; Yildiz, R.; Hatipoglu, F.; Baspinar, N.; Ider, M.; Üney, K.; Ertürk, A.; Durgut, M.K.; & Terzi, F. Use of intestine-related biomarkers for detecting intestinal epithelial damage in neonatal calves with diarrhea. *Am. J. Vet. Res.* 81, 139–146. doi: 10.2460/ajvr.81.2.139 (2020).
95. Klepsch, V., Moschen, A. R., Tilg, H., Baier, G., & Hermann-Kleiter, N. Nuclear receptors regulate intestinal inflammation in the context of IBD. *Front. Immunol.* 10, 1070 (2019).

Figures

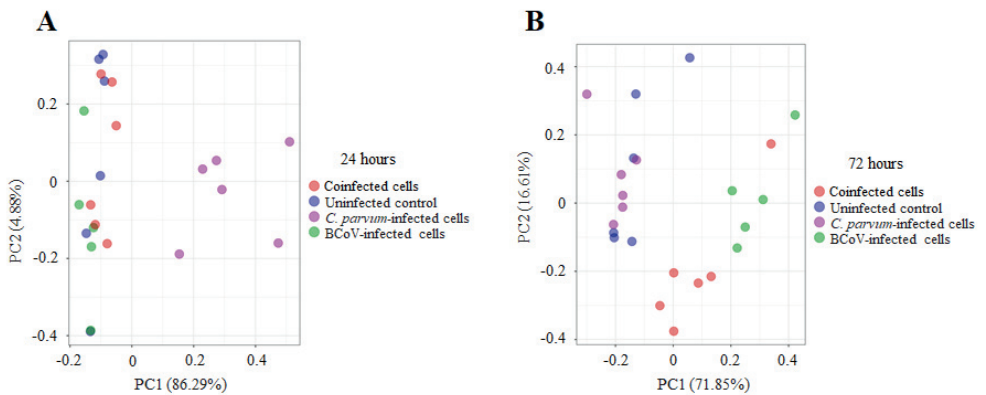


Figure 1

A: PCA plot: Principal Component Analysis of *Homo sapiens* transcriptome at 24 hpi (A) and 72 hpi (B) Analysis based on fragments per kilobase of exon per million mapped reads (FPKM).

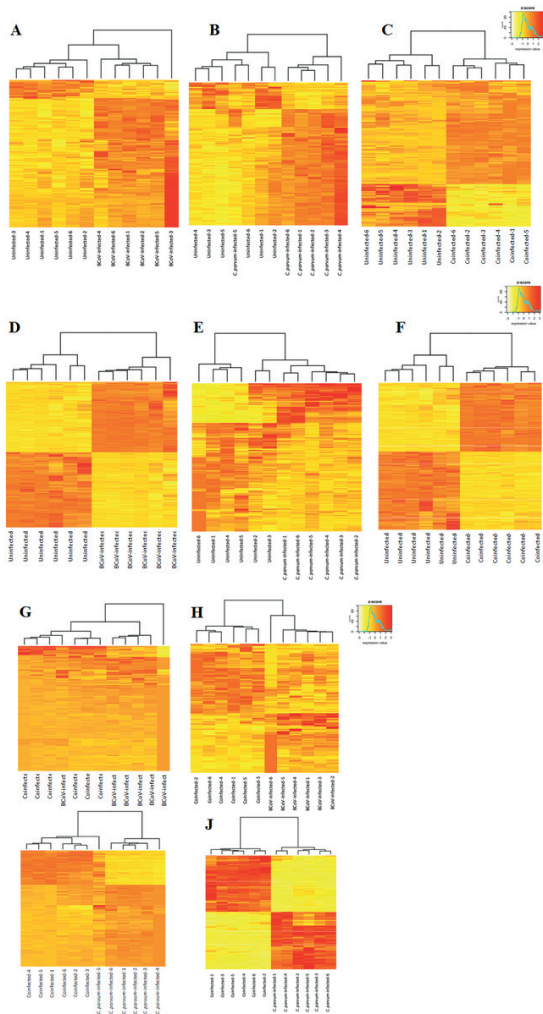


Figure 2

Heatmap of differentially expressed genes of *Homo sapiens* (i.e., uninfected HCT-8 cells; Control) or cells infected with BCoV and/or *C. parvum* at different time points: BCoV-infected cells at (1) 24 and (2) 72 hpi, *C. parvum*-infected cells at (3) 24 and (4) 72 hpi, Co-infected cells at (5) 24 and (6) 72 hpi, BCoV-infected and co-infected cells at (7) 24 hpi and (8) 72 hpi, *C. parvum* and co-infected cells at (9) 24 and (10) 72hpi.

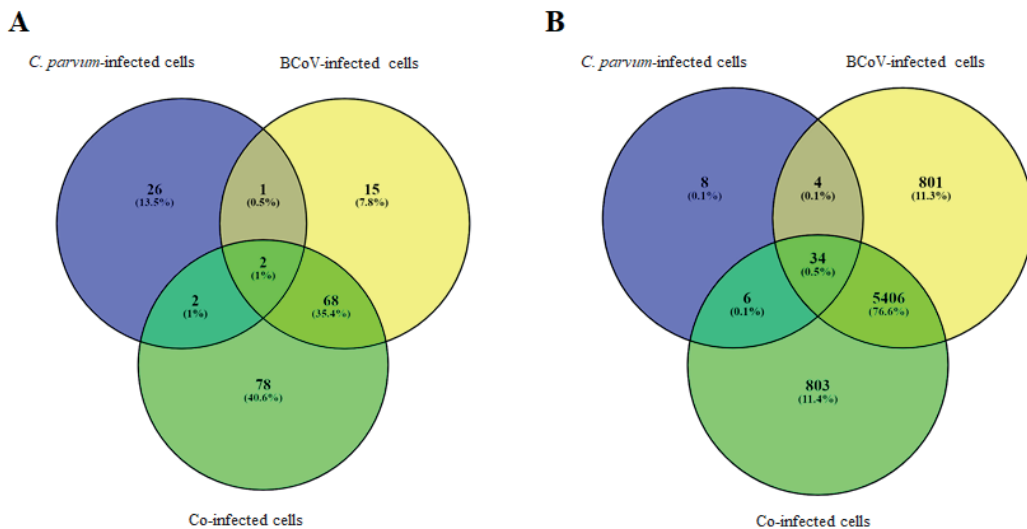


Figure 3

Venn diagrams with *Homo sapiens* differentially expressed genes in the different comparisons assessed in the present work at (A) 24 and (B) 72 hpi.

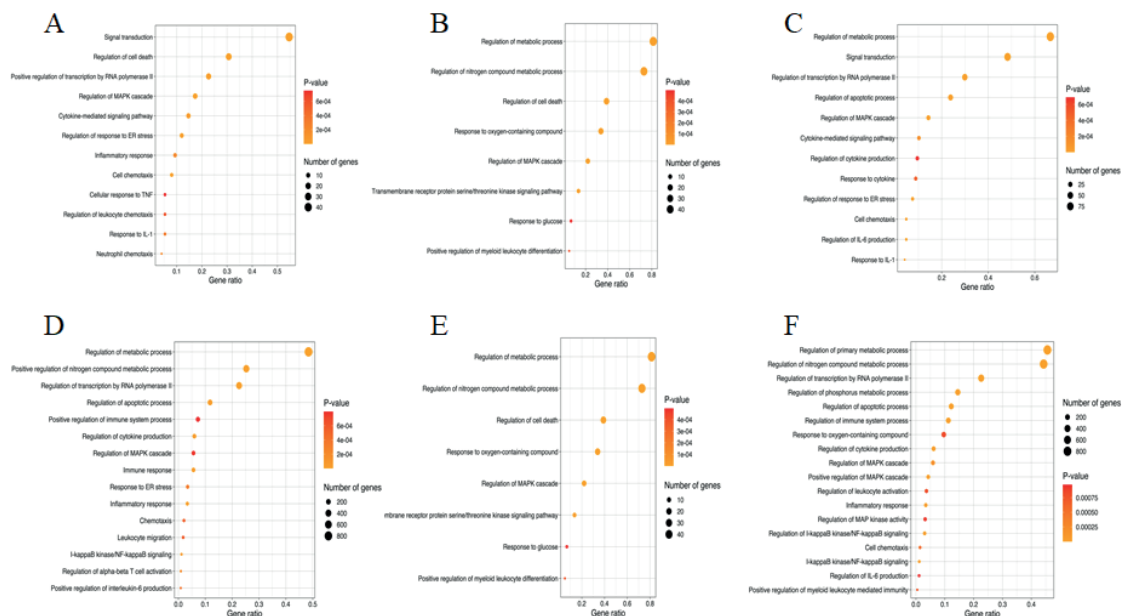


Figure 4

Selected Gene Ontology (GO) terms enriched in the present work among upregulated genes. A: BCoV-infected cells at 24 hpi; B: *C. parvum*-infected cells at 24 hpi; C: Co-infected cells at 24 hpi; D: BCoV-infected cells at 72 hpi; E: *C. parvum*-infected cells at 72 hpi; F: Co-infected cells at 72 hpi.

Supplementary Files

This is a list of supplementary files associated with this preprint. Click to download.

- [Supplementaryfigure1Volcanoplots.pptx](#)
- [Supplementaryfigure2Confocal.pptx](#)
- [Supplementaryfigure3SelectedKEGGs.pptx](#)
- [Supplementarytable1DEGscontrolvssingleinfectionscoinfection.xlsx](#)
- [Supplementarytable2DEGssingleinfectionsvscoinfection.xlsx](#)
- [Supplementarytable3Comparisonthreeinfections24h72h.xlsx](#)
- [Supplementarytable4CntrlvsVirusBioKEGG24hGO.xlsx](#)
- [Supplementarytable5CntrlvsVirusBioKEGG72hGO.xlsx](#)
- [Supplementarytable6CntrlvsCryptoBioKEGG24hGO.xlsx](#)
- [Supplementarytable7CntrlvsCryptoBioKEGG72hGO.xlsx](#)
- [Supplementarytable8CntrlvsCoinfectionBioKEGG24hGO.xlsx](#)
- [Supplementarytable9CntrlvsCoinfectionBioKEGG72hGO.xlsx](#)
- [Supplementarytable10GObpandKEGGsinglevscoinfection.xlsx](#)

Paper III

Article

Bovine Enteroids as an In Vitro Model for Infection with Bovine Coronavirus

Ruchika Shakya , Alejandro Jiménez-Meléndez, Lucy J. Robertson  and Mette Myrmel * 

Department of Paraclinical Sciences, Faculty of Veterinary Medicine, Norwegian University of Life Sciences (NMBU), 1430 Ås, Norway

* Correspondence: mette.myrmel@nmbu.no

Abstract: Bovine coronavirus (BCoV) is one of the major viral pathogens of cattle, responsible for economic losses and causing a substantial impact on animal welfare. Several in vitro 2D models have been used to investigate BCoV infection and its pathogenesis. However, 3D enteroids are likely to be a better model with which to investigate host–pathogen interactions. This study established bovine enteroids as an in vitro replication system for BCoV, and we compared the expression of selected genes during the BCoV infection of the enteroids with the expression previously described in HCT-8 cells. The enteroids were successfully established from bovine ileum and permissive to BCoV, as shown by a seven-fold increase in viral RNA after 72 h. Immunostaining of differentiation markers showed a mixed population of differentiated cells. Gene expression ratios at 72 h showed that pro-inflammatory responses such as IL-8 and IL-1A remained unchanged in response to BCoV infection. Expression of other immune genes, including CXCL-3, MMP13, and TNF- α , was significantly downregulated. This study shows that the bovine enteroids had a differentiated cell population and were permissive to BCoV. Further studies are necessary for a comparative analysis to determine whether enteroids are suitable in vitro models to study host responses during BCoV infection.

Keywords: bovine coronavirus (BCoV); bovine; enteroid; in vitro model; organoid



Citation: Shakya, R.;

Jiménez-Meléndez, A.; Robertson, L.J.; Myrmel, M. Bovine Enteroids as an In Vitro Model for Infection with Bovine Coronavirus. *Viruses* **2023**, *15*, 635. <https://doi.org/10.3390/v15030635>

Academic Editors: Christine Hanssen Rinaldo and Morten Tryland

Received: 19 January 2023

Revised: 24 February 2023

Accepted: 24 February 2023

Published: 27 February 2023



Copyright: © 2023 by the authors. Licensee MDPI, Basel, Switzerland. This article is an open access article distributed under the terms and conditions of the Creative Commons Attribution (CC BY) license (<https://creativecommons.org/licenses/by/4.0/>).

1. Introduction

Bovine coronavirus (BCoV) is one of the major respiratory and enteric viral pathogens of cattle, causing a substantial impact on animal welfare in the beef and dairy industries [1–3]. BCoVs, belonging to the family *Coronaviridae*, genus *Betacoronavirus*, are enveloped, positive-sense, single-stranded RNA (+ssRNA) viruses with a genome of 31 Kb and a diameter of 120–160 nm [4]. The virus is globally distributed [5] and endemic in Scandinavian countries, including Norway. BCoV is transmitted by inhalation of aerosols from nasal discharge, thereby reaching the respiratory epithelium, or reaching the intestine via the faeco-oral route [6]. BCoV is the cause of three distinct clinical syndromes in cattle—calf diarrhoea (CD), winter dysentery (WD) with haemorrhagic diarrhoea in adults, and respiratory infections in cattle of various ages—and is an important contributor to bovine respiratory disease complex [5,7]. The virus is thus able to replicate both in the gastrointestinal and upper respiratory epithelium [8].

Two-dimensional (2D) cell-culture systems have been used to culture BCoV and to study host–pathogen interactions [9] and pathogen–pathogen interactions [10]. The cell lines used to date include human rectal tumour-18 (HRT-18G), human colon adenocarcinoma (HCT-8), African green monkey kidney, Madin Darby bovine kidney, Madin Darby canine kidney 1, bovine embryonic lung, bovine embryonic kidney, and bovine foetal spleen cell lines [11]. Although cell lines are useful experimental models, they lack cellular diversity, and functionality, and some may present genomic abnormalities [12]. On the other hand, primary bovine intestinal epithelial cell lines show a better resemblance to in vivo models. However, they are not well characterized, proliferate slowly, and can be used for only a limited number of passages [13]. Finally, more optimal in vivo animal

studies are more expensive, require large numbers of animals and the necessary facilities, and their use has ethical implications.

To overcome some of the limitations associated with cell lines or animal models, organoids, multicellular three-dimensional (3D) *in vitro* models exhibiting similar architecture as organs [14], could be a good alternative. Organoids can be grown in an extracellular matrix (ECM) supplemented with several growth factors, allowing long-term propagation [15]. Enteroids are organoids derived from the intestine; they form an enclosed system, with the basal regions of the epithelium facing outwards and apical brush borders lying inwards [16–18]. Enteroids comprise a mixed population of stem cells, enterocytes, Paneth cells, goblet cells, and enteroendocrine cells, and can be used to study host interactions with enteric pathogens [19–21].

Recently there has been an upsurge in studies focusing on enteroids as suitable systems for culturing pathogens [22–24]. Human intestinal organoids have proven successful for culturing human rotavirus (HuRoV), norovirus, and enteroviruses [22,25,26], and porcine enteroids have been used to study infection caused by porcine enteric coronaviruses and the host innate response [27]. Although studies on bovine enteroids infected with enteric pathogens are limited to date, there are some studies on the characterization of cell types and culture of bovine rotavirus (BRoV) group A, *Salmonella typhimurium*, *Toxoplasma gondii*, and *Mycobacterium avium* subspecies *paratuberculosis* [17,28,29].

The aim of the present study was to establish bovine enteroids as a replication system for BCoV, to characterize the enteroid cell population, and to compare the expression of selected immune genes during BCoV infection with that previously described in BCoV-infected HCT-8 cells [30]. The gene expression of intestinal stem cells (LGR5+) and differentiation markers (ChrA and Muc2) were analysed using qPCR followed by immunostaining to look for proteins (ChrA, Muc2, sucrose isomaltase, and lysozyme). A panel of three commonly used housekeeping genes (18s rRNA, GAPDH, and ACTB) were tested [31–33], to normalize the gene expression.

2. Materials and Methods

2.1. Isolation of Intestinal Crypts

Tissues used were obtained from post-mortem of a healthy male British Holstein-Friesian (*Bos taurus*) calf less than 1 month old. The isolation of intestinal crypts was carried out at Moredun Research Institute (MRI), Scotland, UK as described in [18]. For all the animal studies carried out at MRI, regulatory licenses had been approved by the University of Edinburgh's Ethics Committee (E50/15).

Briefly, a 10 cm portion of the ileum was collected into ice-cold phosphate-buffered saline (PBS; Gibco, Thermo Fisher Scientific, Scotland, UK) containing 25 µg/mL gentamicin (gen) and 100 U/mL penicillin/streptomycin (pen/str) (Life Technologies, Paisley, UK). The ileum was cut open longitudinally and a glass slide was used to gently remove the mucus layer. The mucosal layer consisting of the intestinal stem cells were then scraped off and suspended in 15 mL of Hank's Balanced Salt Solution (HBSS; Gibco, Thermo Fisher Scientific) with 25 µg/mL gen and 100 U/mL pen/str. The sample was washed several times with HBSS and digested at 37 °C for 40 min in 25 mL of Dulbecco's Modified Eagle's Medium (DMEM; Gibco, Thermo Fisher Scientific) containing 1.0% foetal calf serum (Thermo Fisher Scientific, Grand Island, NY, USA), 25 µg/mL gen, 100 U/mL pen/str, 75 U/mL collagenase type1-A (Sigma-Aldrich, St. Louis, MO, USA) and 20 µg/mL dispase I (Roche, Mannheim, Germany). The number and integrity (finger-like morphology) of isolated crypts were visually assessed by light microscopy at 4× magnification. The crypts were further washed to remove traces of digestion medium and centrifuged at 400× g for 2 min, before finally being re-suspended in 100 µL advanced DMEM/F12 medium (Adv F12; Thermo Fisher Scientific) with 1× B27 supplement minus vitamin A (Thermo Fisher Scientific), 25 µg/mL gen, and 100 U/mL pen/str. After the final wash, the sample consisted of 1000–2000 crypts.

2.2. Enteroid Culture and Differentiation

The enteroids were cultured as previously described [18] and, for long-term storage, enteroids were cryopreserved in Cryostor CS10 medium (STEMCELL Technologies, Cambridge, UK) in liquid nitrogen. Cryopreserved enteroids were resuscitated and passaged at least thrice (P3) before any experimental use in our laboratory.

The crypts (roughly 1000 crypts in 100 μ L Adv F12) were added to 150 μ L of Corning Growth Factor Reduced Matrigel Matrix (AH Diagnostics, Oslo, Norway). Then, 50 μ L of the mix (~200 crypts) was added to each of five wells in a pre-warmed 24-well plate (Nunc, Thermo Fisher Scientific). The Matrigel polymerized for 10 min in a humidified incubator with 5% CO₂ at 37 °C before 500 μ L of growth medium was added to each well. The growth medium consisted of IntestiCult Organoid Growth Medium (Mouse), with Rho-associated kinase inhibitor (Y-27632; Cayman chemicals, Ann Arbor, MI, USA), p38 mitogen-activated protein kinase inhibitor (SB202190; Enzo Life Science, England, UK), and TGF β inhibitor (LY2157299; Cayman chemicals), referred to as medium 1 hereafter (Table S1) [34,35]. Every 2–3 days, the medium was replaced with fresh medium. The enlarged and budding crypts (henceforth referred to as enteroids) were passaged every 7–10 days by removing the medium and dissolving the Matrigel in 500 μ L of cold Adv F12 with 1 \times B27 supplement minus vitamin A, 25 μ g/mL gen, and 100 U/mL pen/str. The enteroids were fragmented into crypts by pipetting, counted, and plated as previously described [18].

A total of four media (Table S1) were prepared to be tested for enteroid differentiation by immunostaining, as described later. Enteroids were grown in medium 1 for 2–3 days and the medium was replaced with 300 μ L of differentiation medium (1–4).

2.3. Inoculation of Crypts with Bovine Coronavirus

The BCoV strain (GenBank accession ID OQ507475) originated from a calf faecal sample and had previously been isolated in our lab using the human rectal tumour cell line (HRT-18G, ATCC CRL-11663) [36]. The isolate was titrated on the cells grown in a 96-well plate by ten-fold serial dilutions, using the Spearman–Karber method [37] (TCID₅₀/mL = 3.16 \times 10⁶).

Inoculation was performed using enteroids that were: A) fragmented into crypts with pipetting only, and B) further dissociated by TrypLE Express enzyme, as detailed below.

Setup A: Approximately 1000 crypts in 100 μ L were inoculated with 100 μ L of BCoV (6.32 \times 10³ TCID₅₀) per well in a 24-well plate. After 1 h incubation at 37 °C, the crypts were transferred into an Eppendorf tube and centrifuged at 300 \times g for 5 min. The pellet was washed once, and the crypts resuspended in 100 μ L Adv F12. After counting, the crypts were mixed with Matrigel, and medium 1 was added after polymerization as described for the enteroid culture.

Setup B: Approximately 1000 crypts in 500 μ L that had already been fragmented by pipetting were further dissociated by incubation with 200 μ L of 1 \times TrypLE Express enzyme (Thermo Fisher Scientific, Newton Drive, Carlsbad, CA, United States) for 10 min at 37 °C, before resuspension in Adv F12 with 300 μ L of 2% foetal bovine serum (FBS; Thermo Fisher Scientific) to stop the dissociation process. The pellet was washed once, and the crypts resuspended in 100 μ L Adv F12. The dissociated crypts were inoculated with same amount of BCoV and grown as described for setup A.

Three individual trials with three replicates were completed for both setups.

Samples and negative controls (mock-infected with Adv F12) were harvested after 1 h and 72 h post-inoculation (hpi), to be checked for virus replication. Prior to harvesting, the crypts were inspected by light microscopy for morphological changes. For harvest, the Matrigel was solubilized in cold Adv F12 and the crypts were centrifuged at 300 \times g for 5 min, washed, centrifuged once more, and lysed with 300 μ L of RLT buffer plus DTT (2M) (Qiagen, Hilden, Germany). Investigation of virus replication was carried out using immunostaining and RT-qPCR [38].

2.4. Immunostaining for Cell Differentiation Markers and BCoV S-Protein

Enteroids were stained for differentiation markers after 2–3 days in medium 1–4, while the infected enteroids were stained for BCoV envelope S-protein and enteroendocrine cells at 72 hpi. The enteroids were rinsed with ice-cold PBS for the removal of Matrigel followed by a fixation and permeabilization step for 20 min as described in [10]. The blocking was performed for 1 h in PBS with 20% horse serum (Thermo Fisher Scientific), and 0.1% Tween-20. The stains and antibodies (Table 1) were diluted in PBS with 2% horse serum and 0.1% Tween 20 and incubated with the enteroids for 1 h at room temperature.

Table 1. Stains and antibodies used for cell nuclei and actin, BCoV envelope S-protein, and markers for cell differentiation.

Stains/Antibodies (Producer)	Dilution	Target
Hoechst 33342 (Invitrogen, Waltham, MA, USA)	1:10,000	Nuclei
Phalloidin iFluor 488 (Abcam, Cambridge, UK)	1:1000	Actin filaments
Monoclonal mouse anti-BCoV, FITC (Bio-X Diagnostics, Rochefort, Belgium)	1:100	BCoV S-protein
Monoclonal mouse anti-sucrase isomaltase, FITC (Santa Cruz Biotechnology, Dallas, TX, USA)	1:100	Enterocytes
Polyclonal anti-bovine chromogranin A (Immunostar, Hudson, WI, USA)	1:100	Enteroendocrine cells
Goat anti-rabbit IgG, Alexa 594 (Life Technologies, Eugene, OR, USA)	1:100	
Polyclonal anti-cattle mucin 2 (MyBioSource Inc., San Diego, CA, USA)	1:100	Goblet cells
Goat anti-rabbit IgG, Alexa 594	1:100	
Polyclonal anti-cattle lysozyme (MyBioSource Inc.)	1:100	Paneth cells
Goat anti-rabbit IgG, Alexa 594	1:100	
Monoclonal mouse anti-BCoV, FITC (Bio-X Diagnostics, Rochefort, Belgium)	1:100	BCoV S-protein
Monoclonal mouse anti-sucrase isomaltase, FITC (Santa Cruz Biotechnology, Dallas, TX, USA)	1:100	Enterocytes
Polyclonal anti-bovine chromogranin A (Immunostar, Hudson, WI, USA)	1:100	Enteroendocrine cells
Goat anti-rabbit IgG, Alexa 594 (Life Technologies, Eugene, OR, USA)	1:100	

A washing step with cold washing buffer and centrifugation was incorporated twice after each incubation step.

After the final centrifugation, the pellet was resuspended in Fluoroshield (Merck) and aliquots of 20 μ L were mounted on glass slides with coverslips. Preparations were examined using a Leica Inverted Confocal SP8 equipped with a White Light Laser, a Leica HyD Detector, and the Leica Application Suite software (Leica microsystems GmbH, Mannheim, Germany), and images were captured at 40 \times and 63 \times magnification under oil immersion. Counting mode was used in the sequential setting, displaying the image based on the number of photons detected per pixel over a constant integration time.

2.5. RNA Isolation and RT-qPCR for Detection of Viral RNA

The enteroids were harvested in 300 μ L of RLT buffer plus DTT (2M) Qiagen as described in Section 2.3 and mixed well by pipetting. Total RNA was isolated from the enteroids using RNeasy Kit (Qiagen), following the manufacturer's instructions. The RNA was eluted in 50 μ L of nuclease-free water and stored at -80° C until analysis.

Information on primers, probe, and RT-qPCR conditions is provided in Table S2. RT-qPCR for BCoV was performed based on a published protocol [38] using the RNA UltraSense™ One-Step Quantitative RT-PCR System kit (Invitrogen, Waltham, MA, USA). A total volume of 20 µL with 2 µL of template RNA was run in a Stratagene AriaMx Real-Time PCR System (Agilent Technologies, Inc., Santa Clara, CA, USA), with Agilent Aria Software v1.5. All samples were run in technical duplicates, with negative and positive controls included in each run.

2.6. Relative Quantification of BCoV RNA and Statistical Analysis

Relative quantification of BCoV genome copies was performed using the formula $Ns1 = Ns2 * (1 + E)^{(Cts2 - Cts1)}$ [39] where Ns1 and Ns2 represent sample copy numbers, Cts1 and Cts2 are sample Ct values, and E the efficiency of the RT-qPCR. Based on a standard curve prepared from a 10-fold dilution series of BCoV RNA, the efficiency was determined to be 98%. To find any statistically significant difference between copy numbers at 1 and 72 hpi, a one-way nonparametric Mann–Whitney *U*-test for independent samples was used.

2.7. Estimation of Gene Expression Ratios

The immune genes included in the present study were selected as they had been shown to be differentially expressed with a high fold change at 72 hpi during BCoV infection of HCT-8 cells [30]. A panel of three commonly used housekeeping genes (18s rRNA, GAPDH, and ACTB) were tested [31–33], and the most stably expressed (similar Ct-values in mock- and BCoV-infected enteroids) were included to normalize the gene expression results. All primers are listed in Table S3 [40–43].

The RNA used for quantification of viral RNA was treated with DNase I (Qiagen) at room temperature (20–25 °C) for 10 min including a final DNase heat inactivation step at 95 °C for 5 min. cDNA was synthesized from 24 µL RNA using SuperScript™ IV VIL0™ Master Mix (Invitrogen, Paisley, UK) in a 48 µL volume, according to the manufacturer’s instructions.

The qPCR was performed in 20 µL volumes using PowerUp™ SYBR™ Green Master Mix (Applied Biosystems, Foster City, CA, USA), 10 pmol each of forward and reverse primer and 2 µL cDNA diluted 1:2. The qPCR was carried out using a Stratagene AriaMx Real-Time PCR instrument and the cycling steps were 2 min at 95 °C followed by 40 cycles of 15 s at 95 °C, 30 s at 60 °C, and a melting curve stage. The amplicon specificity was verified by analysing the melting curve with Agilent Aria Software v1.5. All samples were run in technical triplicates. The qPCR efficiencies (E) were determined by using 4-fold serial dilutions of cDNA and were between 94% and 110%.

A replicate C_t -value that differed by more than 1 from the average of the two others was considered an outlier and omitted. Gene expression ratios were calculated using the Pfaffl method [44] with normalization against the housekeeping genes.

$$\text{Relative gene expression ratio} = \frac{(E_{\text{target}})^{\Delta C_t \text{ target}}}{\text{GeoMean}[(E_{\text{ref}})^{\Delta C_t \text{ ref}}]}$$

where *E* is the efficiency of the qPCRs, ΔC_t is the difference between average C_t -values of the mock-infected and BCoV-infected samples, and *GeoMean* is the geometric mean [45].

To test the statistical significance of gene expression differences between mock- and BCoV-infected enteroids at 72 hpi, average C_t -values from all experiments were assessed in group means using pair-wise fixed reallocation randomization test with at least 2000 randomizations performed in REST software 2009 [46]. The criteria for considering a gene differentially expressed were ratios >1 (upregulated) or <1 (down-regulated), and a *p*-value < 0.05.

3. Results

3.1. Culture, Maintenance, and Staining for Cell Markers

The enteroids were successfully cultured in medium 1, cryopreserved, and resuscitated for experimental use. The crypts formed spheroid-like enteroids after 1–2 days and started budding out, giving enlarged enteroids with a lumen by 5–10 days (Figure S1). The enteroids could be maintained for at least 35 passages, without any obvious signs of degeneration. Staining with Phalloidin showed F-actin rich brush borders on the luminal surface (Figure 1a). The enteroids stained for sucrase isomaltase and ChrA revealed the presence of enterocytes (Figure 1b) and enteroendocrine cells (Figure 1c). However, staining for Muc2 (goblet cells) and lysozyme (Paneth cells) gave only background signals (not shown).

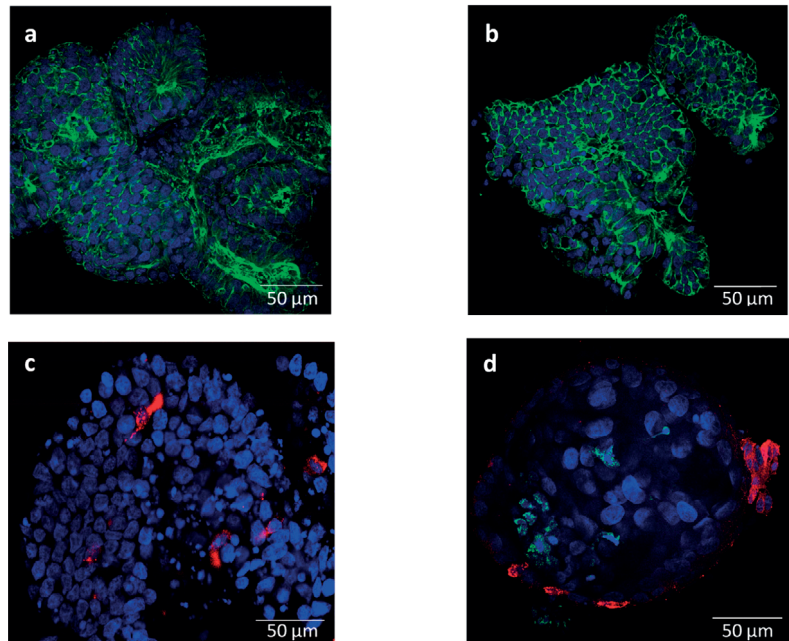


Figure 1. Representative immunofluorescent staining images of bovine enteroids (a–c) mock-infected and (d) infected with bovine coronavirus (BCoV) at 72 h post inoculation: (a) F-actin expressing brush border on the luminal surface (Phalloidin, green); (b) stained for enterocytes (sucrase isomaltase, green); (c) stained for enteroendocrine cells (chromogranin A, red); and (d) stained for BCoV S-protein (green) and enteroendocrine cells (chromogranin A, red). Nuclei were counter-stained with Hoechst (blue). Magnification = 63 \times ; Scale bar = 50 μ m.

The enteroids that were grown in medium 1 before receiving differentiation medium 2–4 (Table S1) survived for only 3–4 days before starting to disintegrate and die (Figure S2b–d) and were not further used.

3.2. BCoV Replication

Regarding the preparation of enteroids for virus inoculation, Setup A gave finger-like crypts surrounded by some cellular debris, while Setup B resulted in smaller disintegrated crypts with small openings and more cellular debris (Figure S3).

The mock- and BCoV-inoculated crypts were morphologically intact, with no cellular debris at 1 and 72 hpi. At 72 hpi, crypts had started budding out, forming lumen-like structures (spheroids), which stained positive for BCoV-S protein (inoculated crypts from

setup B). Nevertheless, relatively few infected cells were identified (Figure 1d), although the samples showed a statistically significant increase in the virus gene copy number from 1 to 72 hpi (Mann–Whitney $U = 14$, $p < 10^{-5}$) (Table 2).

Table 2. Bovine coronavirus (BCoV) gene copy numbers in enteroids at 1 h and 72 h post inoculation (hpi). Samples from Setup A (fragmented enteroids) and B (fragmented and dissociated enteroids), both with $n = 9$ (3 trials with 3 parallels), were analysed by RT-qPCR using Mann–Whitney test for statistical analysis ($p < 0.05$).

Setup	Harvest Time Points (hpi)	Median BCoV Gene Copy Number	IQR	<i>p</i> -Value
A	1	2967	1877–5973	0.3409
	72	3723	1150–6047	
B	1	2962 *	2298–4741	$<10^{-5}$
	72	20,956 *	12,646–32,889	

* Statistically significant difference ($p < 0.05$).

3.3. Gene Expression

For the gene expression, three trials with mock-infected and two of the inoculated enteroids were included in the analysis. The first trial with inoculated samples was excluded as the cDNA concentrations were out of range and the Ct values very high (Figure S4).

Among the three housekeeping genes tested, GAPDH and ACTB were included for the normalization of the expression results, as they were more stably expressed than 18 s rRNA (Table 3).

Table 3. Gene expression ratios for selected genes in BCoV- to mock-infected bovine enteroids. The enteroids were harvested 72 h post inoculation and mRNA was quantified by two-step RT-qPCR. The results were normalized to housekeeping genes GAPDH and ACTB. Three independent trials with mock- ($n = 9$) and two with BCoV-infected ($n = 6$) enteroids are included.

Gene	Type	Reaction Efficiency	Expression Ratio	Std. Error	95% C.I.	P(H1)	Result
<i>GAPDH</i>	REF	0.99	1.127				
<i>ACTB</i>	REF	1.01	0.887				
<i>LGR5</i>	TRG	1.01	2.811	0.915–5.705	0.554–6.948	0.022	UP
<i>ChrA</i>	TRG	1.02	8.356	3.292–18.151	2.046–42.257	0.000	UP
<i>Muc2</i>	TRG	1.09	0.213	0.052–0.835	0.019–2.676	0.008	DOWN
<i>IL-8</i>	TRG	0.95	1.110	0.675–1.782	0.532–2.399	0.537	No diff
<i>IL-1A</i>	TRG	0.94	1.091	0.653–1.733	0.417–2.348	0.662	No diff
<i>MMP13</i>	TRG	1.09	0.036	0.012–0.145	0.010–0.372	0.000	DOWN
<i>CXCL-3</i>	TRG	1.1	0.554	0.287–0.848	0.240–1.031	0.009	DOWN
<i>TNF-α</i>	TRG	1.03	0.556	0.336–0.891	0.235–1.108	0.004	DOWN

P(H1): Probability of alternate hypothesis that the difference in gene expression between BCoV- and mock-infected enteroids is due only to chance. REF: Reference (housekeeping gene). TRG: Target gene. Geometric mean of expression ratio of housekeeping genes = 1.00.

The differentiation markers, LGR5+ (stemness) and ChrA (enteroendocrine cells), were upregulated, while the Muc2 (goblet cells) gene was downregulated in the BCoV-infected enteroids compared to the mock-infected at 72 hpi.

The expression ratios for the immune genes, IL-8 and IL-1A, were similar for mock- and BCoV-infected enteroids, while MMP13, CXCL-3, and TNF- α genes were downregulated.

4. Discussion

The main finding of this study is that bovine enteroids were able to support the replication of BCoV, as indicated by an approximately seven-fold increase in viral RNA after 72 h and the immunostaining of BCoV envelope S-protein. According to our knowledge, this is the first report on BCoV replication in enteroids.

The enteroids were successfully grown from intestinal tissue (ileum) from a healthy young calf less than one month old and could be propagated in medium 1 for at least 35 passages without any signs of degeneration, which is longer than reported in other studies [17,18]. Ref. [18] also isolated crypts from the ileum of young calves (<one month old), but the enteroids could be passaged in medium 1 no more than five to eight times without any sign of degeneration. This indicates that the possible number of passages of bovine enteroids could depend on the donor animal. The region of intestine used, animal age, and breed might also have an influence, as [17] isolated crypts from the jejunum of adults (20 to 30 months) of a different breed and the enteroids could be kept in medium 2 for no more than four to 12 passages before degeneration. In our hands, medium 2 did not support the growth and differentiation of the enteroids.

Staining of enteroids in medium 1 for F-actin rich brush borders on the luminal surface indicated that the epithelium was polarised, as *in vivo*. The stained differentiation markers revealed enterocytes and enteroendocrine cells, while staining for goblet cells and Paneth cells gave largely non-specific signals. In total, the staining results indicate that medium 1 can support differentiation to some extent. Previous studies using bovine, porcine, and murine enteroids [17,47,48] have indicated that WntCM, growth factors R-spondin (Wnt agonist), and Noggin (TGF β superfamily inactivator) are core components for differentiation. Ref [17] demonstrated a differentiated cell population by immunostaining (enteroendocrine and goblet cells) and by proteomic analysis (enterocytes, stem cell markers, mucus components, and villus morphogenesis). Furthermore, EGF (epidermal growth factor) is also considered crucial for the growth and differentiation of the cells. Refs [16,49] also describe the need of developing in-house media to replace IntestiCult to adjust individual growth factors. Bovine supplements/growth factors are, however, not readily available and, therefore, those derived from humans/mice are mostly used. This could be a reason for the difficulty in achieving differentiated bovine enteroids [47,50], as the homology/activity of EGF varies between species [21]. In the present study, several formulations (Table S1) for the manipulation of growth factors and differentiation of the enteroids were tested, but our results did not indicate that modifying the concentration of growth factors mentioned above was necessary for differentiation. Embedding the enteroids in Matrigel could also have contributed to differentiation, as described by [51,52]. To lower any Matrigel-driven differentiation, we used Matrigel with reduced growth factors [18].

In addition to the media 1 and 2, as described by [17,18], we tried two other formulations. Medium 3 was tested as [21] found it to work well for chicken enteroids, which they reported to be the most difficult to grow and differentiate. Ref [34] was able to differentiate human enteroids using medium 4, and to infect them with HuRoV, while [25] also followed the same recipe for human enteroids and found them permissive for human norovirus. Ref [28] also used medium 4 to differentiate bovine enteroids and infect them with BRoV. Nevertheless, of the three formulations in Table S1, only [18] supported persistent growth and some differentiation of bovine enteroids in our study.

The enteroids inoculated with BCoV showed no apparent signs of degeneration after 72 hpi. When the enteroids were mechanically disrupted and exposed to BCoV (setup A), a small increase in viral RNA could be detected, indicating that a limited infection had been established. However, when TrypL Xpress was used for further dissociation (setup B), there was probably an increased exposure of the interior (luminal) surface to virus particles, thus resulting in a clearly recognizable infection despite relatively few infected cells being identified by staining at 72 hpi.

Ref. [6] describes that BCoV infects the enterocytes and the positive staining of sucrase isomaltase in our study showed the enteroids contained a high proportion of these cells at the time of infection. Our results, which show a significant increase in BCoV gene copies only after the dissociation of the enteroids, indicate the need for a sufficient breakdown of the enteroids for the virus to infect the cells. The insufficient opening and, perhaps, early closing of the crypts in our study could be a reason for the relatively few infected enterocytes. According to [53], crypts from fragmented and dissociated enteroids seal

and start growing from intact stem cells at the base of the crypts. It is possible that BCoV target cells are lost during fragmentation and trypsinization, resulting in mainly non-differentiated stem cells at the time of infection. For these reasons, the breakdown of enteroids might need to be optimized to increase virus access to the permissive luminal side of the cells, while minimizing the loss of cells.

In the present gene expression study, LGR5+ was upregulated in infected enteroids, which might indicate that BCoV is able to induce self-renewal of the stem cells in the crypts. A previous study on porcine intestinal organoids infected with the coronavirus transmissible gastroenteritis virus revealed upregulation of Wnt-target genes, including LGR5 with activation of the Wnt/ β -catenin pathway promoting the self-renewal of intestinal stem cells [54].

As shown by the gene expression results, the BCoV-infected enteroids in our study (at least P3 at the time of infection) showed the downregulation of Muc2 at 72 hpi. Transcriptomics data from [18] comparing isolated crypts with progressive passages of organoids (up to passage 6) showed the downregulation of Muc2 at higher passage numbers. However, the absence of staining of the Muc2 indicated that any goblet cells had limited production of the Muc 2 protein. A study on porcine enteroids [27] showed that coronavirus porcine epidemic diarrhoea virus (PEDV) infected multiple intestinal epithelial cells including goblet cells. [55] demonstrated that PEDV infection reduced the number of goblet cells in the small intestine of weaned pigs. A previous study on neonatal calves also indicated BCoV infected the goblet cells, causing a reduction in the number of these cells [56]. These studies suggest that BCoV could possibly infect goblet cells, and further investigation in a well-differentiated enteroid system or *in vivo* would be of interest.

The expression of the immune genes IL-8 and IL-1A showed no significant difference between the mock- and BCoV-infected enteroids at 72 hpi. However, an expression study on BCoV-infected HCT-8 cells showed that both genes were highly upregulated at 24 and 72 hpi [30]. A study by [57] showed that the mean IL-8 serum concentration in BCoV-infected diarrhoeal calves increased from 0 to 24 h compared to non-diarrhoeal calves, but started to decline at 48 hpi, also suggesting that IL-8 could be used as a biomarker of intestinal injury. As these pro-inflammatory responses (IL-8 and IL-1A) are modulated as early immune responses during viral infections [58], earlier timepoints might have been more appropriate for analysis in the present study. According to [30], CXCL-3 was upregulated in BCoV-infected HCT-8 cells both at 24 and 72 hpi, whereas MMP13 expression and the TNF- α signalling pathway were upregulated at 72 hpi. In contrast, these three genes were significantly downregulated in BCoV-infected enteroids in the present study. The downregulation of MMP13 could indicate that the cells were more intact in the enteroids than in the HCT-8 cells, as MMP13 is associated with reduced epithelial barrier function during pathological changes in the cells [59]. A study by [60] showed that bovine enteroids treated with inflammatory cytokines such as TNF- α for 24–48 hpi disrupted the bovine intestinal barrier by altering the junctional morphology and permeability, thereby disrupting the epithelial cells. In contrast, an expression study on calves infected with BCoV showed the downregulation of TNF- α genes at 18 hpi [61], which corroborates with our enteroid results at 72 hpi.

Overall, the gene expression data obtained in the present study suggests that the host response to BCoV infection at 72 hpi differed substantially from that of HCT-8 cells. The discrepancies in the regulation of immune-related genes during the infection of a traditional cell line and enteroids may reflect that the enteroid system is more complex, with different cell populations that may have different modulations and can counteract proinflammatory responses. There are experimental differences between the studies, such as a much lower dose of BCoV used for the enteroids than in the HCT-8 cells, different methods to analyse gene expression (RT-qPCR and RNASeq), use of a BCoV strain that was already adapted to the cell line but not to the enteroids, and *in vitro* infection of cells from different host species.

5. Conclusions

Stem cells isolated from the ileum of a healthy calf were successfully developed into enteroids and used as a tool to increase our knowledge on host–pathogen interaction during BCoV infection. The gene expression study demonstrated a host response that differs from that reported from BCoV-infected HCT-8 cells. Future comparative gene expression studies on BCoV infection are needed to determine whether the enteroid system is a good model for the bovine intestine.

Supplementary Materials: The following supporting information can be downloaded at: <https://www.mdpi.com/article/10.3390/v15030635/s1>, Figure S1: Bovine crypts grown in medium 1 forming (a) spheroid-like structures at day 1–2; (b) budding out at day 3; (c) with enlarged branched out structures and lumen, enteroids at day 5; (d) 7 and (E)10; Figure S2: Bovine enteroids in four of the tested differentiation media on day 4 (a) Medium 1: enteroids budding out with few dark-centred spheroids; (b) Medium 2: enlarged, rounded, and elongated enteroids with few of them starting to disintegrate; (c) Medium 3: rounded and elongated enteroids surrounded by cellular debris, starting to disintegrate; (d) Medium 4: enteroids appear as round spheroids surrounded by cellular debris; Figure S3: (a) Bovine enteroids fragmented by pipetting (setup A) giving finger-like crypts surrounded by some cellular debris. (b) Enteroids further dissociated with TrypL Xpress (setup B) showing more disintegrated crypts with small openings shown with blue arrows surrounded by more cellular debris. Figure S4: Average threshold cycle (Ct) values for eight targeted *Bos taurus* genes of the bovine enteroids either (a) mock-infected or (b) infected with bovine coronavirus at 72 h post inoculation. The dot symbols indicate average mean Ct values while different colours indicate three independent rounds of experiments (R1 = round 1, R2 = round 2, R3 = round 3). The bars indicate standard deviation, Table S1: Formulations of media that were tested for growth (medium 1) and differentiation (media 1–4); Table S2: Nucleotide sequences of the primers and probe, and RT-qPCR cycling conditions used for the amplification of BCoV RNA; Table S3: Primers used for qPCR in the expression study of targeted *Bos taurus* genes.

Author Contributions: Conceptualization, M.M.; methodology, data curation, and formal analysis, R.S., A.J.-M., L.J.R. and M.M.; writing—original draft preparation, R.S.; writing—review and editing, A.J.-M., L.J.R. and M.M.; supervision, L.J.R. and M.M.; funding acquisition and project administration, M.M. All authors have read and agreed to the published version of the manuscript.

Funding: This project was supported by internal funding from the Virology and Parasitology Unit, NMBU.

Institutional Review Board Statement: For all the animal studies carried out at Moredun Research Institute (MRI), Scotland, UK, regulatory licenses had been approved by the University of Edinburgh’s Ethics Committee (E50/15). Tissues used were obtained from the post-mortem of a healthy male British Holstein–Friesian (*Bos taurus*) calf and therefore did not require a Home Office license.

Data Availability Statement: Full genomes of BCoV from several samples used in this study were sequenced and can be accessed with GenBank accession ID OQ507475.

Acknowledgments: We would like to thank Professor Elisabeth A. Innes and Postdoc Alison Bur-rells at Moredun Research Institute (MRI) for facilitating a very positive study visit for the first author (RS) at MRI and for providing the training on working with bovine enteroids, as well as sharing the enteroids for this future work; Mamata Khatri for all the help in the laboratory; and Hilde Raanaas Kolstad at Imaging Centre, NMBU for technical assistance on confocal microscopy.

Conflicts of Interest: The authors declare no conflict of interest. The funders had no role in the design of the study; in the collection, analyses, or interpretation of data; in the writing of the manuscript; or in the decision to publish the results.

References

1. Beaudeau, F.; Björkman, C.; Alenius, S.; Frössling, J. Spatial patterns of bovine corona virus and bovine respiratory syncytial virus in the Swedish beef cattle population. *Acta Vet. Scand.* **2010**, *52*, 33. [CrossRef] [PubMed]
2. Toftaker, I.; Sanchez, J.; Stokstad, M.; Nodtvedt, A. Bovine respiratory syncytial virus and bovine coronavirus antibodies in bulk tank milk—risk factors and spatial analysis. *Prev Vet. Med.* **2016**, *133*, 73–83. [CrossRef] [PubMed]

3. Gulliksen, S.M.; Jor, E.; Lie, K.I.; Hamnes, I.S.; Løken, T.; Åkerstedt, J.; Østerås, O. Enteropathogens and risk factors for diarrhea in Norwegian dairy calves. *J. Dairy Sci.* **2009**, *92*, 5057–5066. [[CrossRef](#)] [[PubMed](#)]
4. Saif, L.J.; Jung, K. Comparative pathogenesis of bovine and porcine respiratory coronaviruses in the animal host species and SARS-CoV-2 in humans. *J. Clin. Microbiol.* **2020**, *58*, e01355-20. [[CrossRef](#)]
5. Hodnik, J.J.; Ježek, J.; Starič, J. Coronaviruses in cattle. *Trop. Anim. Health Prod.* **2020**, *52*, 2809–2816. [[CrossRef](#)]
6. Park, S.J.; Kim, G.Y.; Choy, H.E.; Hong, Y.J.; Saif, L.J.; Jeong, J.H.; Park, S.I.; Kim, H.H.; Kim, S.K.; Shin, S.S.; et al. Dual enteric and respiratory tropisms of winter dysentery bovine coronavirus in calves. *Arch. Virol.* **2007**, *152*, 1885–1900. [[CrossRef](#)]
7. Fulton, R.W.; Ridpath, J.F.; Burge, L.J. Bovine coronaviruses from the respiratory tract: Antigenic and genetic diversity. *Vaccine* **2013**, *31*, 886–892. [[CrossRef](#)]
8. Cho, Y.I.; Yoon, K.J. An overview of calf diarrhea-infectious etiology, diagnosis, and intervention. *J. Vet. Sci.* **2014**, *15*, 1–17. [[CrossRef](#)]
9. Schultze, B.; Herrler, G. Bovine coronavirus uses N-acetyl-9-O-acetylneuraminic acid as a receptor determinant to initiate the infection of cultured cells. *J. Gen. Virol.* **1992**, *73*, 901–906. [[CrossRef](#)]
10. Shakya, R.; Meléndez, A.J.; Robertson, L.J.; Myrmel, M. Interactions between *Cryptosporidium parvum* and bovine corona virus during sequential and simultaneous infection of HCT-8 cells. *Microbes Infect.* **2022**, *24*, 104909. [[CrossRef](#)]
11. Clark, M.A. Bovine coronavirus. *Br. Vet. J.* **1993**, *149*, 51–70. [[CrossRef](#)]
12. Kapalczyńska, M.; Kolenda, T.; Przybyła, W.; Zajączkowska, M.; Teresiak, A.; Filas, V.; Ibbs, M.; Bliźniak, R.; Łuczewski, L.; Lamperska, K. 2D and 3D cell cultures—a comparison of different types of cancer cell cultures. *Arch. Med. Sci.* **2018**, *14*, 910–919. [[CrossRef](#)]
13. Zhan, K.; Lin, M.; Liu, M.M.; Sui, Y.N.; Zhao, G.Q. Establishment of primary bovine intestinal epithelial cell culture and clone method. *Vitr. Cell Dev. Biol.-Anim.* **2017**, *53*, 54–57. [[CrossRef](#)]
14. Clevers, H. Modeling development and disease with organoids. *Cell* **2016**, *165*, 1586–1597. [[CrossRef](#)]
15. Dutta, D.; Clevers, H. Organoid culture systems to study host–pathogen interactions. *Curr. Opin. Immunol.* **2017**, *48*, 15–22. [[CrossRef](#)]
16. Sutton, K.M.; Orr, B.; Hope, J.; Jensen, S.R.; Vervelde, L. Establishment of bovine 3D enteroid-derived 2D monolayers. *Vet. Res.* **2022**, *53*, 1–13. [[CrossRef](#)]
17. Derricott, H.; Luu, L.; Fong, W.Y.; Hartley, C.S.; Johnston, L.J.; Armstrong, S.D.; Randle, N.; Duckworth, C.A.; Campbell, B.J.; Wastling, J.M.; et al. Developing a 3D intestinal epithelium model for livestock species. *Cell Tissue Res.* **2019**, *375*, 409–424. [[CrossRef](#)]
18. Hamilton, C.A.; Young, R.; Jayaraman, S.; Sehgal, A.; Paxton, E.; Thomson, S.; Katzer, F.; Hope, J.; Innes, E.; Morrison, L.J.; et al. Development of in vitro enteroids derived from bovine small intestinal crypts. *Vet. Res.* **2018**, *49*, 1–15. [[CrossRef](#)]
19. Cieza, R.J.; Golob, J.L.; Colacino, J.A.; Wobus, C.E. Comparative analysis of public RNA-sequencing data from human intestinal enteroid (HIEs) infected with enteric RNA viruses identifies universal and virus-specific epithelial responses. *Viruses* **2021**, *13*, 1059. [[CrossRef](#)]
20. Zhou, J.; Li, C.; Liu, X.; Chiu, M.C.; Zhao, X.; Wang, D.; Wei, Y.; Lee, A.; Zhang, A.J.; Chu, H.; et al. Infection of bat and human intestinal organoids by SARS-CoV-2. *Nat. Med.* **2020**, *26*, 1077–1083. [[CrossRef](#)]
21. Holthaus, D.; Delgado-Betancourt, E.; Aebischer, T.; Seeber, F.; Klotz, C. Harmonization of protocols for multi-species organoid platforms to study the intestinal biology of *Toxoplasma gondii* and other protozoan infections. *Front. Cell Infect. Microbiol.* **2021**, *935*, 368. [[CrossRef](#)] [[PubMed](#)]
22. Zou, W.Y.; Blutt, S.E.; Crawford, S.E.; Ettayebi, K.; Zeng, X.L.; Saxena, K.; Ramani, S.; Karandikar, U.C.; Estes, M.K. Human intestinal enteroids: New models to study gastrointestinal virus infections. *Methods Mol. Biol.* **2019**, *1576*, 229–247. [[CrossRef](#)] [[PubMed](#)]
23. Co, J.Y.; Margalef-Català, M.; Monack, D.M.; Amieva, M.R. Controlling the polarity of human gastrointestinal organoids to investigate epithelial biology and infectious diseases. *Nat. Protoc.* **2021**, *16*, 5171–5192. [[CrossRef](#)]
24. Dutta, D.; Heo, I.; O’connor, R. Studying *Cryptosporidium* infection in 3D tissue-derived human organoid culture systems by microinjection. *J. Vis. Exp.* **2019**, *151*, e59610. [[CrossRef](#)]
25. Ettayebi, K.; Crawford, S.E.; Murakami, K.; Broughman, J.R.; Karandikar, U.; Tenge, V.R.; Neill, F.H.; Blutt, S.E.; Zeng, X.L.; Qu, L.; et al. Replication of human noroviruses in stem cell-derived human enteroids. *Science* **2016**, *353*, 1387–1393. [[CrossRef](#)]
26. Drummond, C.G.; Bolock, A.M.; Ma, C.; Luke, C.J.; Good, M.; Coyne, C.B. Enteroviruses infect human enteroids and induce antiviral signaling in a cell lineage-specific manner. *Proc. Natl. Acad. Sci. USA.* **2017**, *114*, 1672–1677. [[CrossRef](#)]
27. Li, L.; Fu, F.; Guo, S.; Wang, H.; He, X.; Xue, M.; Yin, L.; Feng, L.; Liu, P. Porcine intestinal enteroids: A new model for studying enteric coronavirus porcine epidemic diarrhea virus infection and the host innate response. *J. Virol.* **2019**, *93*, e01682-18. [[CrossRef](#)]
28. Alfajaro, M.M.; Kim, J.Y.; Barbé, L.; Cho, E.H.; Park, J.G.; Soliman, M.; Baek, Y.B.; Kang, M.I.; Kim, S.H.; Kim, G.J.; et al. Dual recognition of sialic acid and α Gal epitopes by the VP8* domains of the bovine rotavirus G6P [5] WC3 and of its mono-reassortant G4P [5] RotaTeq vaccine strains. *J. Virol.* **2019**, *93*, e00941-19. [[CrossRef](#)]
29. Blake, R.; Jensen, K.; Mabbott, N.; Hope, J.; Stevens, J. The development of 3D bovine intestinal organoid derived models to investigate *Mycobacterium avium* ssp *paratuberculosis* pathogenesis. *Front. Vet. Sci.* **2022**, *9*, 921160. [[CrossRef](#)]

30. Jiménez-Meléndez, A.; Shakya, R.; Markussen, T.; Robertson, L.J.; Myrmel, M.; Shokouh, M.-N. Virus modulation predominates the gene expression profile of HCT-8 cells following co-infection with *Cryptosporidium parvum* and bovine coronavirus. *Sci. Rep.* 2023; (submitted)
31. Lee, B.R.; Yang, H.; Lee, S.I.; Haq, I.; Ock, S.A.; Wi, H.; Lee, H.C.; Lee, P.; Yoo, J.G. Robust three-dimensional (3D) expansion of bovine intestinal organoids: An in vitro model as a potential alternative to an in vivo system. *Animals* 2021, 11, 2115. [CrossRef]
32. Puech, C.; Dedieu, L.; Chantal, I.; Rodrigues, V. Design, and evaluation of a unique SYBR Green real-time RT-PCR assay for quantification of five major cytokines in cattle, sheep, and goats. *BMC Vet. Res.* 2015, 11, 65. [CrossRef]
33. Horcajo, P.; Jiménez-Pelayo, L.; García-Sánchez, M.; Regidor-Cerrillo, J.; Collantes-Fernández, E.; Rozas, D.; Hambruch, N.; Pfarrer, C.; Ortega-Mora, L.M. Transcriptome modulation of bovine trophoblast cells in vitro by *Neospora caninum*. *Int. J. Parasitol.* 2017, 47, 791–799. [CrossRef]
34. Saxena, K.; Blutt, S.E.; Ettayebi, K.; Zeng, X.L.; Broughman, J.R.; Crawford, S.E.; Karandikar, U.C.; Sastri, N.P.; Conner, M.E.; Opekun, A.R.; et al. Human intestinal enteroids: A new model to study human rotavirus infection, host restriction, and pathophysiology. *J. Virol.* 2016, 90, 43–56. [CrossRef]
35. Miyoshi, H.; Ajima, R.; Luo, C.T.; Yamaguchi, T.P.; Stappenbeck, T.S. Wnt5a potentiates TGF- β signaling to promote colonic crypt regeneration after tissue injury. *Science* 2012, 338, 108–113. [CrossRef]
36. Oma, V.S.; Tråvén, M.; Alenius, S.; Myrmel, M.; Stokstad, M. Bovine coronavirus in naturally and experimentally exposed calves; viral shedding and the potential for transmission. *Virol. J.* 2016, 13, 1–11. [CrossRef]
37. Ramakrishnan, M.A. Determination of 50% endpoint titer using a simple formula. *World J. Virol.* 2016, 5, 85–86. [CrossRef]
38. Christensen, E.; Myrmel, M. Coagulant residues' influence on virus enumeration as shown in a study on virus removal using aluminium, zirconium and chitosan. *J. Water Health* 2018, 16, 600–613. [CrossRef]
39. Livak, K.J.; Schmittgen, T.D. Analysis of relative gene expression data using real-time quantitative PCR and the $2^{-\Delta\Delta CT}$ method. *Methods* 2001, 25, 402–408. [CrossRef]
40. Jiménez-Pelayo, L.; García-Sánchez, M.; Regidor-Cerrillo, J.; Horcajo, P.; Collantes-Fernández, E.; Gómez-Bautista, M.; Hambruch, N.; Pfarrer, C.; Ortega-Mora, L.M. Immune response profile of caruncular and trophoblast cell lines infected by high- (Nc-Spain7) and low-virulence (Nc-Spain1H) isolates of *Neospora caninum*. *Parasit. Vectors* 2019, 12, 218. [CrossRef]
41. Ito, T.; Kodama, M. Demonstration by reverse transcription-polymerase chain reaction of multiple cytokine mRNA expression in bovine alveolar macrophages and peripheral blood mononuclear cells. *Res. Vet. Sci.* 1996, 60, 94–96. [CrossRef]
42. Gärtner, M.A.; Peter, S.; Jung, M.; Drillich, M.; Einspanier, R.; Gabler, C. Increased mRNA expression of selected pro-inflammatory factors in inflamed bovine endometrium in vivo as well as in endometrial epithelial cells exposed to *Bacillus pumilus* in vitro. *Reprod. Fertil. Dev.* 2016, 28, 982–994. [CrossRef] [PubMed]
43. Arranz-Solis, D.; Benavides, J.; Regidor-Cerrillo, J.; Horcajo, P.; Castaño, P.; del Carmen Ferreras, M.; Jiménez-Pelayo, L.; Collantes-Fernández, E.; Ferre, I.; Hemphill, A.; et al. Systemic and local immune responses in sheep after *Neospora caninum* experimental infection at early, mid, and late gestation. *Vet. Res.* 2016, 47, 2. [CrossRef] [PubMed]
44. Pfaffl, M.W. A new mathematical model for relative quantification in real-time RT-PCR. *Nucleic Acids Res.* 2001, 29, e45. [CrossRef]
45. Vandesompele, J.; De Preter, K.; Pattyn, F.; Poppe, B.; Van Roy, N.; De Paepe, A.; Speleman, F. Accurate normalization of real-time quantitative RT-PCR data by geometric averaging of multiple internal control genes. *Genome Biol.* 2002, 3, 1–11. [CrossRef] [PubMed]
46. Pfaffl, M.W.; Horgan, G.W.; Dempfle, L. Relative expression software tool (REST[®]) for group-wise comparison and statistical analysis of relative expression results in real-time PCR. *Nucleic Acids Res.* 2002, 30, e36. [CrossRef]
47. Powell, R.H.; Behnke, M.S. WRN conditioned media is sufficient for in vitro propagation of intestinal organoids from large farm and small companion animals. *Biol. Open* 2017, 6, 698–705. [CrossRef]
48. Sato, T.; Vries, R.G.; Snippert, H.J.; van de Wetering, M.; Barker, N.; Stange, D.E.; Van Es, J.H.; Abo, A.; Kujala, P.; Peters, P.J.; et al. Single Lgr5 stem cells build crypt-villus structures in vitro without a mesenchymal niche. *Nature* 2009, 459, 262–265. [CrossRef]
49. Töpfer, E.; Pasotti, A.; Telopoulou, A.; Italiani, P.; Boraschi, D.; Ewart, M.A.; Wilde, C. Bovine colon organoids: From 3D bioprinting to cryopreserved multi-well screening platforms. *Toxicol. Vitro* 2019, 61, 104606. [CrossRef]
50. Beaumont, M.; Blanc, F.; Cherbuy, C.; Egidy, G.; Giuffra, E.; Lacroix-Lamandé, S.; Wiedemann, A. Intestinal organoids in farm animals. *Vet. Res.* 2021, 52, 33. [CrossRef]
51. Baatout, S.; Cheṭa, N. Matrigel: A useful tool to study endothelial differentiation. *Rom. J. Intern. Med.* 1996, 34, 263–269.
52. Zhang, J.; Li, J.; Yan, P.; He, L.; Zhang, X.; Wang, X.; Shi, Y.; Deng, L.; Zhang, Z.; Zhao, B. In-depth analysis of the relationship between bovine intestinal organoids and enteroids based on morphology and transcriptome. *J. Tissue Eng. Regen Med.* 2022, 16, 1032–1046. [CrossRef]
53. Heo, I.; Clevers, H. Expanding intestinal stem cells in culture. *Cell Res.* 2015, 25, 995–996. [CrossRef]
54. Yang, N.; Zhang, Y.; Fu, Y.; Li, Y.; Yang, S.; Chen, J.; Liu, G. Transmissible gastroenteritis virus infection promotes the self-renewal of porcine intestinal stem cells via Wnt/ β -Catenin pathway. *J. Virol.* 2022, 96, e00962-22. [CrossRef]
55. Jung, K.; Saif, L.J. Goblet cell depletion in small intestinal villous and crypt epithelium of conventional nursing and weaned pigs infected with porcine epidemic diarrhea virus. *Res. Vet. Sci.* 2017, 110, 12–15. [CrossRef]
56. Doughri, A.M.; Storz, J.; Hajer, I.; Fernando, H.S. Morphology and morphogenesis of a coronavirus infecting intestinal epithelial cells of newborn calves. *Exp. Mol. Pathol.* 1976, 25, 355–370. [CrossRef]

57. Ok, M.; Yildiz, R.; Hatipoglu, F.; Baspinar, N.; Ider, M.; Üney, K.; Ertürk, A.; Durgut, M.K.; Terzi, F. Use of intestine-related biomarkers for detecting intestinal epithelial damage in neonatal calves with diarrhea. *Am. J. Vet. Res.* **2020**, *81*, 139–146. [[CrossRef](#)]
58. Mogensen, T.H.; Paludan, S.R. Molecular pathways in virus-induced cytokine production. *Microbiol. Mol. Biol. Rev.* **2001**, *65*, 131–150. [[CrossRef](#)]
59. Vandenbroucke, R.E.; Dejonckheere, E.; Van Hauwermeiren, F.; Lodens, S.; De Rycke, R.; Van Wonterghem, E.; Staes, A.; Gevaert, K.; López-Otin, C.; Libert, C. Matrix metalloproteinase 13 modulates intestinal epithelial barrier integrity in inflammatory diseases by activating TNF. *EMBO Mol. Med.* **2013**, *5*, 1000–1016. [[CrossRef](#)]
60. Crawford, C.K.; Lopez Cervantes, V.; Quilici, M.L.; Armien, A.G.; Questa, M.; Matloob, M.S.; Huynh, L.D.; Beltran, A.; Karchemskiy, S.J.; Crakes, K.R.; et al. Inflammatory cytokines directly disrupt the bovine intestinal epithelial barrier. *Sci. Rep.* **2022**, *12*, 14578. [[CrossRef](#)]
61. Aich, P.; Wilson, H.L.; Kaushik, R.S.; Potter, A.A.; Babiuk, L.A.; Griebel, P. Comparative analysis of innate immune responses following infection of newborn calves with bovine rotavirus and bovine coronavirus. *J. Gen. Virol.* **2007**, *88*, 2749–2761. [[CrossRef](#)]

Disclaimer/Publisher’s Note: The statements, opinions and data contained in all publications are solely those of the individual author(s) and contributor(s) and not of MDPI and/or the editor(s). MDPI and/or the editor(s) disclaim responsibility for any injury to people or property resulting from any ideas, methods, instructions or products referred to in the content.

ISBN: 978-82-575-2091-5

ISSN: 1894-6402



Norwegian University
of Life Sciences

Postboks 5003
NO-1432 Ås, Norway
+47 67 23 00 00
www.nmbu.no